

1 **Control of tissue development and cell diversity by cell cycle dependent transcriptional filtering**

2

3 Maria Abou Chakra, Ruth Isserlin, Thinh Tran and Gary D. Bader\*

4 The Donnelly Centre, University of Toronto, Toronto, M5S 3E1, Canada.

5 \*Correspondence: gary.bader@utoronto.ca

6

7 **Abstract**

8 Cell cycle duration changes dramatically during development, starting out fast to generate cells quickly  
9 and slowing down over time as the organism matures. The cell cycle can also act as a transcriptional  
10 filter to control the expression of long gene transcripts which are partially transcribed in short cycles.  
11 Using mathematical simulations of cell proliferation, we identify an emergent property, that this filter  
12 can act as a tuning knob to control gene transcript expression, cell diversity and the number and  
13 proportion of different cell types in a tissue. Our predictions are supported by comparison to single-cell  
14 RNA-seq data captured over embryonic development. Additionally, evolutionary genome analysis  
15 shows that fast developing organisms have a narrow genomic distribution of gene lengths while slower  
16 developers have an expanded number of long genes. Our results support the idea that cell cycle  
17 dynamics may be important across multicellular animals for controlling gene transcript expression and  
18 cell fate.

19

20 **Keywords**

21 cell cycle, development, cell differentiation, gene regulation, computational model, single cell,  
22 transcriptome, transcriptional filter, gene length

23

24

## 25 **Introduction**

26

27 A fundamental question in biology is how a single eukaryotic cell (e.g. zygote, stem cell) produces the  
28 complexity required to develop into an organism. A single cell will divide and generate many progeny,  
29 diversifying in a controlled and timely manner (Mueller et al., 2015) to generate cells with very different  
30 functions than the parent, all with the same genome (Wilmot et al., 1997). Many regulatory mechanisms  
31 coordinate this process, but much remains to be discovered about how it works (Zoller et al., 2018).  
32 Here, we explore how cell cycle regulation can control gene transcript expression timing and cell fate  
33 during tissue development.

34

35 The canonical view of the cell cycle is a timely stepwise process. Typically, the complete cell cycle is  
36 divided into four phases: first gap phase (G1), synthesis phase (S), second gap phase (G2) and mitotic  
37 phase (M). The length of each phase determines how much time a cell allocates for processes associated  
38 with growth and division. However, the amount of time that is spent in each phase frequently differs  
39 from one cell type to another within the same organism. For example, some cells experience fast cell  
40 cycles, especially in early embryogenesis. Organisms such as the fruit fly (*Drosophila melanogaster*)  
41 and the worm (*Caenorhabditis elegans*) exhibit cell cycle durations as short as 8-10 mins (Edgar et al.,  
42 1994; Foe, 1989). Cell cycle duration also changes over development (Figure 1 and Supplementary File  
43 1). For example, it increases in mouse (*Mus musculus*) brain development from an average of 8 hours at  
44 embryonic day 11 (E11) to an average of 18 hours by E17 (Furutachi et al., 2015; Takahashi et al.,  
45 1995a).

46

47 Interestingly, cell cycle duration can act as a transcriptional filter that constrains transcription (Rothe et  
48 al., 1992; Shermoen and O'Farrell, 1991). In particular, if the cell cycle progresses relatively fast,  
49 transcription of long genes will be interrupted. In typical cells, the gene transcription rate is between 1.4-  
50 3.6 kb per minute (Ardehali and Lis, 2009). Thus, an 8 minute cell cycle would only allow transcription  
51 of the shortest genes, on the order of 10 kb measured by genomic length, including introns and exons,  
52 whereas a 10 hour cell cycle would allow transcription of genes as long as a megabase on the genome.

53

54 Cell cycle dependent transcriptional filtering has been proposed to be important in cell fate control  
55 (Bryant and Gardiner, 2016; Swinburne and Silver, 2008). Most multicellular eukaryotic animals start

56 embryogenesis with short cell cycle durations and a limited transcription state (O’Farrell et al., 2004)  
57 with typically short zygotic transcripts (Heyn et al., 2014). These cells allocate the majority of their  
58 cycle time to S-phase (synthesis), where transcription is inhibited (Newport and Kirschner, 1982a), and  
59 M-phase (division), with little to no time for transcription in the gap phases. However, as the cell cycle  
60 slows down, time available for transcription increases (Edgar et al., 1986; Newport and Kirschner,  
61 1982a, 1982b), enabling longer genes to be transcribed (Djabrayan et al., 2019; Shermoen and O’Farrell,  
62 1991; Yuan et al., 2016).

63

64 We asked what effects cell cycle dependent transcriptional filtering may have over early multicellular  
65 organism development. Through extensive mathematical simulations of developmental cell lineages, we  
66 identify the novel and unexpected finding that a cell cycle dependent transcriptional filter can directly  
67 influence the generation of cell diversity and can provide fine-grained control of cell numbers and cell  
68 type ratios in a developing tissue. Our computational model operates at single-cell resolution, enabling  
69 comparison to single-cell RNA-seq data captured over development, supporting our model by showing  
70 similar trends. Our model also predicts genomic gene length distribution and gene transcript expression  
71 patterns that are consistent with a range of independent data. Our work provides new insight into how  
72 cell cycle parameters may be important regulators of cell type diversity over development.

73

## 74 **Results**

### 75 *Computational model of multicellular development*

76 We model multicellular development starting from a single totipotent cell that gives rise to many  
77 progeny, each with its own transcriptome (Figure 2). We developed a single cell resolution agent-based  
78 computational model to simulate this process (see materials and methods). Each cell behaves according  
79 to a set of rules, and cells are influenced solely by intrinsic factors (e.g. number of genes in the genome,  
80 gene length, transcript levels and transcription rate). We intentionally start with a simple set of rules,  
81 adding more rules as needed to test specific mechanisms. Our analysis is limited to pre-mRNA transcript  
82 expression and we do not consider other gene expression-related factors, such as splicing, translation or  
83 gene-gene interactions. We also omit external cues (e.g. intercellular signaling or environmental  
84 gradients) to focus on the effects of intrinsic factors.

85

86 In our model, each cell is characterised by a fixed genome containing a set of  $G$  genes  
87 ( $\text{gene}_1, \text{gene}_2, \dots, \text{gene}_G$ ), shown in Figure 2A. Each  $\text{gene}_i$  is defined by a length,  $L_i$  (in kb), and in all  
88 our simulations each gene is assigned a different length ( $L_1 < L_2 < \dots < L_G$ ). Since each  $\text{gene}_i$  has a unique  
89 length,  $L_i$ , we label genes by their length ( $\text{gene}_i^{L_i} = \text{gene}^{L_i}$ ; e.g.  $\text{gene}^3$  is a gene of length 3 kb). We  
90 assume transcription time for  $\text{gene}_i$  is directly proportional to its length,  $L_i$ . In the model, each  $\text{cell}_j$  is  
91 initialized with a cell cycle duration ( $\Gamma_{\text{cell}}$ ) which represents the total time available for gene  
92 transcription (see materials and methods). For example, we can initialise  $\text{cell}_1$  with a three-gene genome  
93 ( $\text{gene}^1, \text{gene}^2, \text{gene}^3$ ), where  $L = (1 \text{ kb}, 2 \text{ kb}, 3 \text{ kb})$  and a cell cycle duration  $\Gamma_1$  of 1 hr. We fix  
94 transcription rate,  $\lambda$ , to 1 kb/hr for all genes (though this assumption can be relaxed without changing  
95 our results, Figure 3 and 3-figure supplement 1). As transcription progresses for all genes,  $\text{cell}_1$  will only  
96 express  $\text{gene}^1$ . Increasing cell cycle duration,  $\Gamma_{\text{cell}}$ , will allocate more time for transcription, allowing  
97 longer genes to be transcribed. For example, if we initialise  $\text{cell}_2$  with a cell cycle duration  $\Gamma_2=3$  hrs,  $\text{cell}_2$   
98 will express all three genes, with time to make three copies of  $\text{gene}^1$  (Figure 2B). We assume RNA  
99 polymerase II re-initiation occurs along the gene, a distance  $\Omega$  apart (Figure 3-figure supplement 1).

100

101 Once transcription is complete, the cell enters M-phase, during which it divides, and expressed  
102 transcripts are randomly distributed to the two progeny cells (Figure 2C). This is the main stochastic  
103 component in our model. We assume that transcription begins anew at the start of the cell cycle (i.e. all  
104 transcripts from a gene that can't be finished in one cycle are eliminated), modeling the known  
105 degradation of incomplete nascent transcripts in M-phase (Shermoen and O'Farrell, 1991). Relaxing our  
106 assumption to include parental transcript inheritance and decay (Sharova et al., 2009), where a  
107 proportion of inherited parental transcripts remain after each cell division does not change our overall  
108 results (Figure 3-figure supplement 2). All individual cells and their transcriptomes are tracked over the  
109 course of the simulation, enabling single cell resolution analysis. Transcriptomes are stored as vectors  
110 containing the total number of transcripts per gene. For instance,  $\text{cell}_2$  may have a transcriptome of  
111  $(3,1,1)$ , indicating that three genes are expressed, with  $\text{gene}^1$  expressed at three transcripts per cell and  
112 the other two genes expressed at one transcript per cell (Figure 2D).

113

114 *Model prediction: Cell cycle duration influences transcript count - short genes generate more*  
115 *transcripts than longer genes*

116 We begin by examining how a transcriptional filter impacts transcript counts, as controlled by cell cycle  
117 duration. Shorter cell cycles will interrupt long gene transcription resulting in relatively high expression  
118 of short gene transcripts and low expression of long gene transcripts. Our computational simulations  
119 generate this expected pattern (Figure 3A). Each simulated cell transcriptome is divided into three bins  
120 containing short, medium and long genes and then each bin is summarized with an average transcript  
121 count. In simulations, bins with short genes exhibit the highest average transcript count levels. As cell  
122 cycle duration increases, more cells show an increase in transcript count of longer genes; the trend is  
123 consistent for various genome sizes and gene length distributions (Figure 3A and 3-figure supplement  
124 3).

125

126 Single cell RNA-seq (scRNA-seq) has recently been used to profile mRNA expression of thousands of  
127 cells for one cell type (microglia) across multiple species (Geirsdottir et al., 2019) or for multiple  
128 embryonic developmental time points in one species, such as *Xenopus tropicalis* (Briggs et al., 2018)  
129 and *Danio rerio* (Kimmel et al., 1995; Wagner et al., 2018), or tissue, such as mouse neural cortex  
130 (Yuzwa et al., 2017). We analyzed these data in the same manner as our model (Figure 3B and 3-figure  
131 supplement 4) and found that, in general, short genes have a higher mRNA expression level than longer  
132 genes within a cell. Thus, gene mRNA expression patterns from a range of scRNA-seq data sets,  
133 including developmental time courses, are compatible with our model prediction.

134

135 *Model prediction: Cell cycle duration can control cell diversity*

136 We next asked how three major model parameters (cell cycle duration, maximum gene length, and  
137 number of genes in the genome) can influence the generation and control of cell diversity observed  
138 during normal multicellular development. We conducted simulations for a single cell division step for  
139 simplicity, but these were repeated thousands of times to model cell population effects. We compute cell  
140 diversity in two ways; first, as the number of distinct transcriptomes in the cell population  
141 (transcriptome diversity); and second, as the number of distinct transcriptomic clusters, as defined using  
142 standard single cell transcriptomic analysis techniques (Satija et al., 2015) (see methods). Both measures  
143 model real cell types and states that are distinguished by their transcriptomes, with transcriptome  
144 diversity as an upper bound on cell type number, and cluster number approximating a lower bound. We  
145 first ran simulations with an active transcriptional filter by varying only the cell cycle duration,  $\Gamma$ , for a  
146 genome with 10 genes, with genes ranging in size from 1 to 10 kb, such that it satisfies  $L_1 = 1 \leq$

147 ... $\Gamma$ ...  $\leq L_G = 10$ . Short cell cycle duration parameter values generated a homogenous population of  
148 cells because only short transcripts can be transcribed. As cell cycle duration was increased,  
149 transcriptome diversity also increased. Longer cell cycle duration values generated heterogeneous  
150 populations, because a range of transcripts can be expressed (Figure 4A, brown line). Interestingly, cell  
151 cluster diversity peaks at intermediate cell cycle duration parameter values (Figure 4B, brown line; 4C),  
152 because new genes are introduced with increasing cell cycle lengths, but eventually long cell cycles  
153 provide sufficient time for cells to make all transcripts, which leads to reduced variance between the  
154 progeny. We next repeat this experiment by turning off the transcriptional filter by reducing the  
155 maximum gene length such that  $L_G < \Gamma$ , (Figure 4A,B, blue line). In this case, cell diversity can be  
156 generated, but it quickly saturates (Figure 4B, blue line), as all transcripts are expressed, given a cycle  
157 duration allowing the expression of the longest transcript. Thus, while cellular diversity can be generated  
158 with an active or inactive transcriptional filter, diversity is more easily controlled by cell cycle duration  
159 when the transcriptional filter is active.

160

161 In general, transcriptome diversity increases as a function of cell cycle duration ( $\Gamma$ ), transcription rate  
162 ( $\lambda$ ), and number of genes in the genome ( $G$ ). In particular, transcriptome diversity =  $n \prod_{i=1}^G (T/L_i + 1)$ ,  
163 where  $n$  is the genome ploidy level,  $T = \sum_{a=0}^{L_i} f(a)$ ,  $\forall f(a) \geq 0$ ,  $f(a) = \Gamma * \lambda - \frac{a\Omega}{\lambda}$  (i.e. the maximum  
164 transcribed gene length,  $T$ , is restricted by the product of cell cycle duration,  $\Gamma$ , transcription rate,  $\lambda$  and  
165 RNA polymerase II re-initiation,  $\Omega$ ), and  $L_i$  is the length of gene $_i$ . This analytical solution of cell  
166 transcriptome diversity was validated by comparing it to simulations (Supplementary File 2). While the  
167 number of genes and their length distribution can change over the course of evolution, these numbers are  
168 constant for a given species, and transcription rate is likely highly constrained (Ardehali and Lis, 2009),  
169 leaving only cell cycle duration as a controllable parameter of cell diversity during development,  
170 according to our model.

171

172 *Model prediction: Varying cell cycle duration over developmental time controls tissue cell proportions*  
173 *and number*

174 During multicellular organism development, it is essential to generate the correct numbers of cells and  
175 cell types. Cell cycle duration changes dramatically during development, generally starting out fast to  
176 generate cells quickly and slowing down over time as the organism matures (Supplementary File 1 and

177 Figure 1) (Farrell and O'Farrell, 2014; O'Farrell et al., 2004). Clearly, cells with short cell cycles  
178 generate more progeny compared to those with longer cell cycles. However, we propose that a trade-off  
179 exists, balancing the generation of diversity (longer cell cycle durations) with the fast generation of cells  
180 (shorter cell cycle durations; **Figure 4**Figure 4B). To study this trade-off, we simulated cell propagation  
181 under a “mixed lineage” scenario where, after the first division, one child cell and its progeny maintains  
182 a constant cell cycle duration ( $\Gamma_1 = 1$  hr) and the second child cell and its progeny maintains an equal or  
183 longer constant cell cycle duration over a lineage with 20 cell division events (Figure 5, grey and blue  
184 lineages, respectively). We initialize the starting cell with no prior transcripts (naïve theoretical state)  
185 and a genome containing five genes ranging from length one to two kb (gene<sup>1</sup>, gene<sup>1.25</sup>, gene<sup>1.5</sup>, gene<sup>1.75</sup>,  
186 gene<sup>2</sup>), setting cell cycle duration in the second lineage to range between one and two, controlling the  
187 transcriptional filter threshold in this lineage only. We considered three scenarios: 1) both cell lineages  
188 cycle at the same rate (Fast-Fast, Figure 5A); 2) the first (blue) lineage is slower than the second (gray)  
189 (Slow-Fast, Figure 5B); 3) both slow and fast lineages divide asymmetrically, producing one slow and  
190 one fast cell (Slow-Fast, Figure 5C).

191

192 In the simulation where both cell lineages cycle at the same rate (Figure 5A), both lineages generate the  
193 same number of progeny with the same level of diversity (Figure 5D). When cell cycle duration for the  
194 second (blue) lineage is increased across simulations (Figure 5E), the transcriptional filter acts to  
195 generate more diverse progeny, but with fewer cell numbers and progressively smaller population  
196 proportions due to the slower cell cycle (Figure 5E, blue bars). Meanwhile, the short cell cycle lineage  
197 maintains a steady, low level of diversity generation (Figure 5E, gray bars). When a fast cell can divide  
198 asymmetrically, generating one slow and one fast cell at each division, the number of slow cells in the  
199 population can increase, however this comes with a reduction of the number of fast cells in the  
200 population (Figure 5F). Thus, our simulations show how the cell cycle duration parameter can impose a  
201 trade-off between cell proportion and diversity generation, and mixing lineages with different cell cycle  
202 durations can generate mixed cell populations each with their own diversity levels.

203

204 To more faithfully simulate multicellular animal development where cell cycle duration increases over  
205 time, we next allowed progeny cells to differ in their cell cycle duration from their parents in each  
206 generation (Figure 6A). Increasing the cell cycle duration over time reveals that cell cycle dynamics can  
207 alter the number and proportions of cells as a function of time (cell generations; Figure 6B and 6-figure

208 supplement 1). To compare with a real system, we explore single cell transcriptomics data measured  
209 over four timepoints of mouse cortex development (Yuzwa et al., 2017). Average cell cycle duration  
210 over mouse neural cortex development is known to increase from 8 hours at embryonic day 11 (E11) to  
211 an average of 18 hours by E17 (Furutachi et al., 2015; Takahashi et al., 1995a). Within this range,  
212 progenitor cells are, in general, expected to be characterized by fast cycles with short G1 duration and  
213 neurons by slower cell cycles with long G1 duration (Calegari et al., 2005). In our analysis of the mouse  
214 cortex scRNA-seq data, we find genes with increasing transcript expression across the time course  
215 (E11.5 < E13.5 < E15.5 < E17.5) are associated with neural developmental (maturing cell) pathways  
216 whereas the genes with decreasing transcript expression across time (E11.5 > E13.5 > E15.5 > E17.5) are  
217 associated with transcription and proliferation (stem and progenitor cell) pathways (Figure 6-figure  
218 supplement 2). Furthermore, we observe an overall pattern of an increasing number of cells with long  
219 cell cycle duration and a decrease in fast cycling cells (Figure 6C) following the same general trend as  
220 observed in our simulations (Figure 6A), supporting the idea that cell cycle duration dynamics could  
221 play a role in controlling cell proportions and cell diversity in a developing tissue.

222

223

224 *Hypothesis: A cell cycle dependent transcriptional filter may help control cell proportion and diversity*  
225 *in tissue development*

226 Our theoretical model and agreement with general trends in scRNA-seq data supports the hypothesis that  
227 a cell cycle dependent transcriptional filter has the potential to control cell proportion and diversity in  
228 tissue development. In this section, we use the model to generate specific questions that can be checked  
229 in real data, further supporting our model.

230

231 *Organismal Level*

232 Our model suggests that organisms with long genes will need to maintain long cell cycle durations  
233 during development. Cell cycle duration measurements are not widely available which makes directly  
234 testing this hypothesis difficult. Instead, we explored related questions. We started by asking if  
235 organisms with longer genes would also take longer to develop. We analyze gene length distributions for  
236 twelve genomes spanning budding yeast to human with a diverse range of developmental durations, as  
237 shown in Figure 7 and Supplementary File 3 (Gilbert and Barresi, 2016; Jukam et al., 2017). Non-  
238 mammalian species that we analyze are relatively fast developing, ranging from approximately two

239 hours (e.g. *Saccharomyces cerevisiae*) to a few days (e.g. *Xenopus tropicalis* and *Danio rerio*), while  
240 mammals (*Mus musculus*, *Sus scrofa*, *Macaca mulatta*, and *Homo sapiens*) are relatively slow  
241 developing (20, 114, 168 and 280 days, respectively, Supplementary File 3). These species also have  
242 different gene length distributions; to illustrate this quantitatively, using a typical transcription rate of  
243 1.5 kb/min (Ardehali and Lis, 2009), a cell cycle duration of 1 hr can exclude up to 20% total genes  
244 found in relatively slow developers and not exclude any genes in fast developers (Figure 7A). In  
245 agreement with our hypothesis, the gene length distribution is narrower and left shifted (shorter genes)  
246 for fast developers and broader and right shifted (longer genes) for slower developing species.  
247 Interestingly, one seeming exception to the overall gene length distribution trend in multicellular  
248 animals is the tunicate *Oikopleura dioica*, which has relatively short genes, but also has a rapid gestation  
249 period of four hours to hatched tadpole (approximately twice as fast as *C. elegans* and six times faster  
250 than *D. melanogaster*), supporting our analysis. Broadening this analysis to 101 species, we again find  
251 an association ( $r=0.74$ ) between estimated developmental time and median gene length (Figure 7B and  
252 7-figure supplement 1).

253

254 Our model suggests that short genes will be enriched in pathways that can function independently from  
255 long genes, and that long genes may be enriched in pathways related to mature, differentiated cell types  
256 with slower cell cycles (Figure 8). We examined the functions of short and long genes by conducting a  
257 pathway enrichment analysis on all genes in a genome ranked by their length. In the human genome, the  
258 longest genes are enriched in processes such as, neural development, muscle control, cytoskeleton, cell  
259 polarity and extracellular matrix and the shortest genes are enriched in processes that presumably need  
260 to be quickly activated transcriptionally (e.g. immune, translation, and environment sensing; Figure 8-  
261 figure supplement 1). We performed a similar pathway analysis for human (Figure 8 and 8-figure  
262 supplement 2-3) and 12 other species (Figure 9) and found general agreement with these patterns,  
263 finding the longest genes (gene length in the 95% quantile) enriched for genes involved in mature cell  
264 related processes (e.g. brain and muscle development), whereas the shortest genes (gene length in the  
265 5% quantile) are enriched for genes involved in core processes (e.g. immune, RNA processing, and  
266 olfactory receptors).

267

### 268 *Spatial Level*

269 Within an organism, cell cycle duration and transcript expression vary across many factors, including  
270 spatially. We hypothesize that spatial transcript expression patterns can be initially organized by gene

271 length. To explore this, we study the developing fruit fly embryo (*D. melanogaster*) where the average  
272 cell cycle rates differ spatially (Foe, 1989). At the onset of cell cycle 14, cells in different embryo  
273 regions start to divide at different rates, caused by an increase in their gap phase length, varying from 30  
274 mins to 170 mins (Foe, 1989; Foe and Alberts, 1983). Cell cycle duration lengthening is spatially  
275 organized, with anterior regions dividing faster than posterior regions, with the mid-ventral region being  
276 the slowest (Figure 10). The embryo also exhibits spatial segregation patterns due to Hoxd gene family  
277 transcript expression (Mallo and Alonso, 2013). Overlaying the spatial patterns of hox gene family  
278 transcript expression and cell cycle duration obtained from independent studies, we observe that fast  
279 cycling regions express the shortest hox genes (Dfd 10.6kb, lab 17.2kb) and slow cycling regions  
280 express the longest hox genes (Ubx 77.8kb and Antp 103.0kb )(Foe, 1989; Lemons and McGinnis,  
281 2006) in agreement with our model.

282

## 283 **Discussion**

284 How cellular processes support the carefully orchestrated timing of tissue development that results in a  
285 viable multicellular organism is still unclear. While a combination of many potential cell autonomous  
286 and non-autonomous mechanisms, such as cytoplasmic molecules and gradients, cell-cell  
287 communication, microenvironment signals, and effective cell size (Edgar et al., 1986; Mukherjee et al.,  
288 2020; Tabansky et al., 2013; Yoon et al., 2017), are likely important, one hypothesis is that gene length  
289 can be used as a mechanism to control transcription time in this process (Artieri and Fraser, 2014; Gubb,  
290 1986; Keane and Seoighe, 2016; Swinburne et al., 2008). Bryant and Gardiner further hypothesize that  
291 cell cycle duration may play a role in filtering genes that influence pattern formation and regeneration  
292 (Bryant and Gardiner, 2018; Ohsugi et al., 1997), as cell cycle lengthens over development (Figure 1  
293 and Supplementary File 1) (Foe, 1989; Foe and Alberts, 1983; Newport and Kirschner, 1982b;  
294 Takahashi et al., 1995b). Early experiments using embryos suggested that cell cycle duration has a role  
295 in transcription initiation, however these experiments lacked the temporal resolution necessary to  
296 dissociate the effects of cell cycle duration and transcriptional control from other mechanisms (Edgar et  
297 al., 1986, 1994; Kimelman et al., 1987; Newport and Kirschner, 1982b, 1982a). It is also well known  
298 that cell cycle length changes can control cell fate and development (Coronado et al., 2013; Mummery et  
299 al., 1987; Pauklin and Vallier, 2013; Singh et al., 2013), however, this has remained observational and  
300 not linked to a mechanism. To help address these limitations, we developed an *in silico* cell growth  
301 model to directly study the relationship between cell cycle duration and gene transcription in a

302 developmental context. The new discovery we make is that a transcriptional filter can be controlled by  
303 cell cycle duration and used to simultaneously control the generation of cell diversity, the overall cell  
304 growth rate and cellular proportions during development (defining an emergent property of our  
305 computational model – see Appendix). Genomic information (gene number and gene length distribution)  
306 and cell cycle duration are critical parameters in this model. Across evolutionary time scales, cell  
307 diversity can be achieved by altering gene length (Keane and Seoighe, 2016), however, in terms of  
308 developmental time scales, we propose that cell cycle duration is an important factor that may control  
309 cell diversity and proportions within a tissue.

310

311 We predict that increasing the gene length distribution across a genome over evolution can provide more  
312 cell cycle dependent transcriptional control in a developing system, leading to increased cellular  
313 diversity. Examining a range of genomes and associated data provides support for this novel idea. We  
314 observe that fast developing organisms have shorter median gene lengths relative to the broad  
315 distributions, including many long genes, exhibited by slow developers (mammals). This aspect of  
316 genome structure may help explain the observed rates of cell diversity and organism complexity, as  
317 measured by number of different cell types, over a wide range of species, Figure 7-figure supplement 1  
318 (Valentine et al., 1994; Vogel and Chothia, 2006).

319

320 While we hypothesize that a cell cycle dependent transcriptional filter is a fundamental regulatory  
321 mechanism operating during development (because gene length is fixed in the genome and transcription  
322 rate is expected to lie in a narrow range), multiple other regulatory mechanisms could modulate its  
323 effects. Furthermore, exploring these mechanism may even result in similar conclusions, as it can be  
324 evolutionary advantageous to have multiple paths to the same outcome; These include, but are not  
325 limited to, silencing or deactivating genes, gene regulatory networks, blocking gene clusters, e.g. Hoxd  
326 (Rodríguez-Carballo et al., 2019) changing the transcription or re-initiation rate of RNA polymerase II  
327 (Figure 3-figure supplement 1), or inheriting long transcripts maternally at the zygote stage (Figure 3-  
328 figure supplement 2). Our current model only explores the effects of transcription and re-initiation rates  
329 of RNA polymerase II, mRNA transcript degradation rates, and maternally introduced transcripts. For  
330 the latter mechanism, we expect longer transcripts to be major contributors during the early maternal  
331 phase (Jukam et al., 2017), which agrees with zebrafish (*D. rerio*) experiments showing that maternal  
332 transcripts are longer and have evolutionary conserved functions (Heyn et al., 2014). Indeed, if we add

333 maternal transcript inheritance to our model, we see the same pattern of a small number of long  
334 transcripts present early, as expected (Figure 3-figure supplement 2). Future work would entail curating  
335 experimental data about more regulatory mechanisms in cell systems and testing their association with  
336 cell cycle duration.

337

338 Our analysis raises interesting directions for future work. We focus on development, but transcriptional  
339 filtering may be important in any process involving cell cycle dynamics, such as regeneration (Bryant  
340 and Gardiner, 2018), wound repair, immune activation and cancer. We must also more carefully  
341 consider cell cycle phase, as transcription mainly occurs in the gap phases (Bertoli et al., 2013; Newport  
342 and Kirschner, 1982b). Experiments indicate that a cell will have different fates depending on its phase  
343 (Dalton, 2013; Pauklin and Vallier, 2013; Vallier, 2015). This agrees with our model, as a cell at the  
344 start of its cell cycle will have a different transcriptome in comparison to the end of the cell cycle.  
345 Induced pluripotent cell state is also associated with cell cycle phases (Dalton, 2015) and efficient  
346 reprogramming is only seen in cell subsets with fast cell cycles (Guo et al., 2014). Our model could  
347 explain these observations, as slower cycling cells could express long genes that push a cell to  
348 differentiate rather than reprogram. However, our model is limited to total transcription duration for  
349 interphase (G1, S and G2), thus a future direction would be to explore different durations for each cell  
350 cycle phase. Collecting more experimental data about cell phase in developing systems will help explore  
351 these effects. Further, it will be important to explore how cell cycle duration is controlled. Molecular  
352 mechanisms of cell cycle and cell size (Liu et al., 2018) control could be added to our model to provide  
353 a more biochemically realistic perspective on this topic. Ultimately, a better appreciation of the effects  
354 of cell cycle dynamics will help improve our understanding of a cell's decision-making process during  
355 differentiation, and may prove useful for the advancement of tools to control development, regeneration  
356 and cancer. Finally, it is important to note that we have not provided experimental model support, only  
357 analyses that do not disagree with model predictions. We have also not proven the generality of the  
358 results across species. However, we hope the hypotheses we explore here motivate new experimental  
359 studies to directly test the validity and generality of our model.

360

## 361 **Materials and Methods**

### 362 *Mathematical model*

363 Our mathematical model is agent and rule-based. A single cell behaves and interacts according to a fixed  
364 set of rules. Our major rule involves a gene-length mechanism, where each cell is defined by a genome  
365 and a cell cycle duration. The cell cycle duration determines which gene transcripts are expressed within  
366 the cell, based on the transcription rate. All decisions are based on a cell's autonomous information and  
367 we omit external factors. We deliberately choose to consider this simple baseline setup to clarify the  
368 contribution of cell cycle duration to overall cell population growth.

369  
370 Each cell is defined by a genome  $G$  (containing a set of genes), cell cycle duration in hours and the  
371 transcripts inherited or recently transcribed. In the genome, each gene is defined by a length,  $\text{gene}^{\text{Length}}$ .  
372 For example, in a genome with three genes,  $(\text{gene}^1, \text{gene}^2, \text{gene}^3)$  represents genes of length 1, 2, 3 kb,  
373 respectively.

374  
375 Each cell can divide and make two progeny cells. This process can continue many times to simulate the  
376 growth of a cell population and we keep track of the entire simulated cell lineage. For each cell division  
377 (one time step in the simulation): each  $\text{Cell}_i$  will transcribe its genes based on the time available, defined  
378 by the cell cycle duration. We assume the time it takes to transcribe a gene depends on its length and a  
379 fixed transcription rate, although a simplification, there are examples where this occurs, for instance the  
380 human dystrophin gene is 2241765bp long and takes about 16 hrs to transcribe (Tennyson et al., 1995).  
381 Once a cell cycle is finished, the cell divides. When cells are synchronized, the first cell division  $T = \Gamma_i$ .  
382 When the cells are asynchronized then the algorithm identifies the time allocated as the shortest cell  
383 cycle duration in the population as the time step and each cell division will have a different duration. In  
384 this case, we keep track of the exact duration such that cells with short cell cycles, for example  $\Gamma = 1$  hr,  
385 will register 10 divisions in 10 hrs while cells with long cell cycles, for example  $\Gamma = 10$  hrs, will register 1  
386 division in over the same time. We limited the model to two modes of division, symmetric (where the  
387 cell gives rise to identical cells, e.g. Figure 5A) and asymmetric (where the cell gives rise to a fast and  
388 slow cell, e.g. Figure 5C). We do not consider mechanisms that reduce cell numbers (cell death). For  
389 certain experiments (e.g. Figure 6), the cell cycle duration for each progeny is allowed to diverge from  
390 the parental duration using a monotonic function (increasing or decreasing) and a stochastic variable  
391 based on a Gaussian distribution with a mean equal to  $\Gamma_i$  (parental cell cycle duration). This models a  
392 more realistic noisy distribution of cell cycle durations in the simulated cell population. The cell cycle

393 and division rules are repeated for all cells in the population until a set number of cell divisions have  
394 been reached.

395

396 During a cycle, each cell contains a certain number of transcripts. The number of transcripts for each  
397 gene is calculated by a function of cell cycle duration,  $\Gamma$ , transcription rate,  $\lambda$ , re-initiation distance,  $\Omega$ ,

398 and gene length,  $L$ :  $\sum_{a=0}^{\frac{\text{gene}^{L_i}}{\Omega}-1} \Gamma * \lambda - \frac{a\Omega}{\lambda}$ . If the cell does not divide, then the number of transcripts

399 reflects the current cell cycle phase, which is computed and stored. If the cell can divide within the time  
400  $T=(\Gamma * \lambda)$ , then it will randomly, according to a uniform distribution, assign its transcripts between its

401 two progeny cells. Typically simulations were conducted with  $\lambda = 1$ , simplifying the analysis to

402  $(\Gamma - a\Omega)/\text{gene}^{L_i}$ , however, we also explored the effects of transcript re-initiation and transcription rate  
403 on the system as shown in Figure 3-figure supplement 1.

404

405 Our model tracks single cells, with each cell identified by a transcriptome and cell cycle duration. The

406 transcriptome data resemble a single cell RNA-seq matrix to aid comparison between simulation and

407 experimental data. We allow cells without any transcripts e.g. (0,0,0) to exist – due to the low numbers

408 of genes considered in our simplified model and results, and that parental transcripts are distributed

409 between progeny, there is a probability of  $2/(\text{the total number of transcripts})$  that all the transcripts will

410 end up in only one of the new cells, leaving the other one empty (Zhou et al., 2011). Theoretically we

411 have no reason to omit these cells and they may represent the most naïve theoretical state of a cell

412 without any prior information. Early embryos, such as in xenopus stages that lack zygotic transcription,

413 may be similar real systems to such a state (Newport and Kirschner, 1982b).

414

415 Parameters tracked for each cell<sub>i</sub>= (number of divisions, current cell cycle phase, current time in cell

416 cycle, length until next division, relative time passed, total cell cycle duration, transcriptome list, cell

417 name, and lineage history). All cells are set with the same genome, ploidy level and RNA polymerase II

418 transcription rate and RNA polymerase II re-initiation distance.

419

420 Our model was developed and simulated using Mathematica (Wolfram-Research, 2017).

421

422 ***Quantification and statistical analysis***

423 *Gene length analysis*

424 All protein coding genes were downloaded from Ensembl genome database version 95 or 100 (Yates et  
425 al., 2016) using the R (3.6.1) Biomart package version 3.10 (Durinck et al., 2005). The length of each  
426 gene was calculated using start\_position and end\_position for each gene, as extracted from the Ensembl  
427 database (Yates et al., 2016).

428

429 *Single cell analysis pipeline*

430 Simulated data sets were pre-processed and clustered in R using the standard workflow implemented in  
431 the Seurat package version 3.1.2 (Satija et al., 2015). We used default parameters unless otherwise  
432 stated. Data were log-normalized and scaled before principal component analysis (PCA) was used to  
433 reduce the dimensionality of each data set. Due to the small number of simulated genes in our  
434 experiments, the maximum number of PCs (one fewer than the number of genes  $\text{dims}=1:3$ ) was  
435 calculated and used in clustering. FindVariableFeatures was used with loess.span set to 0.3 unless the  
436 number of genes were less than 5, then (0.4, 0.7 and 1 was used for simulations with 4, 3 and 2 genes,  
437 respectively). Cells were clustered using a shared nearest neighbor (SNN)-based ‘Louvain’ algorithm  
438 implemented in Seurat with reduction set as “pca”. The clustering resolution was set to 1 for all  
439 experiments, and all calculated PCs were used in the downstream clustering process using the Louvain  
440 algorithm accessed via Seurat. Data was visualized with t-SNE after clustering.

441

442 *Developmental time curation*

443 Estimated developmental time was curated from encyclopedia of life or PubMed accessible articles  
444 (Supplementary File 3). We used gestation time for mammals and hatching time for species who lay  
445 eggs (since it is difficult to accurately define a comparative stage for all species). Species were grouped  
446 based on their taxonomic class and their developmental time was estimated by calculating the average  
447 number of days from zygote to birth or hatching.

448

449 *Pathway Enrichment Analysis*

450 We used Gene Set Enrichment Algorithm (GSEA version 4.0.2), in pre-ranked analysis mode, to  
451 identify pathways enriched among all genes in a genome ranked by gene length (Subramanian et al.,  
452 2005). Gene ranks started at  $(\text{number of genes})/2$  to its negative equivalent and were normalised such  
453 that we generated a ranked list from 1 to -1, with 1 specifying the shortest gene and -1 the longest. The

454 ranked gene length list was analyzed for pathway enrichment GSEA with parameters set to 1000 gene  
455 set permutations and gene set size between 15 and 200. Pathways used for the analysis were from Gene  
456 Ontology biological process (Ashburner et al., 2000), MSigDB c2 (Ashburner et al., 2000),  
457 WikiPathways (Slenter et al., 2017), Panther (Mi et al., 2005), Reactome (Croft et al., 2011), NetPath  
458 (Kandasamy et al., 2010), and Pathway Interaction database (Schaefer et al., 2009) downloaded from the  
459 Bader lab pathway resource (<http://baderlab.org/GeneSets>). An enrichment map, created using the  
460 EnrichmentMap Cytoscape app version 3.3.0 (Merico et al., 2010), was generated using Cytoscape  
461 (version 3.8.0) using only enriched pathways with p value of 0.05 and FDR threshold of 0.01 (Reimand  
462 et al., 2019). Cross talk (shared genes) between pathways was filtered by Jaccard similarity greater than  
463 0.25. Pathways were automatically summarized using the AutoAnnotate App to assign pathways to  
464 themes (Kucera et al., 2016). Themes were further summarized by grouping pathways into more general  
465 themes with a mixture of automatic classification using key words and manual identification.

466

#### 467 *Pathway word cloud analysis*

468 All Gene Ontology pathway (GO biological processes) downloaded from the Ensembl genome database,  
469 version 100, (Yates et al., 2016) using the R Biomart package version 3.5 (Durinck et al., 2005). We  
470 restricted analysis to pathways with at least three genes. We grouped genes based on their gene length  
471 (see *Gene length analysis* for details) and identified the pathways associated with each gene. The  
472 description of each pathway was collected and the frequency of each word within the pathway name was  
473 calculated. We defined themes (Supplementary File 5-6) for all *Homo sapiens* available pathways (using  
474 only GO biological processes). Common, generic and uniformly distributed themes (such as cellular-  
475 response, metabolic-biosynthesis, protein-processes, signalling, and transcription) were manually  
476 removed from the list. The frequencies were visualised as word clouds using Mathematica (Wolfram-  
477 Research, 2017).

478

#### 479 *Data and code availability*

480 Our simulation code is available at [https://github.com/BaderLab/Cell\\_Cycle\\_Theory](https://github.com/BaderLab/Cell_Cycle_Theory)

481

#### 482 *Key Resources Table*

<b>Key Resources Table</b>
----------------------------

Reagent type (species) or resource	Designation	Source or reference	Identifiers	Additional information
Software, algorithm	(Wolfram-Research, 2017)			Mathematica (Wolfram Research Inc, Mathematica Versions 11.0-12, Champlain, IL, 2017) <a href="http://www.wolfram.com/mathematica/">http://www.wolfram.com/mathematica/</a>
Software, algorithm		This paper		Cell developmental model <a href="https://github.com/BaderLab/Cell_Cycle_Theory">https://github.com/BaderLab/Cell_Cycle_Theory</a>
Software, algorithm	(Satija et al., 2015)	PMID: 25867923		Seurat (3.1.2) <a href="https://satijalab.org/seurat/">https://satijalab.org/seurat/</a>
Software, algorithm	(Yates et al., 2016)	PMID: 26687719		Ensembl (95) and (100) <a href="https://useast.ensembl.org/index.html">https://useast.ensembl.org/index.html</a>
Software, algorithm	(Ashburner et al., 2000)	PMID: 10802651		Gene Ontology <a href="http://geneontology.org/">http://geneontology.org/</a>
Software, algorithm	(Durinck et al., 2005)	PMID: 16082012		BioMart (3.10) <a href="http://useast.ensembl.org/biomart/martview/">http://useast.ensembl.org/biomart/martview/</a>
Software, algorithm	(Merico et al., 2010)	PMID: 21085593		Enrichment Map software (3.3.0) <a href="https://www.baderlab.org/Software/EnrichmentMap">https://www.baderlab.org/Software/EnrichmentMap</a>
Software, algorithm	(Kucera et al., 2016)	PMID: 14597658		AutoAnnotate App <a href="https://baderlab.org/Software/AutoAnnotate">https://baderlab.org/Software/AutoAnnotate</a>
Software, algorithm	(Shannon et al., 2003)	PMID: 14597658		Cytoscape (3.8.0) <a href="https://cytoscape.org/">https://cytoscape.org/</a>

Software, algorithm	(Reimand et al., 2019)	PMID: 30664679		Baderlab pathway resource (updated June 01,2020) <a href="http://download.baderlab.org/EM_Genesets/">http://download.baderlab.org/EM_Genesets/</a>
------------------------	---------------------------	-------------------	--	--

483

484 **Appendix**

485

486 Why is cell cycle duration changing?

487

488 While defining a general mathematical representation of cell cycle kinetics for a developing system, we  
 489 assembled available cell cycle length measurements from published studies for various species and  
 490 tissues. Figure 1 shows measurements obtained from *Mus musculus*. For other data see Supplementary  
 491 File 1. The data motivated us to ask “why is cell cycle duration changing over development?” and  
 492 propose that changes in cell cycle duration can be used to guide the progression of cell development.

493

494 Theoretically we devised a simple model that can test this idea by assuming:

- 495 • Cell cycle duration can change across developmental time
- 496 • Gene length distribution is constant among all cells in the same organism, such that we can  
 497 denote the length by L
- 498 • The difference in cell cycle can affect the time a cell spends transcribing genes
- 499 • All active genes are transcribed and transcription rate is constant in a cell

500

501 The novel aspect of our work is the proposal that a cell cycle dependent transcriptional filter can control  
 502 cellular diversity within a tissue over development. However, some of the concepts that we build on are  
 503 known and are recognized in the community to varying degrees. We bring these together for the first  
 504 time to support the model and generate predictions. In particular, we list these concepts below and  
 505 clarify our novel contribution.

506

507 Prior contributions:

- 508 • Cell cycle lengthens over development
  - 509 ○ “The *Xenopus* embryo undergoes 12 rapid synchronous cleavages followed by a period  
 510 of slower asynchronous divisions more typical of somatic cells.” after which the cell  
 511 cycle duration continues to increase. (Newport and Kirschner, 1982)  
 512 <https://pubmed.ncbi.nlm.nih.gov/6183003>

- 513           ○ In *D. melanogaster* early development, the first 10 cell divisions are fast and  
514           synchronous, then progressively increase in cell cycle duration. (Foe, 1989; Foe and  
515           Alberts, 1983)  
516           <https://pubmed.ncbi.nlm.nih.gov/6411748>  
517           <https://pubmed.ncbi.nlm.nih.gov/2516798>
- 518           ○ The cell cycle lengthens during *Mus musculus* brain development. “The length of the cell  
519           cycle increases from 8.1 to 18.4 hr, which corresponds to a sequence of 11 integer cell  
520           cycles over the course of neuronal cytotogenesis in mice. The increase in the length of the  
521           cell cycle is due essentially to a fourfold increase in the length of G1 phase which is the  
522           only phase of the cell cycle which varies systematically.” (Takahashi et al., 1995)  
523           <https://pubmed.ncbi.nlm.nih.gov/7666188>
- 524           ○ We also compiled cell cycle duration from 25 papers, which clearly support this  
525           statement (see Figure 1 and Supplementary File 1).
- 526       • Gene length controls transcription timing. Short cell cycles limit transcription and long cell  
527       cycles allow transcription of longer genes
- 528           ○ Cell cycle duration can limit transcripts based on their size
- 529               ▪ Short cell cycles can constrain transcription in *D. melanogaster*. “the length of  
530               mitotic cycles provides a physiological barrier to transcript size, and is therefore a  
531               significant factor in controlling developmental gene activity during short  
532               'phenocritical' periods.” (Rothe et al., 1992)  
533               <https://pubmed.ncbi.nlm.nih.gov/1522901>
- 534           ○ Zygotic transcripts are encoded by short genes and start being expressed when cell cycle  
535           lengthens.
- 536               ▪ “We propose that early development in *Drosophila* operates according to a  
537               hierarchy of events. The first 13 division cycles are driven by a maternal  
538               mechanism which responds to the increasing nuclear density by extending the  
539               interphase periods of successive cycles. This lengthening of interphases allows  
540               transcriptional activation, and the expression of new zygotic gene products  
541               triggers events such as cellularization of the blastoderm, gastrulation, and further  
542               rounds of mitosis.” (Edgar et al., 1986)  
543               <https://pubmed.ncbi.nlm.nih.gov/3080248>
- 544               ▪ *Danio rerio* zygotic transcript lengths are shorter than maternally provided ones;  
545               The earliest zygotic genes are without introns. (Heyn et al., 2014; Kwasnieski et  
546               al., 2019; Shermoen and O’Farrell, 1991)  
547               <https://pubmed.ncbi.nlm.nih.gov/1680567>  
548               <https://pubmed.ncbi.nlm.nih.gov/24440719>  
549               <https://pubmed.ncbi.nlm.nih.gov/31235656>
- 550           ○ Longer genes, with larger introns, take longer to transcribe (“intron delay”)
- 551               ▪ Intron delay and transcriptional timing can affect development. (Artieri and  
552               Fraser, 2014; Gubb, 1986; Swinburne and Silver, 2008)  
553               DOI:10.1002/dvg.1020070302  
554               <https://pubmed.ncbi.nlm.nih.gov/18331713>  
555               <https://pubmed.ncbi.nlm.nih.gov/2506953>
- 556       • Cell-cycle dependent transcriptional filter is a mechanism for gene transcript expression  
557       regulation

- 558           ○ Hypothesized in (Bryant and Gardiner, 2016), but no analysis or experimental data to  
559           support this statement is provided in this publication.
- 560       • Cell cycle length changes can control cell fate and development
- 561           ○ In cell lines
- 562               ▪ Differentiation can be induced in G1-phase isolated pluripotent embryonal  
563               carcinoma cells by treating with retinoic acid (RA) while other cell cycle phases  
564               are not RA stimulated. (Mummery et al., 1987)  
565               <https://pubmed.ncbi.nlm.nih.gov/2883052>
- 566               ▪ “A short G1 phase is an intrinsic determinant of naïve embryonic stem cell  
567               pluripotency” (Coronado et al., 2013)  
568               <https://pubmed.ncbi.nlm.nih.gov/23178806>
- 569               ▪ “The cell-cycle state of stem cells determines cell fate propensity” (Pauklin and  
570               Vallier, 2013)  
571               <https://pubmed.ncbi.nlm.nih.gov/24074866>
- 572               ▪ Embryonic stem cells are more responsive to differentiation signals in G1 than in  
573               other phases of the cell cycle. (Singh et al., 2013)  
574               <https://pubmed.ncbi.nlm.nih.gov/24371808>
- 575           ○ In an organism
- 576               ▪ Alteration of cell cycle length can cause changes in *Gallus gallus* limb pattern.  
577               Gene transcripts normally expressed in mesenchyme cells are sensitive to cell  
578               cycle length. (Ohsugi et al., 1997)  
579               <https://pubmed.ncbi.nlm.nih.gov/9281333>
- 580       • Transcription rate and duration
- 581           ○ Transcription elongation rate is about 1.4kb/min
- 582               ▪ Transcript elongation rates tend to be uniform within a cell type. (Ardehali and  
583               Lis, 2009)  
584               <https://pubmed.ncbi.nlm.nih.gov/19888309>
- 585               ▪ Transcription of human dystrophin gene requires 16 hours (Tennyson et al. 1995)  
586               <https://pubmed.ncbi.nlm.nih.gov/7719>
- 587           ○ Transcription is repressed in S phase.
- 588               ▪ Early evidence that transcription is repressed in synthetic phase (S). (Newport and  
589               Kirschner, 1982b)  
590               <https://pubmed.ncbi.nlm.nih.gov/7139712>
- 591               ▪ “Upon G1–S transcriptional activation, cells progress to S phase, initiate DNA  
592               replication and subsequently inactivate transcription.” (Bertoli et al., 2013)  
593               <https://pubmed.ncbi.nlm.nih.gov/23877564>
- 594

595   Our novel contributions

- 596       • Our main novel claim: We are the first to link cell cycle duration to control of cell diversity and  
597       proportions of cells in tissues
- 598       • We are the first to support the idea that a cell-cycle dependent transcriptional filter is a  
599       mechanism for gene transcript expression regulation that affects development using quantitative  
600       modeling
- 601       • First to link gene length distribution in genomes of multiple species to length of organism  
602       development

- 603
- First to show major functional differences between short and long genes in animal genomes
  - Our single cell transcriptomic mathematical model is novel and shared as a community resource
- 604
- 605

606 **Acknowledgements**

607 We thank our reviewers for insightful comments. We thank Zain Patel, Brendan Innes, Derek van der  
608 Kooy, Peter Zandstra, Nika Shakiba, Janet Rossant, Eszter Posfai, Maria Shutova, Andras Nagy and  
609 Rudy Winklbauer for thoughtful discussions about this work. This work was funded by the University of  
610 Toronto Medicine by Design initiative, by the Canada First Research Excellence Fund.

611

612 **Declaration of Interests**

613 The authors declare no competing interests

614

615 **Figure Legends**

616 **Figure 1: Cell cycle duration changes during mouse development.** The data was curated from several  
617 publications (PubMed identifiers: 5859018, 14105210, 5760443, 5542640, 4041905, 7666188,  
618 12151540, 18164540), shown in the legend as authors and (year). For other species and tissues see  
619 Supplementary File 1.

620 **Figure 2: A novel mathematical model of cell lineage generation.** A) a single cell is defined by a  
621 given number of genes in its genome as well as their gene lengths (e.g. three genes,  $\text{gene}^1 < \text{gene}^2 <$   
622  $\text{gene}^3$ ). Cell cycle duration defines the time a cell has available to transcribe a gene. B) For example, a  
623 cell with cell cycle duration = 1 hour will only enable transcription of  $\text{gene}^1$ ; cell cycle duration = 2  
624 hours will enable transcription of  $\text{gene}^1$  and  $\text{gene}^2$ ; cell cycle duration = 3 hours enables transcription of  
625 all three genes. C) Our model assumes transcripts passed from parental cell to its progeny will be  
626 randomly distributed during division (M-phase). D) Each cell is characterized by its transcriptome,  
627 represented as a vector.

628

629 **Figure 3: Short genes produce more transcripts than longer genes at multiple cell cycle duration**  
630 **lengths.** The transcriptome for each cell is subdivided into short, medium, and long gene bins and  
631 transcript counts are averaged per bin per cell. A) Simulations predict that short gene transcripts will be  
632 more highly expressed than long gene transcripts, irrespective of the genome size. The top panel shows  
633 the total number genes expected from each genome per bin. Simulation results are shown for cell cycle

634 durations of 1, 5 and 10 hours and gene lengths ( $\text{gene}^{L_1-L_{10}}$ ), see Figure 3-figure supplement 3 for  
635 additional simulations (other parameters ploidy=1, one cell division, iterations = 5000000, genome  $G =$   
636 10,  $\text{gene}^{L_1-L_{10}}$ , transcription rate,  $\lambda = 1$  kb/hr, RNA polymerase II re-initiation,  $\Omega = 0.25\text{kb}$ ). Bins are  
637 defined such that genes are evenly distributed across them. B) Single cell microglia data obtained from  
638 GSE134707 (Geirsdottir et al., 2019) displaying expected patterns where short genes (lengths  $<10$  kb)  
639 have a higher transcript expression than both medium genes (lengths  $> 10\text{kb}$ ) and longer genes (lengths  
640  $>25$  kb) -- Kolmogorov-Smirnov test  $p < 10^{-16}$ , the upper bound p-value for all short-medium and short-  
641 long comparisons -- across nine different species (age): *Macaca fascicularis* (3 years), *Callithrix jacchus*  
642 (7 years), *Mus musculus* (8-16 weeks), *Rattus norvegicus* (11-14 weeks), *Mesocricetus auratus* (8-16  
643 weeks), *Nannospalax galili* (2-4 years), *Ovis aries* (18-20 months), *Gallus gallus* (24 weeks) and *Danio*  
644 *rerio* (4-5 months). The top part of the plot shows the total number genes possible in each bin, given the  
645 gene length distribution of each genome. Bins are defined such that they are both consistent across all  
646 species and also approximately evenly filled with genes.

647 **Figure 4: Cell cycle duration can control cell diversity.** Simulations explore the effects of cell cycle  
648 duration,  $\Gamma$ , gene number,  $G$ , and gene length distribution. A) Simulations show that cell diversity  
649 (transcriptome diversity) increases as a function of cell cycle duration. Short cell cycle durations can  
650 constrain the effects of gene number as long as a transcriptional filter is active (gene length distributions  
651 are broad,  $L_1 < \dots (\Gamma * \lambda) \dots < L_G$ ). When  $L_G < (\Gamma * \lambda)$ , cell cycle duration does not control cell  
652 diversity. Cell cycle duration effects are relative to the gene length distribution in the genome. B) We  
653 use Seurat to cluster the simulated single cell transcriptomes (10,000 cells) using default parameters and  
654 report the number of cell clusters over the simulations. This shows that cell diversity increases with gene  
655 number but the number of clusters identified decreases when all the gene transcripts can be expressed  
656 similarly among all cells. C) Representative examples (10,000 cells) of t-SNE visualizations (RunTSNE  
657 using Seurat version 3.1.2) are shown for simulations with cell cycle durations 2, 6 and 10 hours  
658 (genome  $G = 10$ ,  $\text{gene}^{L_1-L_{10}}$ , ploidy  $n = 1$  and transcription rate,  $\lambda = 1$  kb/hr, RNA polymerase II re-  
659 initiation,  $\Omega = 0.25\text{kb}$ ).

660

661 **Figure 5: Cell cycle duration can control the generation of cell proportions and cell types within a**  
662 **population.** Simulations start with two cells and run for 18 divisions (generating  $2^{19}$  cells when cell  
663 cycles are the same). Cell<sub>1</sub> is initialized with cell cycle duration  $\Gamma_1 = 1$  hour, Cell<sub>2</sub> has cell cycle

664 duration,  $\Gamma_2$ , ranging from 1 to 2 hours. All progeny are tracked based on their cell cycle duration  
665 (lineage  $\Gamma_1=1$  cell cycle duration, gray, or lineage  $\Gamma_2$  cell cycle duration, blue). Tree plot depicting  
666 lineages when the cell cycle duration A) are the same,  $\Gamma_1=\Gamma_2$  (scenario 1), or B-C) differ,  $\Gamma_1<\Gamma_2$   
667 (scenarios 2 and 3). Scenario 2 captures a situation when the cell cycle is determined by the parental  
668 lineage, while scenario 3 captures a situation when a cell splits asymmetrically into a fast and slow cell,  
669 resulting with the fast lineage having just one cell. D-F) Müller visualizations show that when the cell  
670 cycle duration is the same, both cells contribute the same number of progeny and cell proportions (%)  
671 are 50:50 (bottom left panel). The visualization is stacked, down-scaling the blue lineage slightly to  
672 reduce occlusion of the grey lineage. Cells with longer cell cycle duration (blue lineage) generate fewer  
673 progeny with respect to the cells with a short cell cycle duration of 1 hour (gray lineage). However, the  
674 slower cells contribute more to the diversity observed in the population, shown as the blue and grey  
675 transcriptome diversity bars. Thus, increasing cell cycle duration increases cell diversity, but also limits  
676 the number of progeny generated. The system can overcome the limit on cell number by using scenario  
677 3, where more slow cells can be generated (other parameters  $G=5$ , gene lengths ( $\text{gene}^L_{-L_2}$ ),  
678 genome= $\{1,1.25,1.5,1.75,2\}$  and ploidy =1, RNA polymerase II re-initiation,  $\Omega = 0.25\text{kb}$ ).

679

680 **Figure 6: Varying cell cycle duration across time affects cell type proportions.** A) Cell cycle  
681 duration increases after each cell division, with amount of increase defined using a Gaussian  
682 distribution. B) Simulation of gradually increasing cell cycle duration over time, such that  $\Gamma$ =Gaussian  
683 (mean  $\Gamma_{\text{parent}} \pm 6$ , standard deviation  $\sigma=0.06$ ), affects the relative proportion of cells with different cell  
684 cycle durations (pie charts). All cell progeny are labeled based on their cell cycle duration (inherited  
685 from parent). See Figure 6-figure supplement 1 for results using other increment rates. Parameters:  
686 genome=10, gene lengths ( $\text{gene}^L_{-L_{10}}$ ),  $\lambda=1$  kb/hr, 18 cell divisions, iterations= 500, ploidy  $n=1$ , , RNA  
687 polymerase II re-initiation,  $\Omega = 0.25\text{kb}$ . C) Single cell transcriptomics data from GSE107122 (Yuzwa et  
688 al., 2017) for embryonic mouse cortex development, known to exhibit increasing cell cycle duration  
689 over time. This data includes identified cell types, is a time series, and we know the average cell cycle  
690 duration at each time point; At E11.5 the average cell cycle duration is 8 hrs and by E17.5 it is 18 hrs  
691 (Furutachi et al., 2015; Takahashi et al., 1995a). Cells were defined as relatively fast cycling cells  
692 (apical progenitors), relatively medium cycling (intermediate progenitors) and relatively slow cycling  
693 (neurons), with cell type annotation based on cell clustering analyses conducted in (Yuzwa et al., 2017).

694 We show how cell proportions (pie charts) change across time, with apical progenitors (relatively fast  
695 cycling cells) decreasing in frequency as the average cell cycle duration increases.

696

697 **Figure 7: Gene length distribution and developmental time are correlated.** A) Model organisms  
698 exhibit a large diversity in gene length distributions over their genomes. Species that have narrower gene  
699 length distributions tend to develop faster, while slow developers (mammals) exhibit broad and right  
700 shifted gene length distributions. Demarcating a 1 hour cell cycle duration using an average transcription  
701 rate of 1.5 kb/min illustrates the proportion of genes that would be interrupted before transcript  
702 completion for each organism. *Saccharomyces cerevisiae* (budding yeast), *Caenorhabditis elegans*  
703 (worm), *Drosophila melanogaster* (fruit fly), *Oikopleura dioica* (tunicate), *Danio rerio* (zebrafish),  
704 *Takifugu rubripes* (fugu), *Xenopus tropicalis* (frog), *Gallus gallus* (chicken), *Mus musculus* (mouse),  
705 *Sus scrofa* (pig), *Macaca mulatta* (monkey), *Homo sapiens* (human). B) There is a clear positive  
706 correlation between developmental time and median gene length (101 species, Figure 7-figure  
707 supplement 1). Estimated developmental time was curated from encyclopedia of life or articles found in  
708 PubMed (Supplementary File 3). We used gestation time for mammals and hatching time for species  
709 who lay eggs (since it is difficult to accurately define a comparative stage for all species). We analyzed  
710 the data using a Pearson correlation test, shown as  $r$ . For each species we calculated median gene length:  
711 All protein coding genes were downloaded from Ensembl version 95 (Yates et al., 2016) using the R  
712 Biomart package (Durinck et al., 2009, 2005). The length of each gene was calculated using  
713 start\_position and end\_position for each gene as extracted from Ensembl data.

714

715 **Figure 8: Short genes and long genes participate in different pathways.** The plot shows the *H.*  
716 *sapiens* gene length distribution. We selected the shortest 5% quantile as a list of short genes and the  
717 95% quantile as a list of long genes. Short genes < 1.6Kb (n=1124) are involved in immune defense,  
718 environment-sensing, and olfactory, and long genes >243kb (n=1125) are represented in processes  
719 involving muscle and brain development, as well as morphogenesis. For each gene group we identified  
720 all corresponding Gene Ontology (Ashburner et al., 2000) biological process terms downloaded from the  
721 Ensembl genome database version 100 (Yates et al., 2016), grouped the terms into themes  
722 (Supplementary File 5-6) and visualized the resulting term frequencies as word clouds using  
723 Mathematica. Refer to Figure 8-figure supplement 2-3 for a more detailed analysis of the themes across  
724 all gene groups.

725

726 **Figure 9: Short genes exhibit different pathways than long genes and this trend is consistent**

727 **across a wide species range.** We selected the shortest 5% quantile as a list of short genes (top panels in  
728 blue) and genes above the 95% quantile to define a list of long genes (bottom panels in gray.

729 *Saccharomyces cerevisiae* (short<0.24kb long>3.5kb), *Ashbya gossypii* (short<0.36kb long>3.5kb),  
730 *Komagataella pastoris* (short<0.37kb long>3.3kb), *Yarrowia lipolytica* (short<0.39kb long>3.5kb),  
731 *Caenorhabditis elegans* (short<0.47kb long>9.6kb), *Drosophila melanogaster* (short<0.56kb  
732 long>29kb), *Danio rerio* (short<1.3kb long>127kb), *Takifugu rubripes* (short<0.72kb long>27kb),  
733 *Xenopus tropicalis* (short<0.93kb long>83kb), *Gallus gallus* (short<0.67kb long>104kb), *Mus musculus*  
734 (short<1.2kb long>183kb), *Sus scrofa* (short<0.57kb long>197kb). For each gene group we identified all  
735 corresponding Gene Ontology biological process terms from the Ensembl genome database (100) and  
736 visualized the resulting term frequencies as word clouds using Mathematica.

737 **Figure 10: Hox gene length is correlated with spatial expression and cell cycle duration in the *D.***

738 ***melanogaster* embryo.** Drosophila Hoxd family genes are each represented by a colored rectangle,  
739 containing the length of the gene in base pairs. Spatial expression of a gene transcript is marked by its  
740 corresponding color on the Drosophila embryo map. Hoxd gene length is correlated with the cell cycle  
741 duration of the embryo location where the gene transcript is expressed, with short Hox gene transcripts  
742 expressed in regions with short mitotic cycles and long Hox gene transcripts expressed in regions of  
743 long mitotic cycles. Spatial map of cell cycle duration from (Foe, 1989; Foe and Alberts, 1983) and gene  
744 transcript expression from (Mallo and Alonso, 2013).

745

746 **Figure 3-figure supplement 1: Simulations exploring the effects of cell cycle duration and RNA**

747 **Polymerase II (rnaPol II)** for different re-initiation distances,  $\Omega$  and transcription rates,  $\lambda$ . A) We  
748 conducted simulations for different re-initiation distances (Default assumes that re-initiation only occurs  
749 one rnaPol II reaches the end of the gene). B) We conducted simulations for different transcription rate.  
750 Rates were randomized using a Gaussian distribution (mean= $\lambda$ , standard deviation= $\lambda$ ) such that  
751 transcription time  $T=\Gamma\lambda/L$ . We generally assumed a fixed rate  $\lambda=1$ , where all genes exhibit the same  
752 rate. Changing parameters in A and B does not alter the overall trend we observe, that short genes  
753 produce more transcripts than longer genes. Other parameters for panels A-B were: ploidy=1,  
754  $Li=\{1,2,3,4,5,6,7,8,9\}$  and  $G=9$ , one cell division, iterations=1000. We also show in the case where all

755 genes are the same length,  $L=9$ , and cell cycle duration is constant (panels C-D) that when cell cycle  
756 durations are short,  $\Gamma=1$  hour, only high transcription rates can quench the constraint of short cell cycle.  
757 E-F) When cell cycle duration is long,  $\Gamma=10$  hours, changing transcription parameters can directly affect  
758 transcript number. Other parameters for panels C-F were: ploidy=1,  $L_i=\{9\}$ ,  $G=9$ , genome= $\{\text{gene}_1^9,$   
759  $\text{gene}_2^9 \dots, \text{gene}_9^9\}$ , one cell division, iterations=1000 per panel.

760

761 **Figure 3-figure supplement 2: Effects of maternal transcript inheritance.** A) Simulation of expected  
762 transcript count when cells are initiated without maternal transcripts in comparison to cells with  
763 maternal transcripts. Parameters: gene lengths ( $\text{gene}_1^L \dots \text{gene}_{10}^L$ ), ploidy=1, one cell division, 10 hours cell  
764 cycle duration, iterations=10000. B) Simulation of expected transcript count where a proportion (zero or  
765 half) of inherited parental transcripts remain after each cell division. Parameters: gene lengths ( $\text{gene}_1^L \dots$   
766  $\text{gene}_{10}^L$ ), ploidy=1, two cell divisions, 10 hours cell cycle duration, iterations=1000.

767

768 **Figure 3-figure supplement 3: Simulations exploring the effects of cell cycle duration on transcript**  
769 **count per cell.** We find that short genes produced more transcripts than longer genes. We conducted  
770 simulations for different gene numbers (10, 100, and 1000) and distributions across various cell cycle  
771 durations (1-10 hours), always resulting in the same overall trend being observed. The transcriptome for  
772 each cell is subdivided into short, medium, and long gene bins. Transcript counts in each bin are  
773 averaged for each cell. Prediction from simulation shows that cells will have higher expression of short  
774 gene transcripts and longer genes irrespective the number of genes in each bin. However, simulation  
775 shows that longer cycle durations will increase relative transcript count per cell (other parameters  
776 ploidy=1, one cell division, iterations=1000, RNA polymerase II re-initiation,  
777  $\Omega$  occurs at the end of the gene).

778

779 **Figure 3-figure supplement 4: Single cell data exploring the effects of cell cycle duration on**  
780 **transcript count per cell.** We find that short genes produce more transcripts than longer genes. A)  
781 *Xenopus tropicalis* (*Xenopus*) single cell data obtained from GSE113074 (Lib2) B) *Danio rerio*  
782 (zebrafish) single cell data obtained from GSE112294 and C) *Mus Musculus* (mouse) cortex single cell  
783 data obtained from GSE107122, displaying predicted patterns where short genes have a higher average  
784 transcript expression than longer genes.

785

786 **Figure 6-figure supplement 1: Varying cell cycle duration across time affects cell type proportions.**

787 All cell progeny are labeled based on their cell cycle duration (inherited from parent). Each line  
788 represents a different rate of increase in average cell cycle duration, following rate increments 0  
789 (shallowest constant curve), 1, 3, 6 and 9 (steepest curve). Cell cycle duration increases after each  
790 division using a Gaussian distribution, such that  $\Gamma = \text{Gaussian}(\text{mean } \Gamma_{\text{parent}} \pm \text{rate increment, standard}$   
791  $\text{deviation } \sigma = 0.06)$ . Gradual cell cycle duration changes affect the relative proportion of cells with  
792 different cell cycle durations (pie charts). Parameters genome=10, gene lengths ( $\text{gene}^L_1 - L_{10}$ ),  $\lambda = 1$  kb/hr,  
793 15 cell divisions, iterations=500, ploidy n=1, RNA polymerase II re-initiation,  $\Omega = 0.25\text{kb}$ .

794

795 **Figure 6-figure supplement 2: Genes with increasing transcript expression are associated with**  
796 **neuronal and synaptic pathways.** We used the mouse cortex time series single cell transcriptomics  
797 data, obtained from GSE107122 (Yuzwa et al., 2017), to identify gene transcripts that increase or  
798 decrease in expression level over development (with gene transcript expression following the pattern:  
799  $E_{11.5} < E_{13.5} < E_{15.5} < E_{17.5}$  for increasing and  $E_{11.5} > E_{13.5} > E_{15.5} > E_{17.5}$  for decreasing genes).  
800 To summarize pathway annotation information for each gene, we identified all corresponding Gene  
801 Ontology biological process terms for each gene from the Ensembl genome database and visualized term  
802 frequencies as word clouds using Mathematica. We find the genes (n=2186) that increase across time are  
803 associated with neural developmental (brain, neuron and synapse) pathways whereas the genes (n=1834)  
804 that decrease across time are associated with DNA-repair and proliferation pathways.

805

806 **Figure 7-figure supplement 1: Illustrating the association between developmental time and median**  
807 **gene length across 101 species, grouped by taxonomy class** (Supplementary File 3). A) The  
808 association between number of cell types and species appearance in the fossil record according to  
809 (Valentine et al., 1994) B) The association between median gene length and emergence time. C) The  
810 association between median gene length and developmental time across 12 species taxonomy classes  
811 (Saccharomycetes, Chromadorea, Ascidiacea, Insecta, Hyperoartia, Amphibia, Actinopterygii, Aves,  
812 Reptilia, Mammalia, Sarcopterygii and Myxini). For each species we calculated median gene length:  
813 The length of each gene was calculated using start and end positions for each gene as extracted from the  
814 Ensembl genome database (version 95). Estimated developmental time was curated from the  
815 encyclopedia of life or articles found in PubMed (Supplementary File 3). We used gestation time for

816 mammals and hatching time for species who lay eggs (since it is difficult to accurately define a  
817 comparative stage for all species). We analyzed the data using a Pearson correlation test shown as  $r$ .

818

819 **Figure 8-supplement 1: Enriched pathways in short(A) and long(B) genes in Human.** Enrichment  
820 map (Merico et al., 2010) showing the pathways enriched in short genes compared to long gene. Circles  
821 represent pathway gene sets. Lines connecting circles represent overlap between pathways. Similar  
822 pathways are grouped in larger bubbles and manually labeled using the AutoAnnotate (Kucera et al.,  
823 2016), Cytoscape app (Reimand et al., 2019) and custom scripts (Supplementary File 4). Blue pathways  
824 (nodes) are enriched in long genes and red pathways are enriched in short genes ( $p$  value  $< 0.05$ , FDR  $<$   
825  $0.01$ , Jaccard coefficient  $> 0.25$ ). Long genes were enriched in many more functional groups than short  
826 genes with 798 and 152 enriched pathways, respectively.

827

828 **Figure 8-supplement 2: Genes participate in different pathways.** The plot shows the *H. sapiens*  
829 genes divided into 20 groups from shortest genes to the longest genes. For each gene group we identified  
830 all corresponding Gene Ontology (Ashburner et al., 2000) biological process terms downloaded from the  
831 Ensembl genome database version 100 (Yates et al., 2016), grouped the terms into themes  
832 (Supplementary File 5-6) and visualized the resulting term frequencies as word clouds using  
833 Mathematica.

834 **Figure 8-supplement 3: Moving average across gene length.** *H. sapiens* genes were divided into 20  
835 groups from shortest genes to longest genes. For each gene group, we identified all corresponding Gene  
836 Ontology (Ashburner et al., 2000) biological process terms downloaded from the Ensembl genome  
837 database version 100 (Yates et al., 2016) and grouped the terms into themes (Supplementary File 5-6).  
838 We calculated a moving average to explore the trend across gene groups by theme. For example, we  
839 identified the 15 most frequent themes between the shortest (blue) and longest (black) gene groups. We  
840 found themes such as ‘environment-sensing’, ‘immune’, and ‘olfactory’ show a trend with a decreasing  
841 average and are found only in the shortest gene group (blue). On the other hand, themes such as ‘brain’,  
842 ‘muscle’, ‘neuron’, and ‘synapse’, show an increasing trend and are found only in the longest genes  
843 group (black).

844

845 **Figure 8-supplement 4: Pathway themes are associated with gene length.** The plot shows the *H.*  
846 *sapiens* genes divided into 20 groups from shortest genes to the longest genes. For each gene group we  
847 identified all corresponding Gene Ontology (Ashburner et al., 2000) biological process terms  
848 downloaded from the Ensembl genome database version 100 (Yates et al., 2016), grouped the terms  
849 into themes (Supplementary File 5-6) and visualized the resulting term relative frequencies in a matrix  
850 plot using Mathematica. Darker shading indicates higher term frequency.

851

## 852 **Supplementary Files**

853

854 Supplementary File 1: Curated cell cycle duration data

855

856 Supplementary File 2: Simulations supporting transcriptome diversity analytical solution

857

858 Supplementary File 3: Curated developmental time for species and their corresponding median gene  
859 length. The length of each gene was calculated using start and end positions for each gene as extracted  
860 from the Ensembl genome database (version 95). Estimated developmental time was curated from the  
861 encyclopedia of life or articles found in PubMed

862

863 Supplementary File 4: General pathway themes from Figure 8-figure supplement 1 generated by using a  
864 mixture of automatic classification applying key words and manual identification.

865

866 Supplementary File 5: General pathway themes their corresponding the list of words that were used to  
867 manually classify the pathways in Figure 8 and 8- figure supplement 2-3.

868

869 Supplementary File 6: General pathway themes in Figure 8 and 8- figure supplement 2-3 applied to *H.*  
870 *sapiens* and their corresponding and Gene Ontology identifiers descriptions extracted from the Ensembl  
871 genome database.

872

## 873 **References**

874 Ardehali MB, Lis JT. 2009. Tracking rates of transcription and splicing in vivo. *Nat Struct Mol Biol*  
875 **16**:1123–1124. doi:10.1038/nsmb1109-1123

876 Artieri CG, Fraser HB. 2014. Transcript Length Mediates Developmental Timing of Gene Expression  
877 Across *Drosophila*. *Mol Biol Evol* **31**:2879–2889. doi:10.1093/molbev/msu226

878 Ashburner M, Ball CA, Blake JA, Botstein D, Butler H, Cherry JM, Davis AP, Dolinski K, Dwight SS,  
879 Eppig JT, Harris MA, Hill DP, Issel-Tarver L, Kasarskis A, Lewis S, Matese JC, Richardson JE,  
880 Ringwald M, Rubin GM, Sherlock G. 2000. Gene Ontology: tool for the unification of biology. *Nat*  
881 *Genet* **25**:25–29. doi:10.1038/75556

882 Bertoli C, Skotheim JM, Bruin RAM de. 2013. Control of cell cycle transcription during G1 and S  
883 phases. *Nat Rev Mol Cell Bio* **14**:518–528. doi:10.1038/nrm3629

884 Briggs JA, Weinreb C, Wagner DE, Megason S, Peshkin L, Kirschner MW, Klein AM. 2018. The  
885 dynamics of gene expression in vertebrate embryogenesis at single-cell resolution. *Science*  
886 **360**:eaar5780. doi:10.1126/science.aar5780

887 Bryant SV, Gardiner DM. 2018. Regeneration: sooner rather than later. *Int J Dev Biology* **62**:363–368.  
888 doi:10.1387/ijdb.170269dg

889 Bryant SV, Gardiner DM. 2016. The relationship between growth and pattern formation. *Regen* **3**:103–  
890 122. doi:10.1002/reg2.55

891 Calegari F, Haubensak W, Haffner C, Huttner WB. 2005. Selective Lengthening of the Cell Cycle in the  
892 Neurogenic Subpopulation of Neural Progenitor Cells during Mouse Brain Development. *J Neurosci*  
893 **25**:6533–6538. doi:10.1523/jneurosci.0778-05.2005

894 Coronado D, Godet M, Bourillot P-Y, Tapponnier Y, Bernat A, Petit M, Afanassieff M, Markossian S,  
895 Malashicheva A, Iacone R, Anastassiadis K, Savatier P. 2013. A short G1 phase is an intrinsic  
896 determinant of naïve embryonic stem cell pluripotency. *Stem Cell Res* **10**:118–131.  
897 doi:10.1016/j.scr.2012.10.004

898 Croft D, O’Kelly G, Wu G, Haw R, Gillespie M, Matthews L, Caudy M, Garapati P, Gopinath G, Jassal  
899 B, Jupe S, Kalatskaya I, Mahajan S, May B, Ndegwa N, Schmidt E, Shamovsky V, Yung C, Birney  
900 E, Hermjakob H, D’Eustachio P, Stein L. 2011. Reactome: a database of reactions, pathways and  
901 biological processes. *Nucleic Acids Res* **39**:D691–D697. doi:10.1093/nar/gkq1018

902 Dalton S. 2015. Linking the Cell Cycle to Cell Fate Decisions. *Trends Cell Biol* **25**:592–600.  
903 doi:10.1016/j.tcb.2015.07.007

904 Dalton S. 2013. G1 Compartmentalization and Cell Fate Coordination. *Cell* **155**:13–14.  
905 doi:10.1016/j.cell.2013.09.015

906 Djabrayan NJ-V, Smits CM, Krajnc M, Stern T, Yamada S, Lemon WC, Keller PJ, Rushlow CA,  
907 Shvartsman SY. 2019. Metabolic Regulation of Developmental Cell Cycles and Zygotic  
908 Transcription. *Curr Biology Cb* **29**:1193-1198.e5. doi:10.1016/j.cub.2019.02.028

909 Durinck S, Moreau Y, Kasprzyk A, Davis S, Moor BD, Brazma A, Huber W. 2005. BioMart and  
910 Bioconductor: a powerful link between biological databases and microarray data analysis. *Bioinform*  
911 *Oxf Engl* **21**:3439–40. doi:10.1093/bioinformatics/bti525

912 Durinck S, Spellman PT, Birney E, Huber W. 2009. Mapping identifiers for the integration of genomic  
913 datasets with the R/Bioconductor package biomaRt. *Nat Protoc* **4**:1184–1191.  
914 doi:10.1038/nprot.2009.97

915 Edgar BA, Kiehle CP, Schubiger G. 1986. Cell cycle control by the nucleo-cytoplasmic ratio in early  
916 *Drosophila* development. *Cell* **44**:365–372. doi:10.1016/0092-8674(86)90771-3

917 Edgar LG, Wolf N, Wood WB. 1994. Early transcription in *Caenorhabditis elegans* embryos. *Dev Camb*  
918 *Engl* **120**:443–51.

919 Farrell JA, O’Farrell PH. 2014. From Egg to Gastrula: How the Cell Cycle Is Remodeled During the  
920 *Drosophila* Mid-Blastula Transition. *Annual Review of Genetics*. pp. 1–26.  
921 doi:10.1146/annurev-genet-111212-133531

922 Foe VE. 1989. Mitotic domains reveal early commitment of cells in *Drosophila* embryos. *Dev Camb*  
923 *Engl* **107**:1–22.

924 Foe VE, Alberts BM. 1983. Studies of nuclear and cytoplasmic behaviour during the five mitotic cycles  
925 that precede gastrulation in *Drosophila* embryogenesis. *J Cell Sci* **61**:31–70.

926 Furutachi S, Miya H, Watanabe T, Kawai H, Yamasaki N, Harada Y, Imayoshi I, Nelson M, Nakayama  
927 KI, Hirabayashi Y, Gotoh Y. 2015. Slowly dividing neural progenitors are an embryonic origin of  
928 adult neural stem cells. *Nat Neurosci* **18**:657–665. doi:10.1038/nn.3989

929 Geirsdottir L, David E, Keren-Shaul H, Weiner A, Bohlen SC, Neuber J, Balic A, Giladi A, Sheban F,  
930 Dutertre C-A, Pfeifle C, Peri F, Raffo-Romero A, Vizioli J, Matiasek K, Scheiwe C, Meckel S, Mätz-  
931 Rensing K, Meer F van der, Thormodsson FR, Stadelmann C, Zilkha N, Kimchi T, Ginhoux F,  
932 Ulitsky I, Erny D, Amit I, Prinz M. 2019. Cross-Species Single-Cell Analysis Reveals Divergence of  
933 the Primate Microglia Program. *Cell* **179**:1609-1622.e16. doi:10.1016/j.cell.2019.11.010

934 Gilbert SF, Barresi MJ. 2016. *Developmental Biology*. pp. 1–810.

935 Gubb D. 1986. Intron-delay and the precision of expression of homoeotic gene products in *Drosophila*.  
936 *Dev Genet* **7**:119–131. doi:10.1002/dvg.1020070302

937 Guo S, Zi X, Schulz VP, Cheng J, Zhong M, Koochaki SHJ, Megyola CM, Pan X, Heydari K,  
938 Weissman SM, Gallagher PG, Krause DS, Fan R, Lu J. 2014. Nonstochastic Reprogramming from a  
939 Privileged Somatic Cell State. *Cell* **156**:649–662. doi:10.1016/j.cell.2014.01.020

940 Heyn P, Kircher M, Dahl A, Kelso J, Tomancak P, Kalinka AT, Neugebauer KM. 2014. The Earliest  
941 Transcribed Zygotic Genes Are Short, Newly Evolved, and Different across Species. *Cell Reports*  
942 **6**:285–292. doi:10.1016/j.celrep.2013.12.030

943 Jukam D, Shariati SAM, Skotheim JM. 2017. Zygotic Genome Activation in Vertebrates. *Dev Cell*  
944 **42**:316–332. doi:10.1016/j.devcel.2017.07.026

945 Kandasamy K, Mohan SS, Raju R, Keerthikumar S, Kumar GSS, Venugopal AK, Telikicherla D,  
946 Navarro JD, Mathivanan S, Pecquet C, Gollapudi SK, Tattikota SG, Mohan S, Padhukasahasram H,  
947 Subbannayya Y, Goel R, Jacob HK, Zhong J, Sekhar R, Nanjappa V, Balakrishnan L, Subbaiah R,  
948 Ramachandra Y, Rahiman BA, Prasad TK, Lin J-X, Houtman JC, Desiderio S, Renauld J-C,  
949 Constantinescu SN, Ohara O, Hirano T, Kubo M, Singh S, Khatri P, Draghici S, Bader GD, Sander  
950 C, Leonard WJ, Pandey A. 2010. NetPath: a public resource of curated signal transduction pathways.  
951 *Genome Biol* **11**:R3. doi:10.1186/gb-2010-11-1-r3

952 Keane PA, Seoighe C. 2016. Intron Length Coevolution across Mammalian Genomes. *Mol Biol Evol*  
953 **33**:2682–2691. doi:10.1093/molbev/msw151

954 Kimelman D, Kirschner M, Scherson T. 1987. The events of the midblastula transition in *Xenopus* are  
955 regulated by changes in the cell cycle. *Cell* **48**:399–407. doi:10.1016/0092-8674(87)90191-7

956 Kimmel CB, Ballard WW, Kimmel SR, Ullmann B, Schilling TF. 1995. Stages of embryonic  
957 development of the zebrafish. *Dev Dynam* **203**:253–310. doi:10.1002/aja.1002030302

958 Kucera M, Isserlin R, Arkhangorodsky A, Bader GD. 2016. AutoAnnotate: A Cytoscape app for  
959 summarizing networks with semantic annotations. *F1000research* **5**:1717.  
960 doi:10.12688/f1000research.9090.1

961 Lemons D, McGinnis W. 2006. Genomic Evolution of Hox Gene Clusters. *Science* **313**:1918–1922.  
962 doi:10.1126/science.1132040

963 Liu S, Ginzberg MB, Patel N, Hild M, Leung B, Li Z, Chen Y-C, Chang N, Wang Y, Tan C, Diena S,  
964 Trimble W, Wasserman L, Jenkins JL, Kirschner MW, Kafri R. 2018. Size uniformity of animal cells  
965 is actively maintained by a p38 MAPK-dependent regulation of G1-length. *Elife* **7**:e26947.  
966 doi:10.7554/elife.26947

967 Mallo M, Alonso CR. 2013. The regulation of Hox gene expression during animal development.  
968 *Development* **140**:3951–3963. doi:10.1242/dev.068346

969 Merico D, Isserlin R, Stueker O, Emili A, Bader GD. 2010. Enrichment Map: A Network-Based Method  
970 for Gene-Set Enrichment Visualization and Interpretation. *Plos One* **5**:e13984.  
971 doi:10.1371/journal.pone.0013984

972 Mi H, Lazareva-Ulitsky B, Loo R, Kejariwal A, Vandergriff J, Rabkin S, Guo N, Muruganujan A,  
973 Doremieux O, Campbell MJ, Kitano H, Thomas PD. 2005. The PANTHER database of protein  
974 families, subfamilies, functions and pathways. *Nucleic Acids Res* **33**:D284–D288.  
975 doi:10.1093/nar/gki078

976 Mueller WA, Hassel M, Greal M. 2015. Development and Reproduction in Humans and Animal Model  
977 Species, Development and Reproduction in Humans and Animal Model Species. Springer.  
978 doi:10.1007/978-3-662-43784-1

979 Mukherjee RN, Sallé J, Dmitrieff S, Nelson KM, Oakey J, Minc N, Levy DL. 2020. The Perinuclear ER  
980 Scales Nuclear Size Independently of Cell Size in Early Embryos. *Dev Cell*.  
981 doi:10.1016/j.devcel.2020.05.003

982 Mummery CL, Brink CE van den, Laat SW de. 1987. Commitment to differentiation induced by retinoic  
983 acid in P19 embryonal carcinoma cells is cell cycle dependent. *Dev Biol* **121**:10–19.  
984 doi:10.1016/0012-1606(87)90133-3

985 Newport J, Kirschner M. 1982a. A major developmental transition in early xenopus embryos: II. control  
986 of the onset of transcription. *Cell* **30**:687–696. doi:10.1016/0092-8674(82)90273-2

987 Newport J, Kirschner M. 1982b. A major developmental transition in early xenopus embryos: I.  
988 characterization and timing of cellular changes at the midblastula stage. *Cell* **30**:675–686.  
989 doi:10.1016/0092-8674(82)90272-0

990 O’Farrell PH, Stumpff J, Su TT. 2004. Embryonic Cleavage Cycles: How Is a Mouse Like a Fly? *Curr*  
991 *Biol* **14**:R35–R45. doi:10.1016/j.cub.2003.12.022

992 Ohsugi K, Gardiner DM, Bryant SV. 1997. Cell Cycle Length Affects Gene Expression and Pattern  
993 Formation in Limbs. *Dev Biol* **189**:13–21. doi:10.1006/dbio.1997.8665

994 Pauklin S, Vallier L. 2013. The Cell-Cycle State of Stem Cells Determines Cell Fate Propensity. *Cell*  
995 **155**:135–147. doi:10.1016/j.cell.2013.08.031

996 Reimand J, Isserlin R, Voisin V, Kucera M, Tannus-Lopes C, Rostamianfar A, Wadi L, Meyer M, Wong  
997 J, Xu C, Merico D, Bader GD. 2019. Pathway enrichment analysis and visualization of omics data

998 using g:Profiler, GSEA, Cytoscape and EnrichmentMap. *Nat Protoc* **14**:482–517.  
999 doi:10.1038/s41596-018-0103-9

1000 Rodríguez-Carballo E, Lopez-Delisle L, Yakushiji-Kaminatsui N, Ullate-Agote A, Duboule D. 2019.  
1001 Impact of genome architecture on the functional activation and repression of Hox regulatory  
1002 landscapes. *Bmc Biol* **17**:55. doi:10.1186/s12915-019-0677-x

1003 Rothe M, Pehl M, Taubert H, Jäckle H. 1992. Loss of gene function through rapid mitotic cycles in the  
1004 *Drosophila* embryo. *Nature* **359**:359156a0. doi:10.1038/359156a0

1005 Satija R, Farrell JA, Gennert D, Schier AF, Regev A. 2015. Spatial reconstruction of single-cell gene  
1006 expression data. *Nat Biotechnol* **33**:495–502. doi:10.1038/nbt.3192

1007 Schaefer CF, Anthony K, Krupa S, Buchoff J, Day M, Hannay T, Buetow KH. 2009. PID: the Pathway  
1008 Interaction Database. *Nucleic Acids Res* **37**:D674–D679. doi:10.1093/nar/gkn653

1009 Shannon P, Markiel A, Ozier O, Baliga NS, Wang JT, Ramage D, Amin N, Schwikowski B, Ideker T.  
1010 2003. Cytoscape: A Software Environment for Integrated Models of Biomolecular Interaction  
1011 Networks. *Genome Res* **13**:2498–2504. doi:10.1101/gr.1239303

1012 Sharova LV, Sharov AA, Nedorezov T, Piao Y, Shaik N, Ko MSH. 2009. Database for mRNA Half-  
1013 Life of 19 977 Genes Obtained by DNA Microarray Analysis of Pluripotent and Differentiating  
1014 Mouse Embryonic Stem Cells. *Dna Res* **16**:45–58. doi:10.1093/dnares/dsn030

1015 Shermoen AW, O’Farrell PH. 1991. Progression of the cell cycle through mitosis leads to abortion of  
1016 nascent transcripts. *Cell* **67**:303–310. doi:10.1016/0092-8674(91)90182-x

1017 Singh AM, Chappell J, Trost R, Lin L, Wang T, Tang J, Matlock BK, Weller KP, Wu H, Zhao S, Jin P,  
1018 Dalton S. 2013. Cell-cycle control of developmentally regulated transcription factors accounts for  
1019 heterogeneity in human pluripotent cells. *Stem Cell Rep* **1**:532–44. doi:10.1016/j.stemcr.2013.10.009

1020 Slenter DN, Kutmon M, Hanspers K, Riutta A, Windsor J, Nunes N, Mélius J, Cirillo E, Coort SL,  
1021 Digles D, Ehrhart F, Giesbertz P, Kalafati M, Martens M, Miller R, Nishida K, Rieswijk L,  
1022 Waagmeester A, Eijssen LMT, Evelo CT, Pico AR, Willighagen EL. 2017. WikiPathways: a  
1023 multifaceted pathway database bridging metabolomics to other omics research. *Nucleic Acids Res*  
1024 **46**:gkx1064-. doi:10.1093/nar/gkx1064

1025 Subramanian A, Tamayo P, Mootha VK, Mukherjee S, Ebert BL, Gillette MA, Paulovich A, Pomeroy  
1026 SL, Golub TR, Lander ES, Mesirov JP. 2005. Gene set enrichment analysis: A knowledge-based  
1027 approach for interpreting genome-wide expression profiles. *P Natl Acad Sci Usa* **102**:15545–15550.  
1028 doi:10.1073/pnas.0506580102

1029 Swinburne IA, Miguez DG, Landgraf D, Silver PA. 2008. Intron length increases oscillatory periods of  
1030 gene expression in animal cells. *Gene Dev* **22**:2342–2346. doi:10.1101/gad.1696108

1031 Swinburne IA, Silver PA. 2008. Intron Delays and Transcriptional Timing during Development. *Dev*  
1032 *Cell* **14**:324–330. doi:10.1016/j.devcel.2008.02.002

1033 Tabansky I, Lenarcic A, Draft RW, Loulier K, Keskin DB, Rosains J, Rivera-Feliciano J, Lichtman JW,  
1034 Livet J, Stern JNH, Sanes JR, Eggan K. 2013. Developmental Bias in Cleavage-Stage Mouse  
1035 Blastomeres. *Curr Biol* **23**:21–31. doi:10.1016/j.cub.2012.10.054

1036 Takahashi T, Nowakowski R, Caviness V. 1995a. The cell cycle of the pseudostratified ventricular  
1037 epithelium of the embryonic murine cerebral wall. *J Neurosci* **15**:6046–6057.  
1038 doi:10.1523/jneurosci.15-09-06046.1995

1039 Takahashi T, Nowakowski R, Caviness V. 1995b. Early ontogeny of the secondary proliferative  
1040 population of the embryonic murine cerebral wall. *J Neurosci* **15**:6058–6068.  
1041 doi:10.1523/jneurosci.15-09-06058.1995

1042 Tennyson CN, Klamut HJ, Worton RG. 1995. The human dystrophin gene requires 16 hours to be  
1043 transcribed and is cotranscriptionally spliced. *Nat Genet* **9**:ng0295-184. doi:10.1038/ng0295-184

1044 Valentine JW, Collins AG, Meyer CP. 1994. Morphological complexity increase in metazoans.  
1045 *Paleobiology* **20**:131–142. doi:10.1017/s0094837300012641

1046 Vallier L. 2015. Cell Cycle Rules Pluripotency. *Cell Stem Cell* **17**:131–132.  
1047 doi:10.1016/j.stem.2015.07.019

1048 Vogel C, Chothia C. 2006. Protein Family Expansions and Biological Complexity. *Plos Comput Biol*  
1049 **2**:e48. doi:10.1371/journal.pcbi.0020048

1050 Wagner DE, Weinreb C, Collins ZM, Briggs JA, Megason SG, Klein AM. 2018. Single-cell mapping of  
1051 gene expression landscapes and lineage in the zebrafish embryo. *Science* **360**:981–987.  
1052 doi:10.1126/science.aar4362

1053 Wilmut I, Schnieke AE, McWhir J, Kind AJ, Campbell KHS. 1997. Viable offspring derived from fetal  
1054 and adult mammalian cells. *Nature* **385**:810–813. doi:10.1038/385810a0

1055 Wolfram-Research. 2017. Mathematica version 11.0–12.0.

1056 Yates A, Akanni W, Amode MR, Barrell D, Billis K, Carvalho-Silva D, Cummins C, Clapham P,  
1057 Fitzgerald S, Gil L, Girón CG, Gordon L, Hourlier T, Hunt SE, Janacek SH, Johnson N, Juettemann  
1058 T, Keenan S, Lavidas I, Martin FJ, Maurel T, McLaren W, Murphy DN, Nag R, Nuhn M, Parker A,  
1059 Patricio M, Pignatelli M, Rahtz M, Riat HS, Sheppard D, Taylor K, Thormann A, Vullo A, Wilder

1060 SP, Zadissa A, Birney E, Harrow J, Muffato M, Perry E, Ruffier M, Spudich G, Trevanion SJ,  
1061 Cunningham F, Aken BL, Zerbino DR, Flicek P. 2016. Ensembl 2016. *Nucleic Acids Res* **44**:D710–  
1062 D716. doi:10.1093/nar/gkv1157

1063 Yoon K-J, Ringeling FR, Vissers C, Jacob F, Pokrass M, Jimenez-Cyrus D, Su Y, Kim N-S, Zhu Y,  
1064 Zheng L, Kim S, Wang X, Doré LC, Jin P, Regot S, Zhuang X, Canzar S, He C, Ming G, Song H.  
1065 2017. Temporal Control of Mammalian Cortical Neurogenesis by m6A Methylation. *Cell* **171**:877–  
1066 889.e17. doi:10.1016/j.cell.2017.09.003

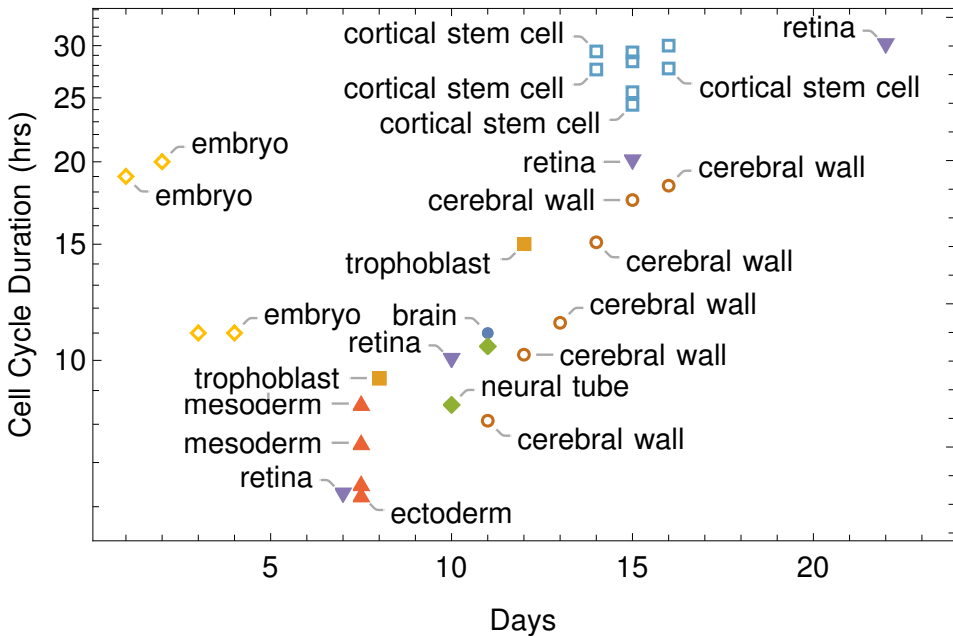
1067 Yuan K, Seller CA, Shermoen AW, O’Farrell PH. 2016. Timing the Drosophila Mid-Blastula  
1068 Transition: A Cell Cycle-Centered View. *Trends Genet* **32**:496–507. doi:10.1016/j.tig.2016.05.006

1069 Yuzwa SA, Borrett MJ, Innes BT, Voronova A, Ketela T, Kaplan DR, Bader GD, Miller FD. 2017.  
1070 Developmental Emergence of Adult Neural Stem Cells as Revealed by Single-Cell Transcriptional  
1071 Profiling. *Cell Reports* **21**:3970–3986. doi:10.1016/j.celrep.2017.12.017

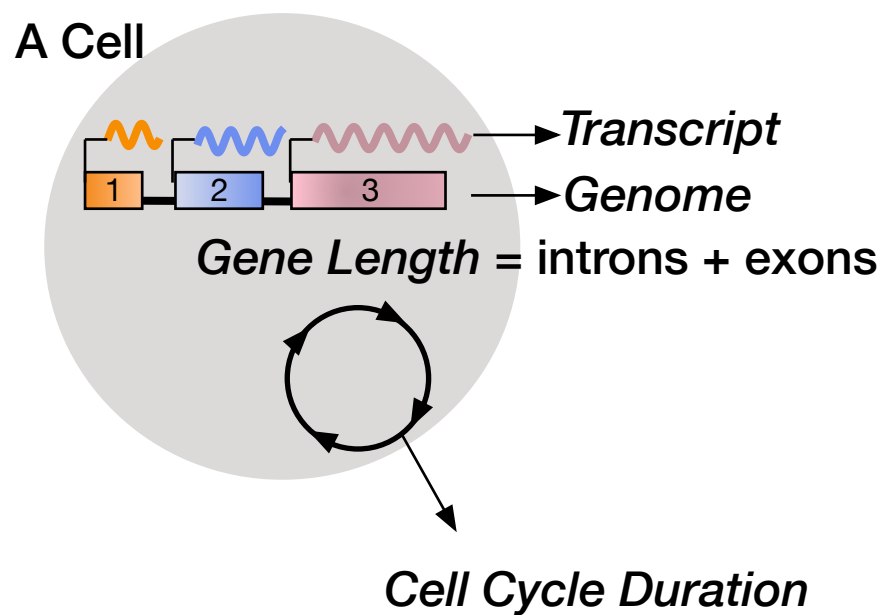
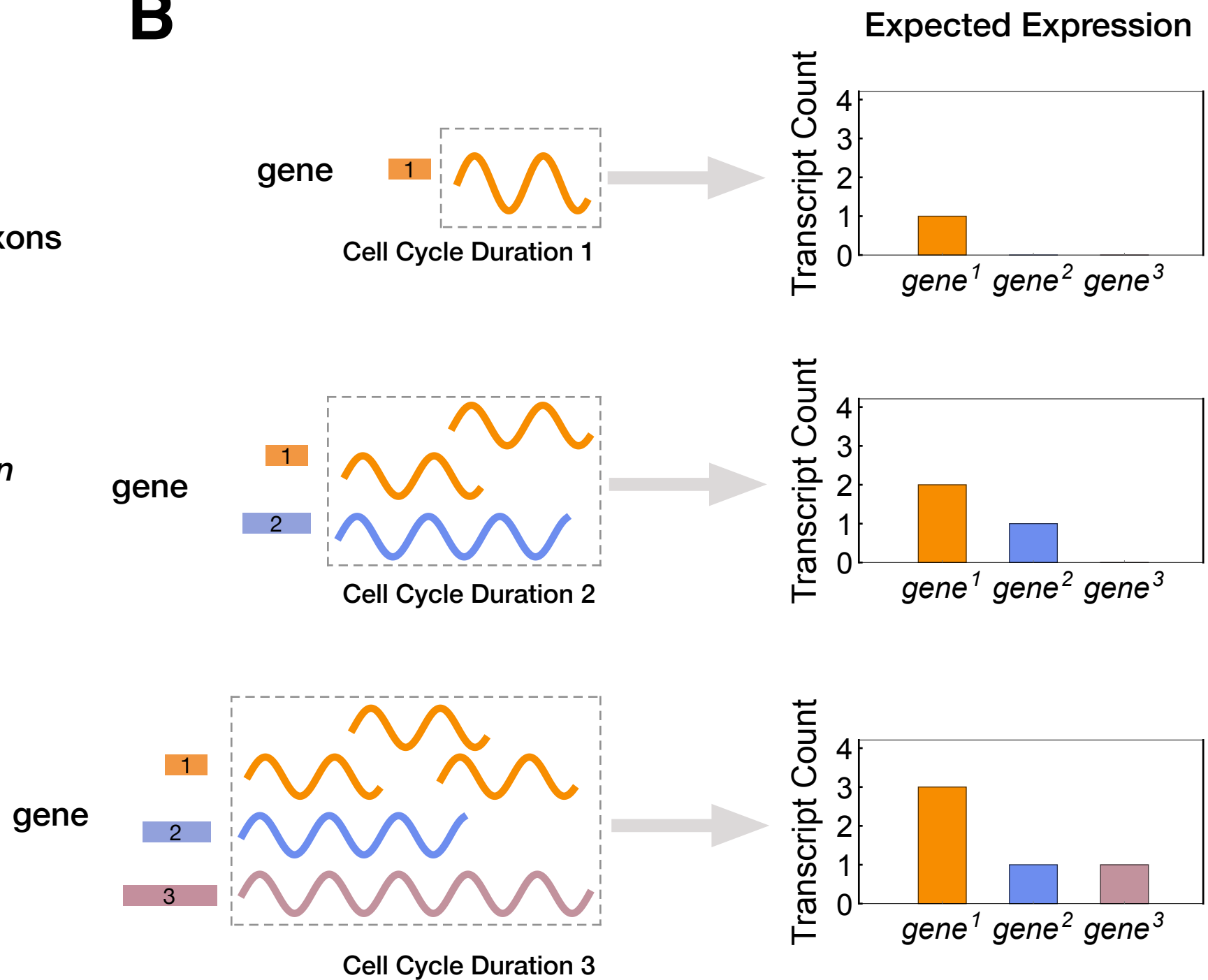
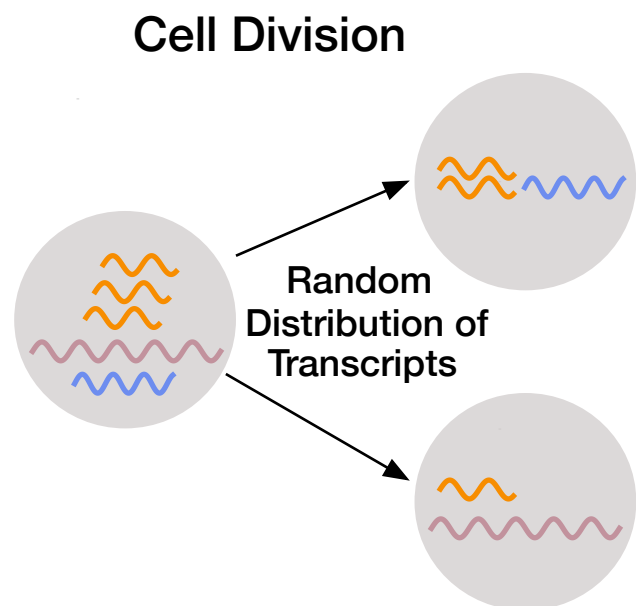
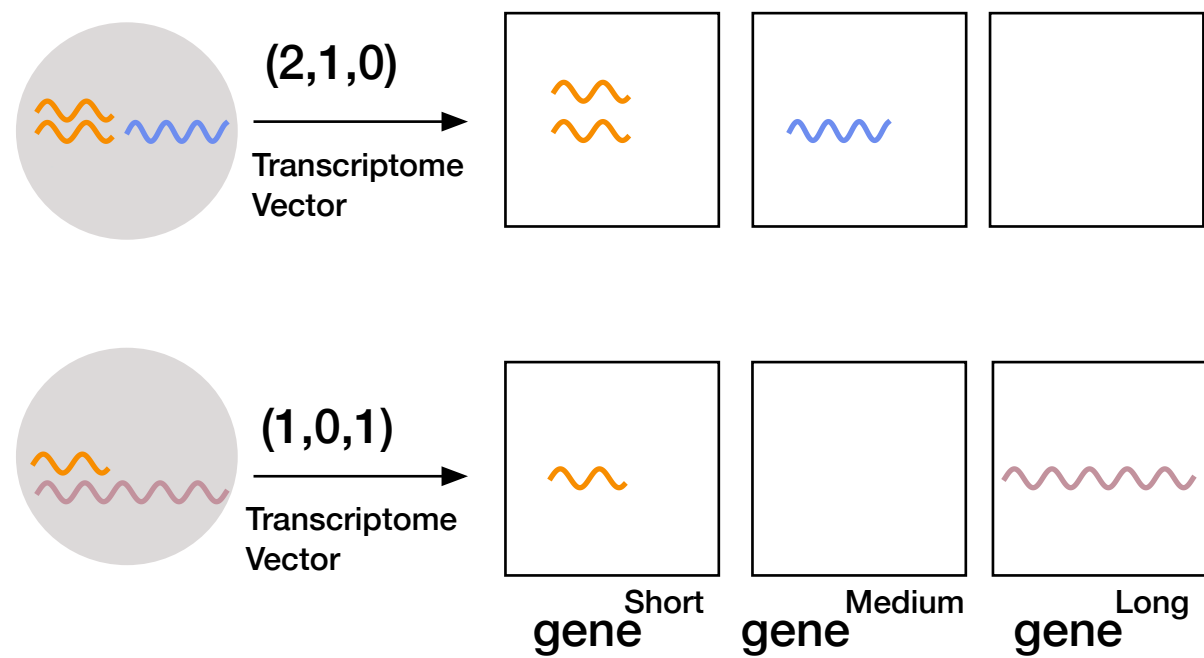
1072 Zhou C, Slaughter BD, Unruh JR, Eldakak A, Rubinstein B, Li R. 2011. Motility and Segregation of  
1073 Hsp104-Associated Protein Aggregates in Budding Yeast. *Cell* **147**:1186–1196.  
1074 doi:10.1016/j.cell.2011.11.002

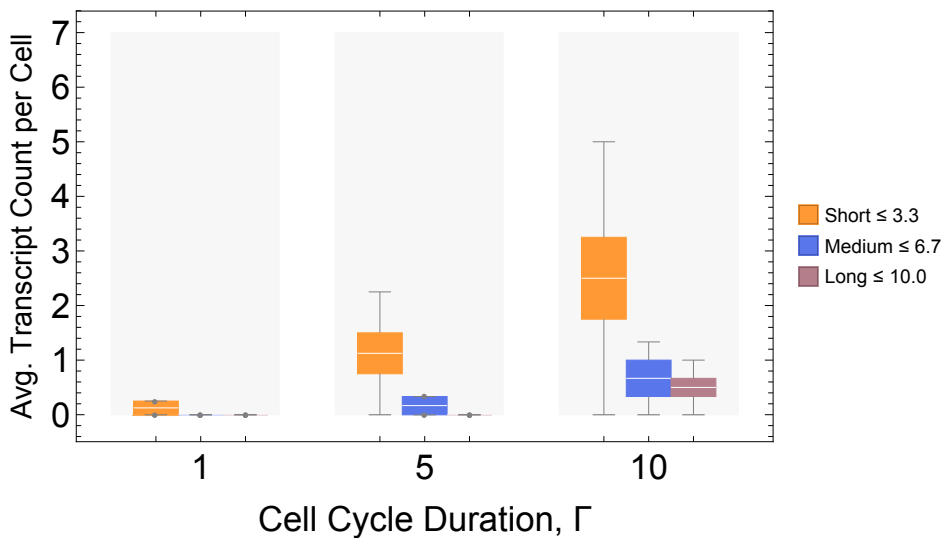
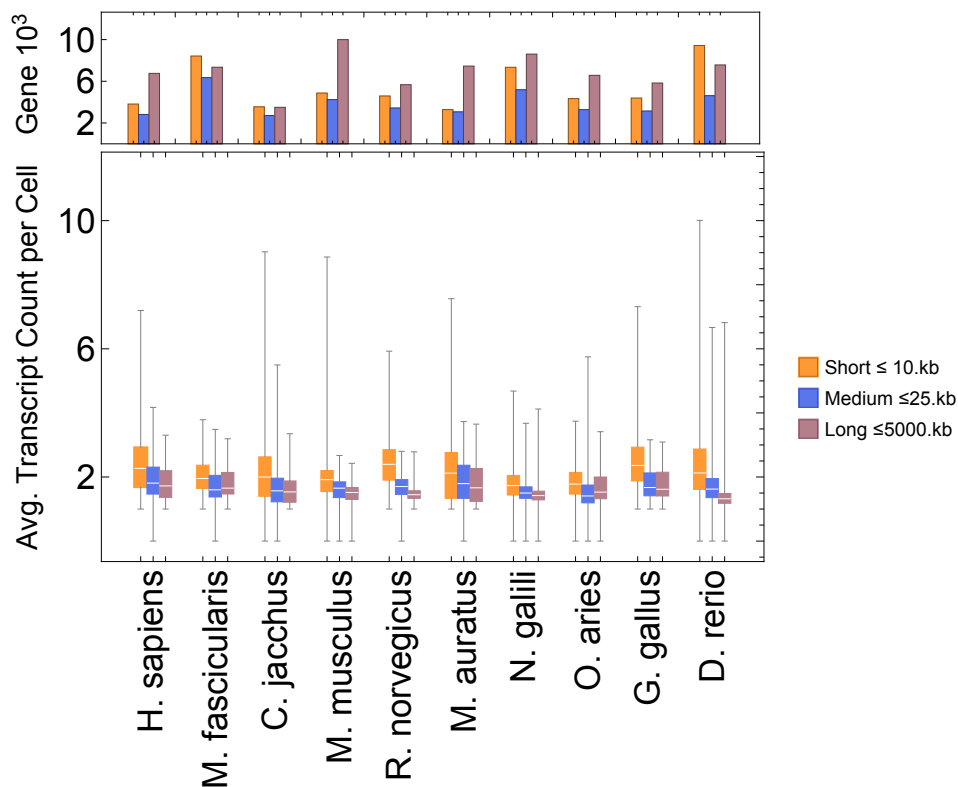
1075 Zoller B, Little SC, Gregor T. 2018. Diverse Spatial Expression Patterns Emerge from Unified Kinetics  
1076 of Transcriptional Bursting. *Cell* **175**:835–847.e25. doi:10.1016/j.cell.2018.09.056  
1077  
1078  
1079  
1080  
1081  
1082

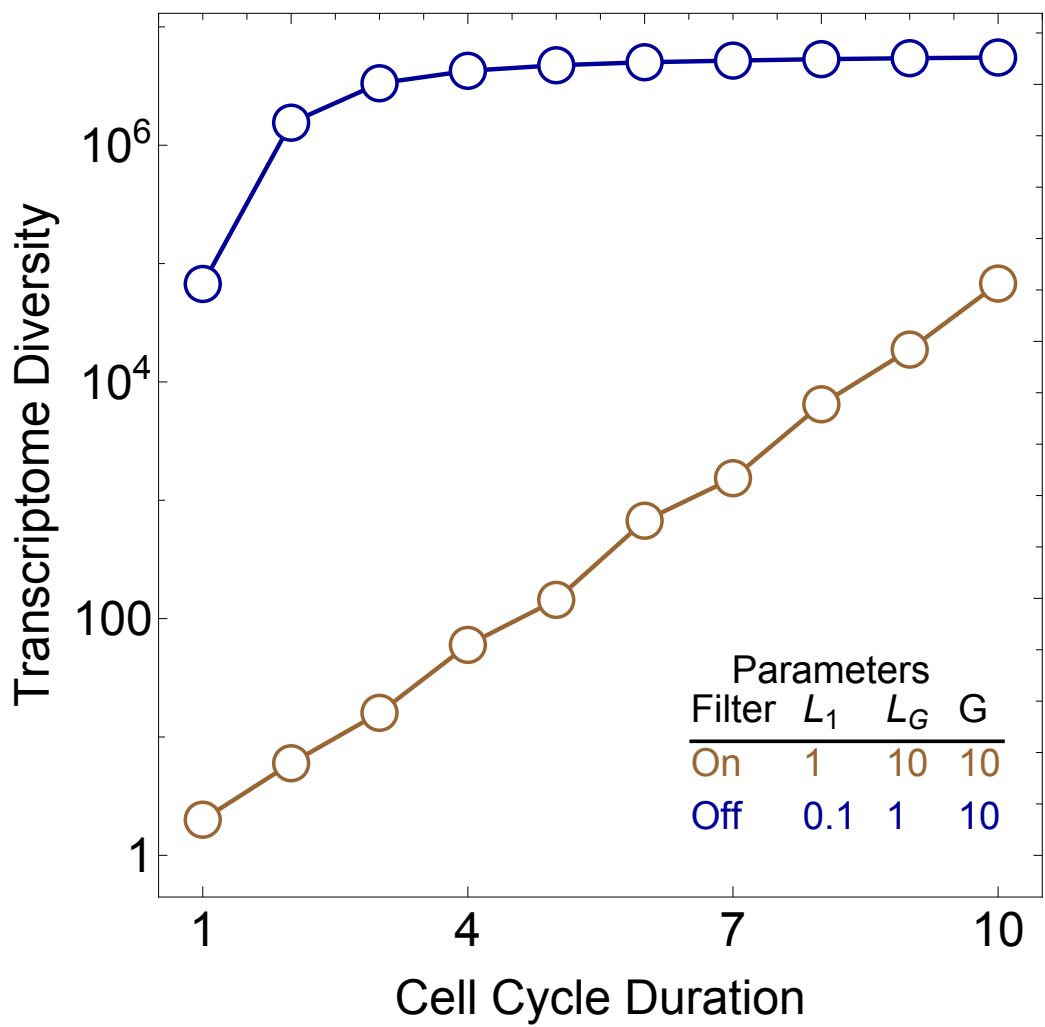
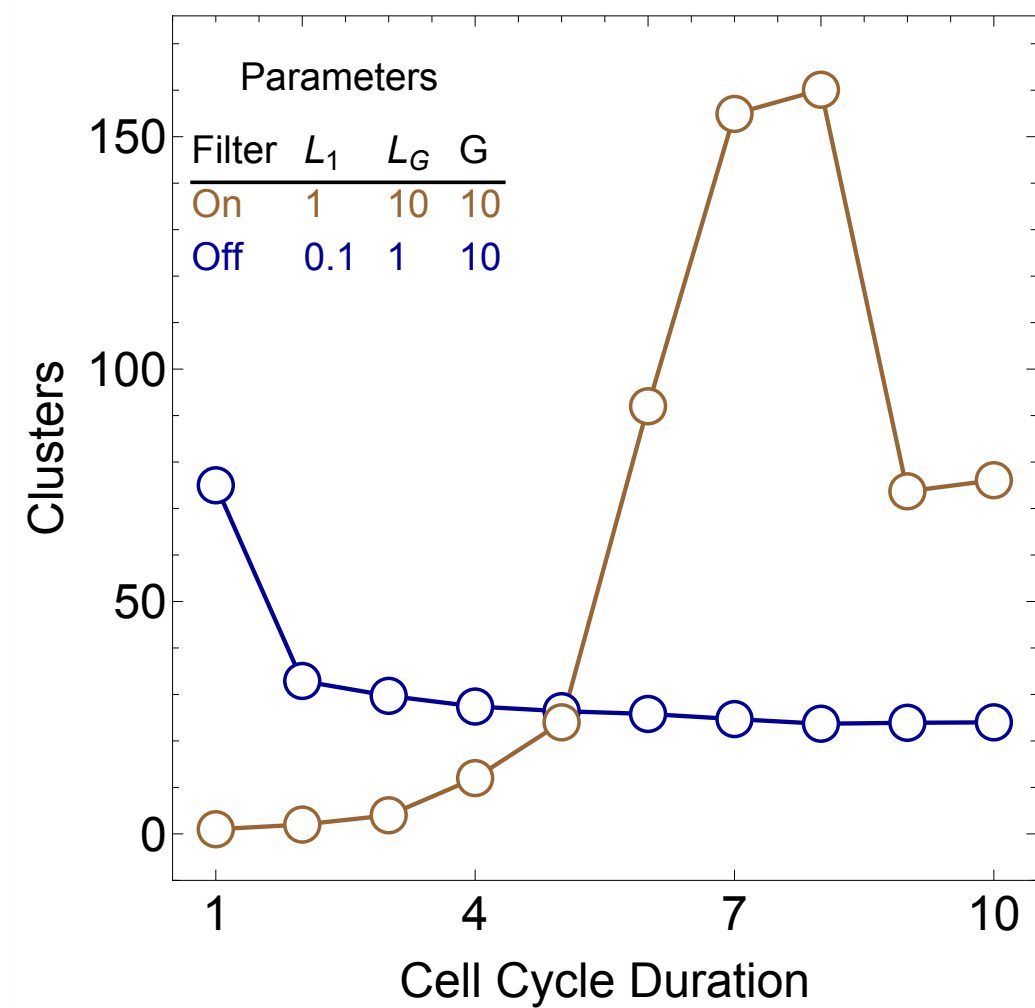
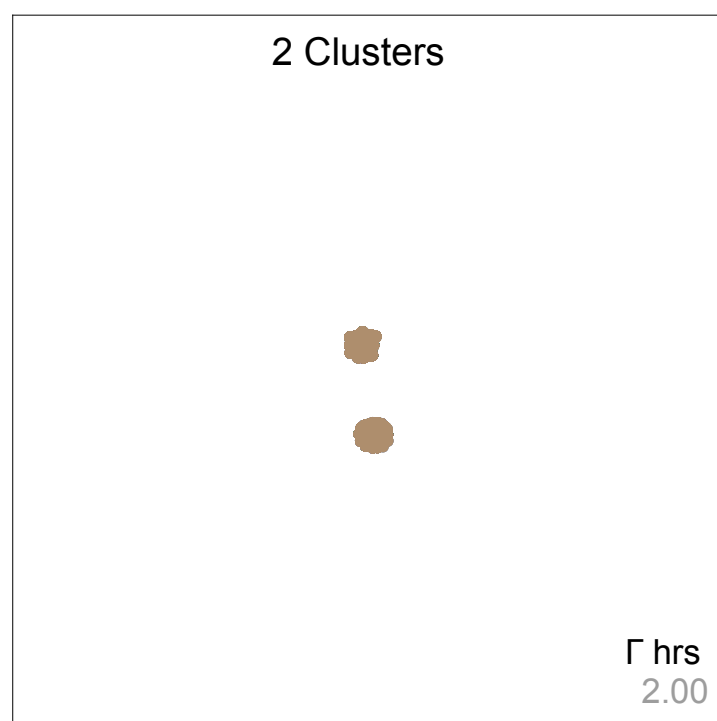
# M. musculus



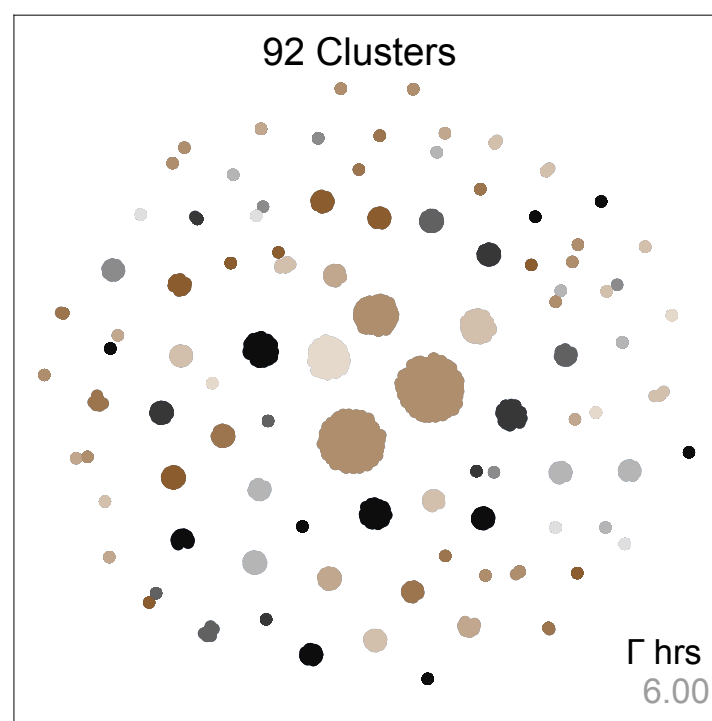
- Altas M., Bond VP. (1965)
- Cameron IL. (1964)
- ◆ Kauffman SL. (1968)
- ▲ Solter D. et al (1971)
- ▼ Young RW. (1985)
- Takahashi T. (1995)
- Lukaszewicz A. et al (2002)
- ◇ Artus J., Cohen-Tannoudji M. (2008)

**A****B****C****D**

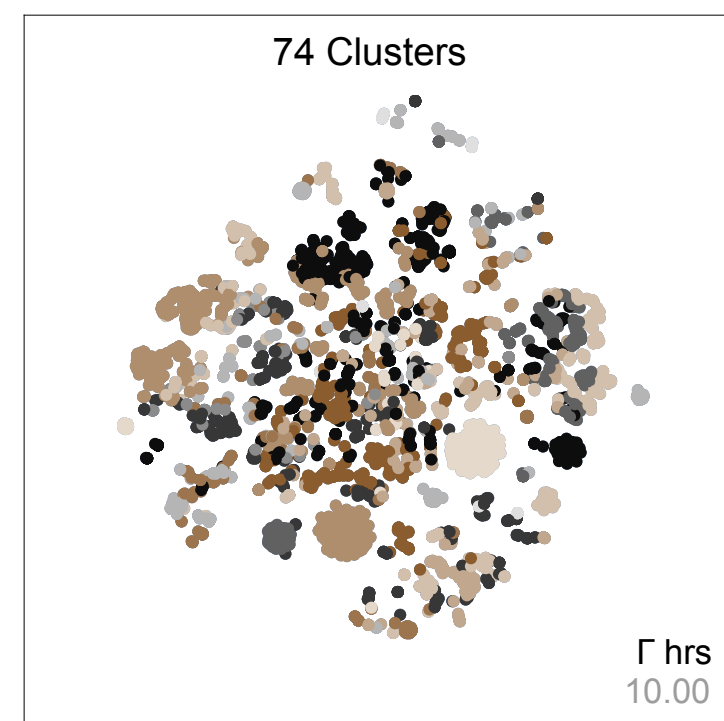
**A****Simulations****B****Species**

**A****B****C**

tsne



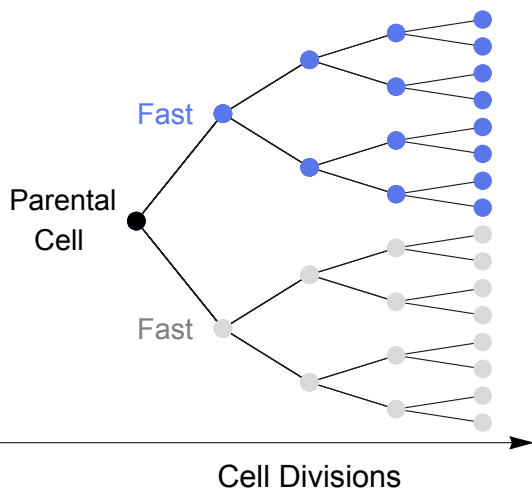
tsne



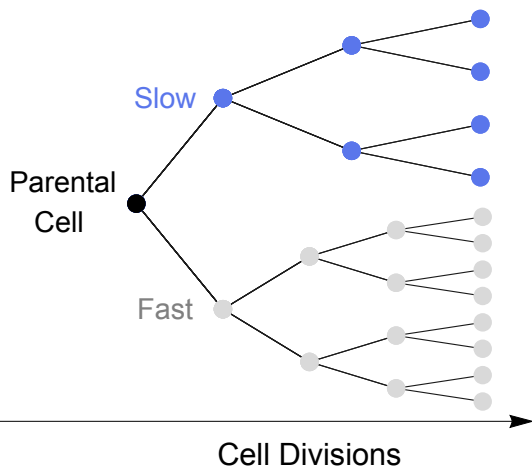
tsne

A

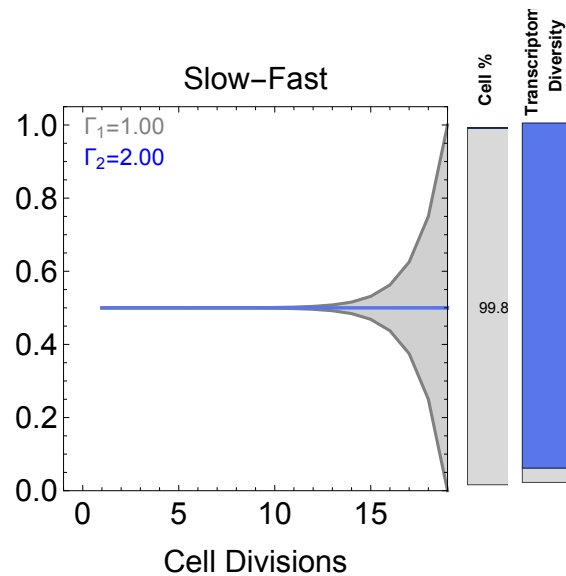
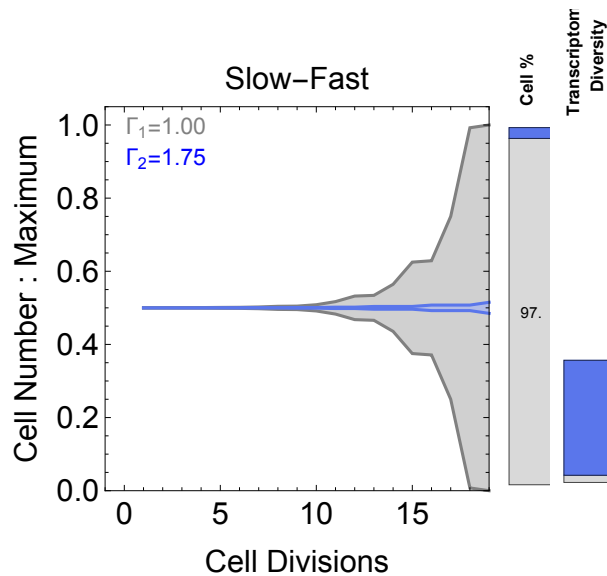
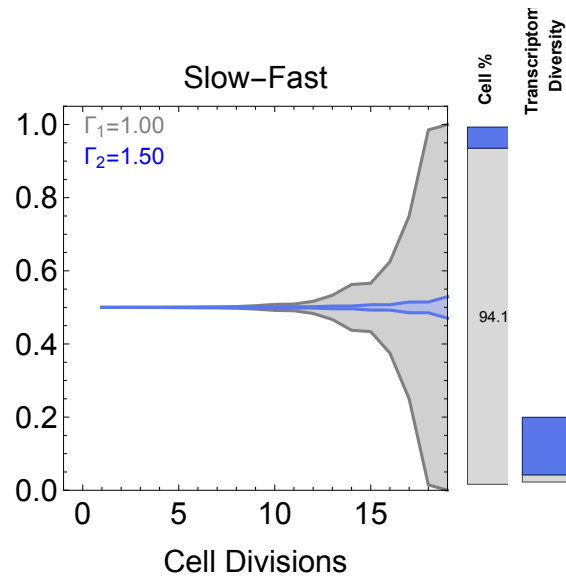
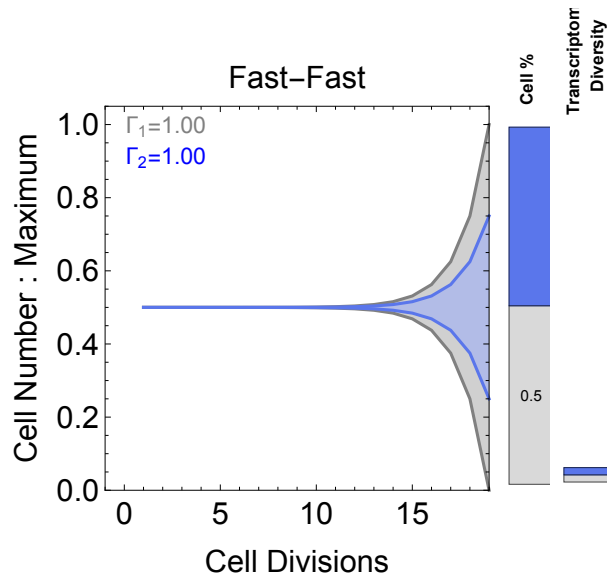
Scenario 1: Fast-Fast

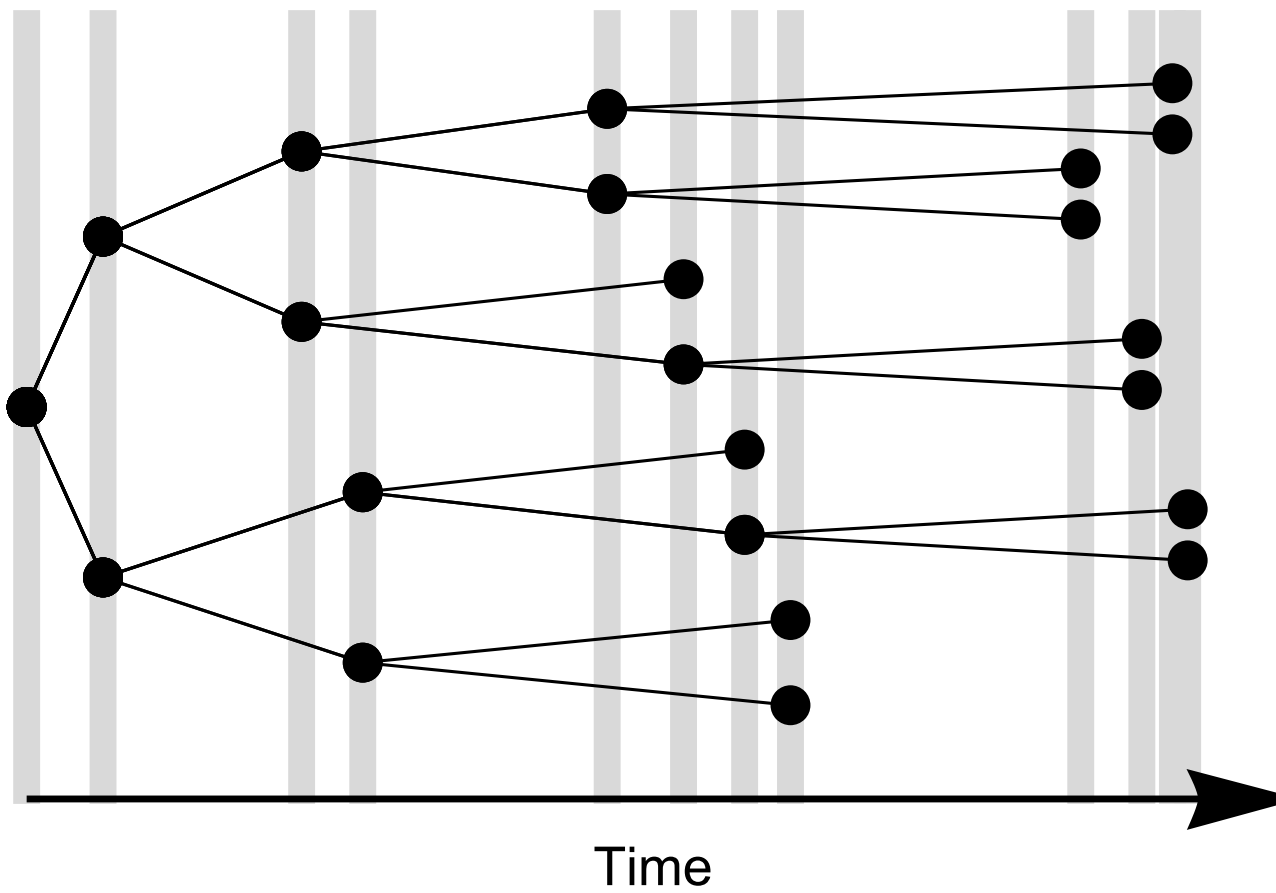
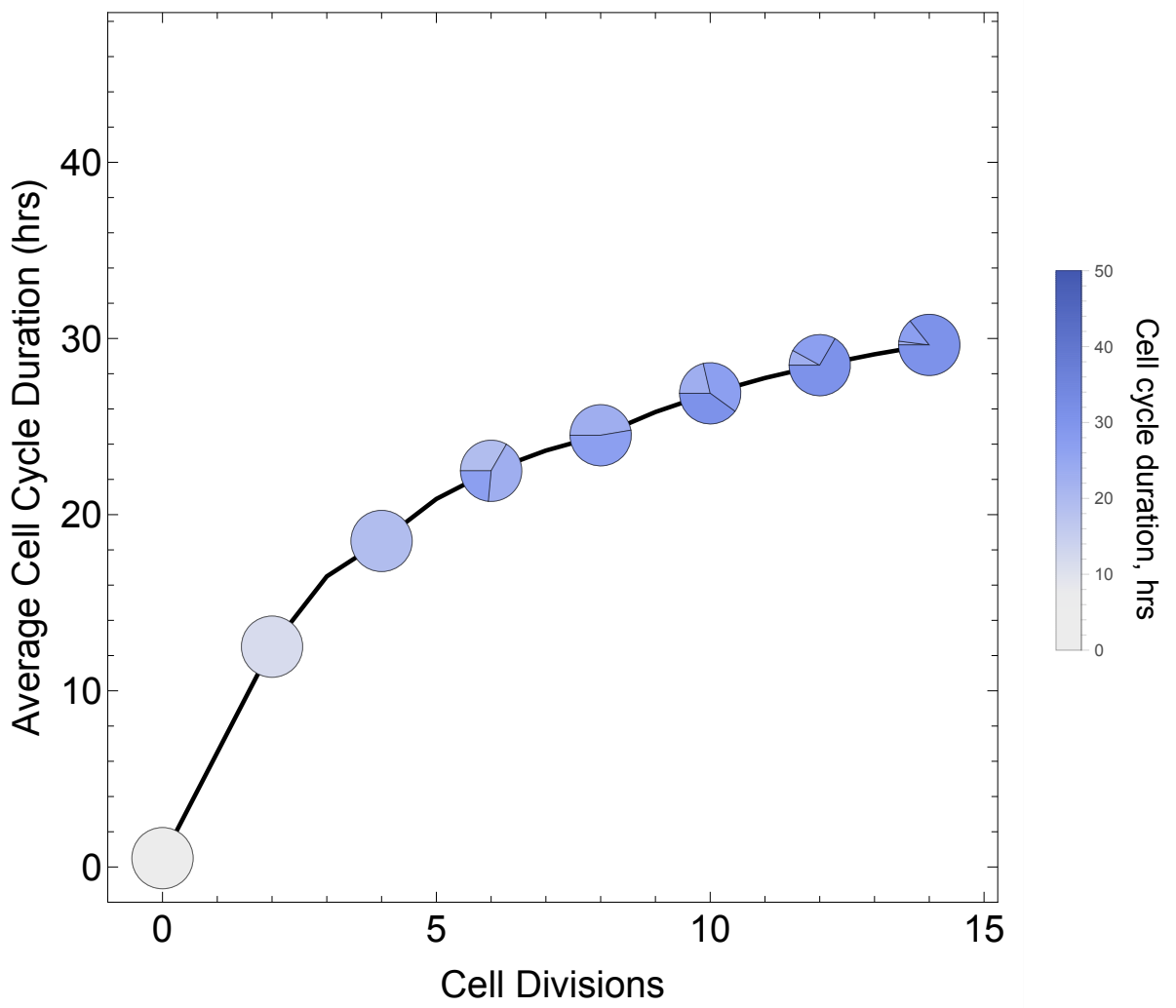
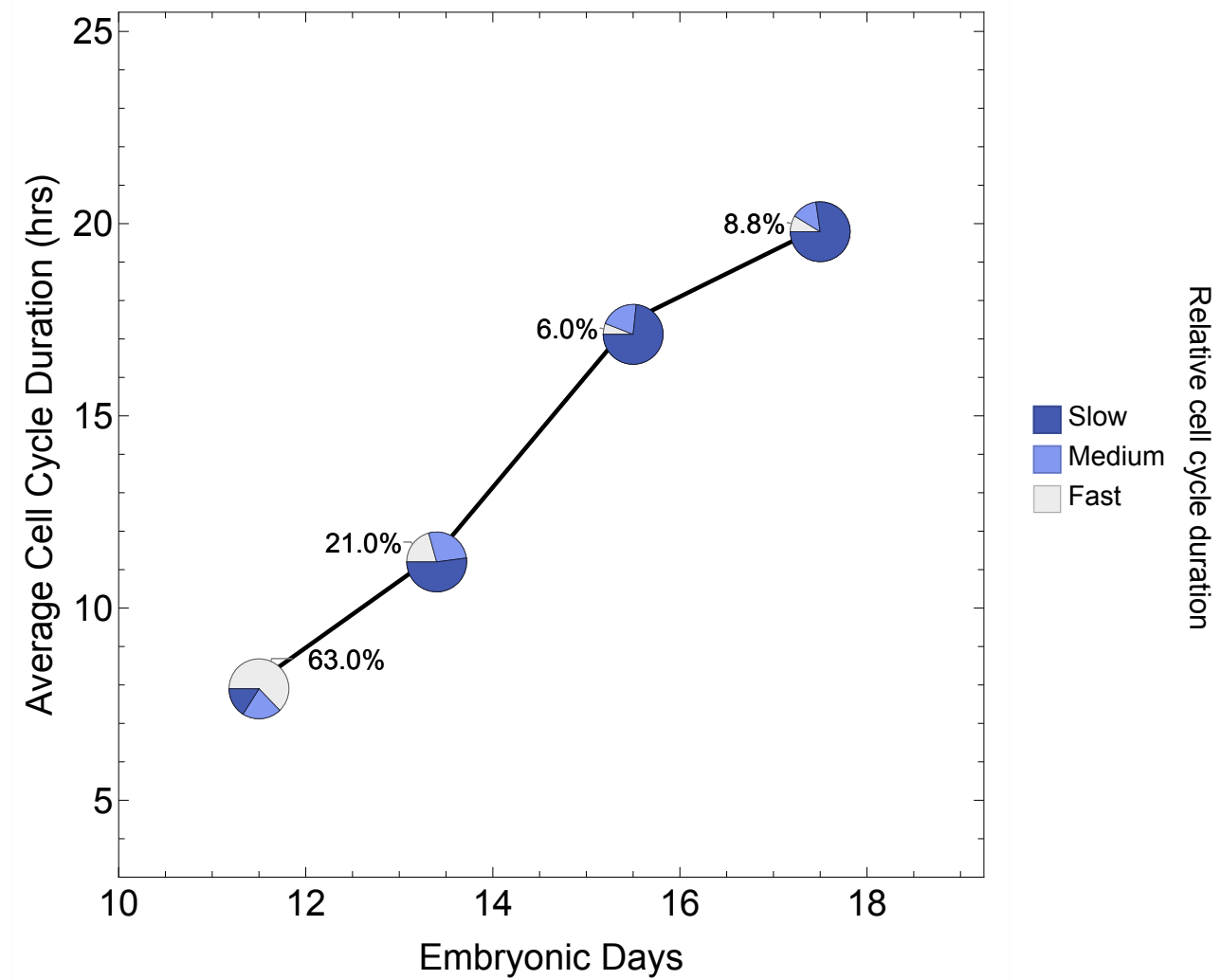


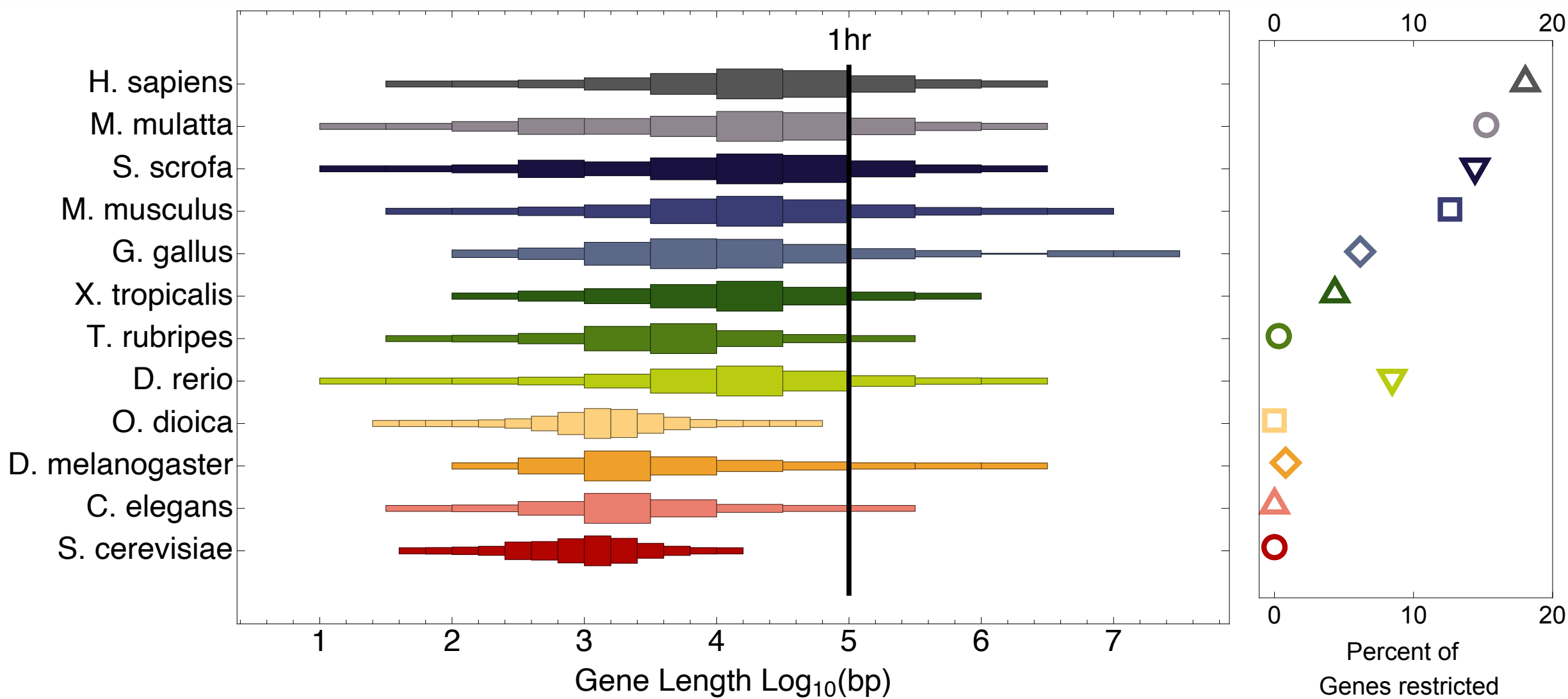
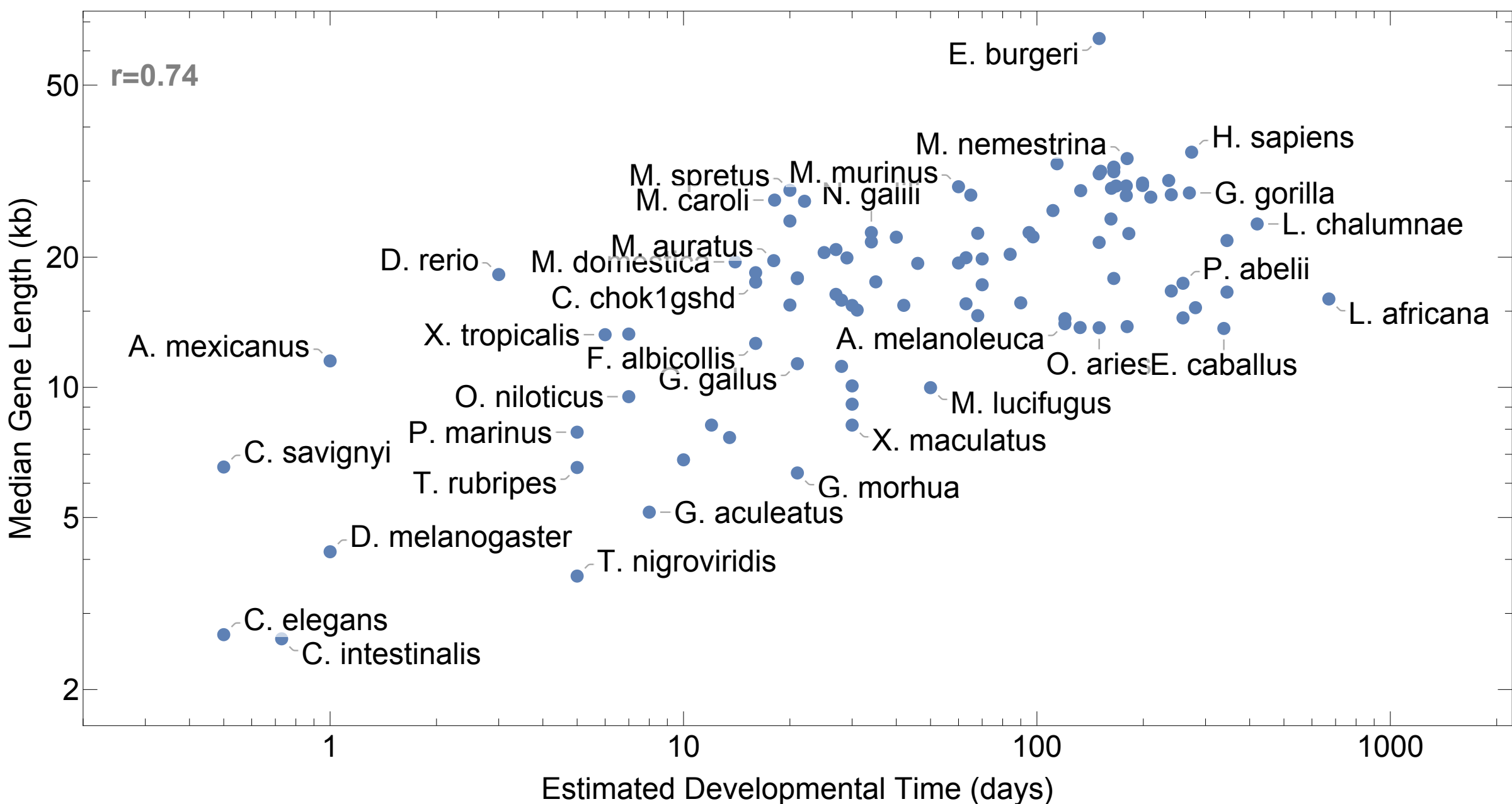
Scenario 2: Slow-Fast



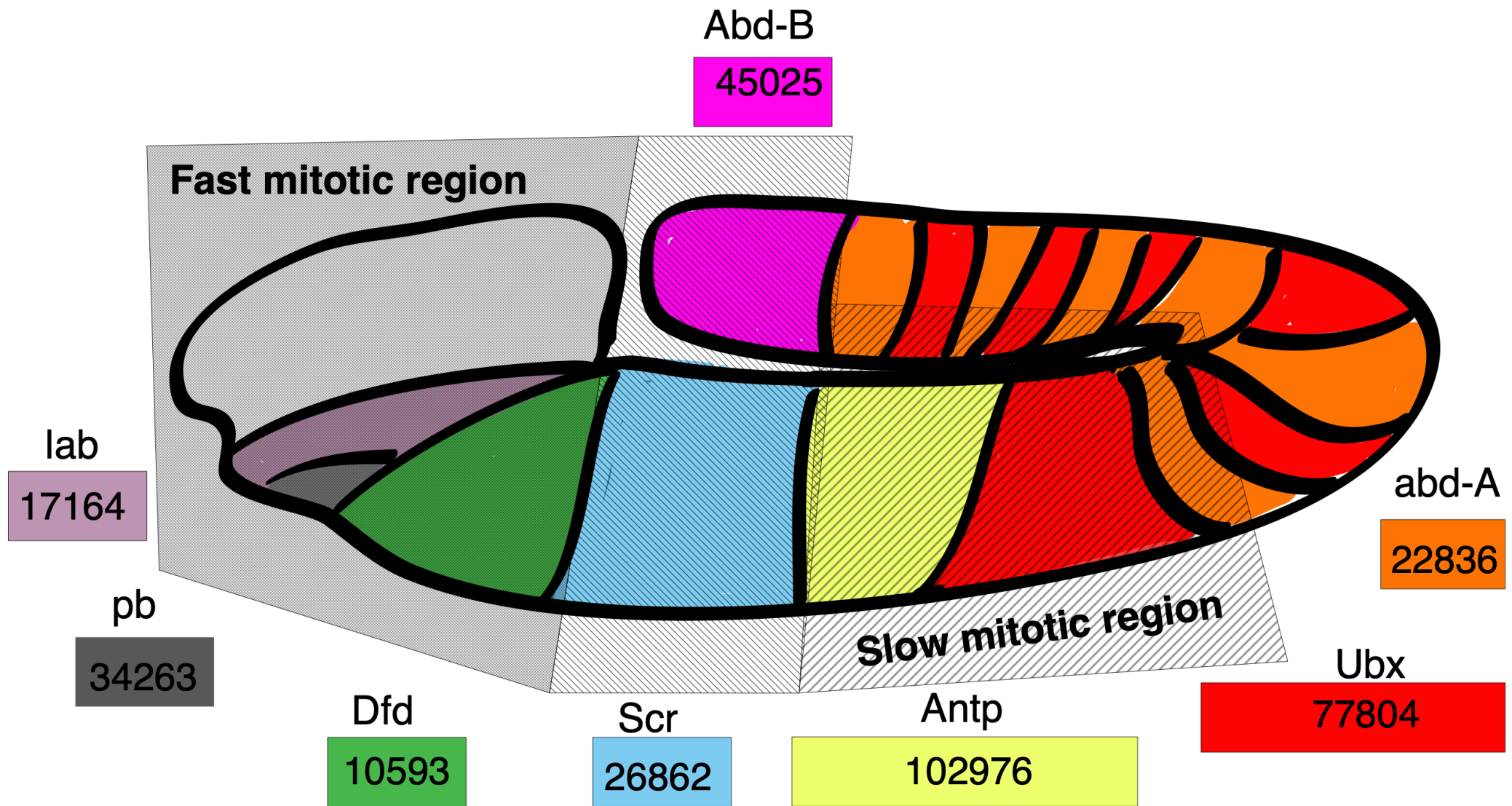
B



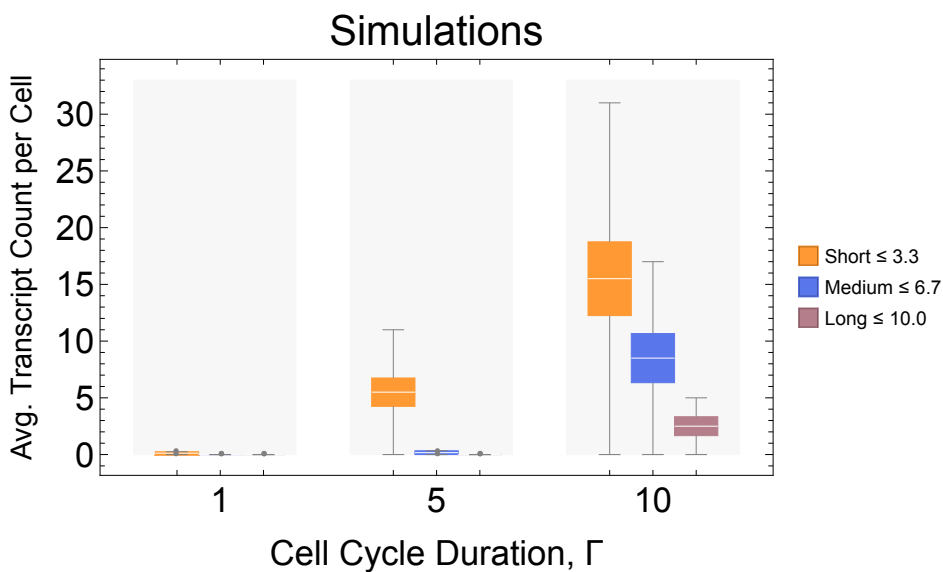
**A****Cell Divisions****B****Simulations****C****M. musculus cortex**

**A****B**

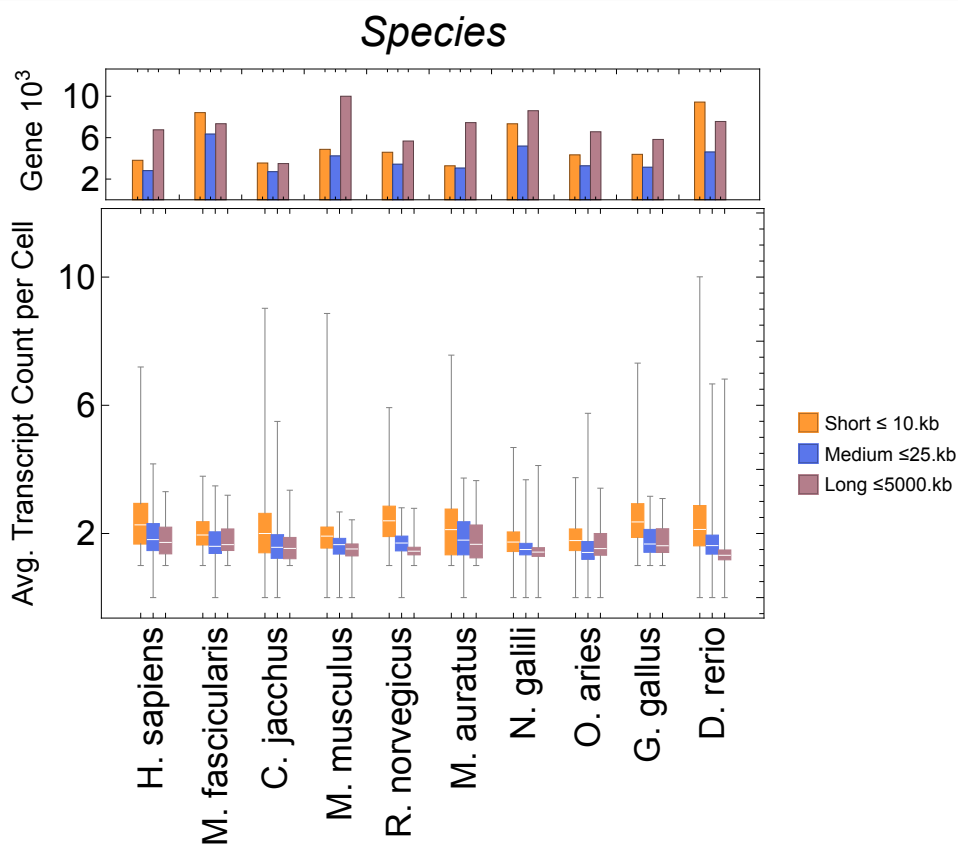




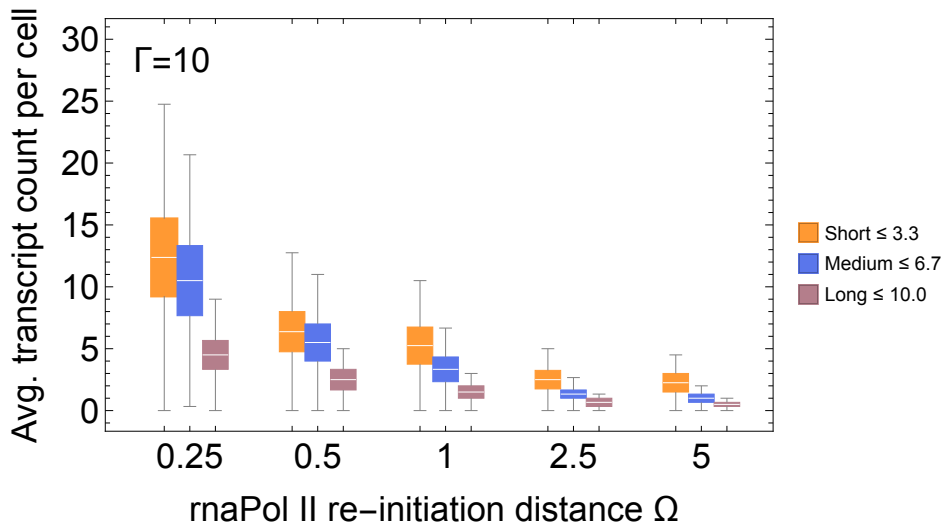
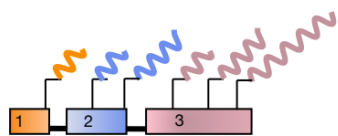
A



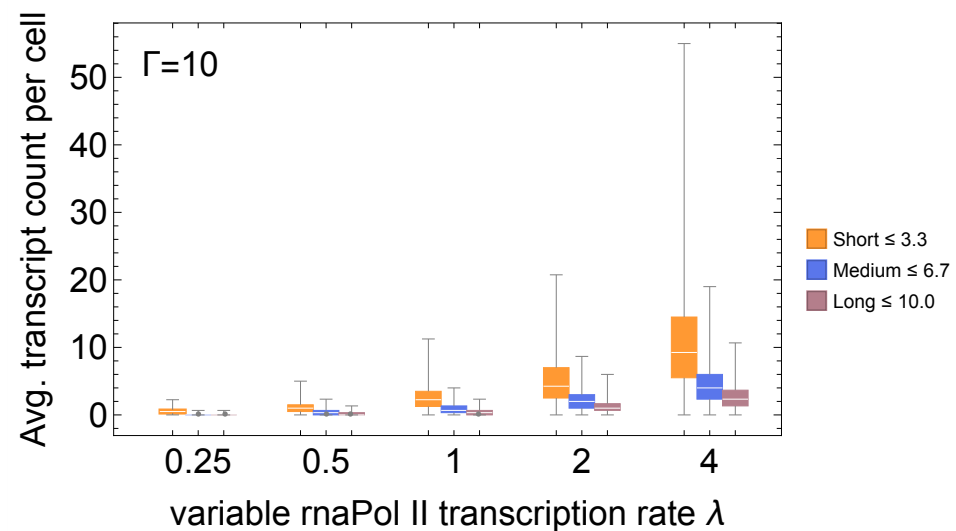
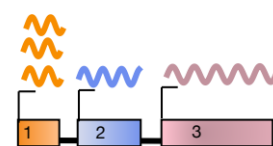
B



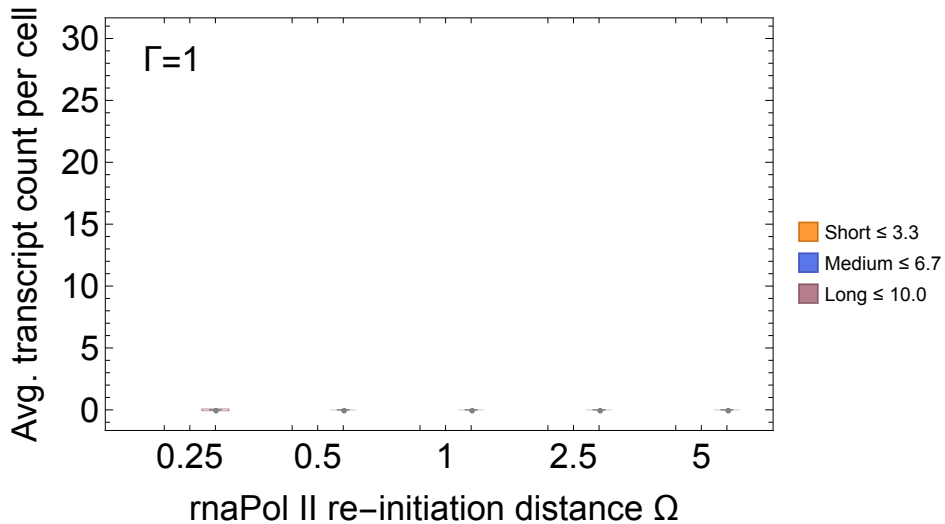
A



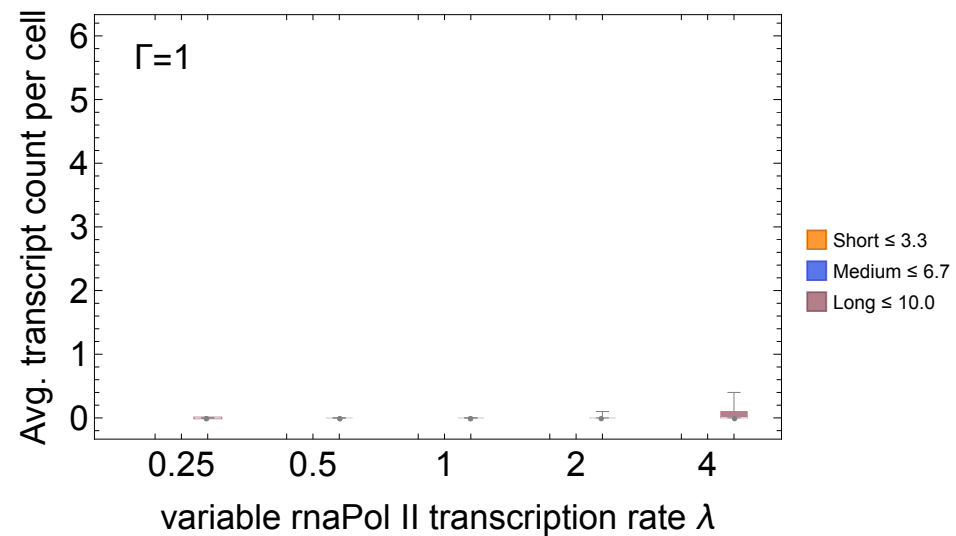
B



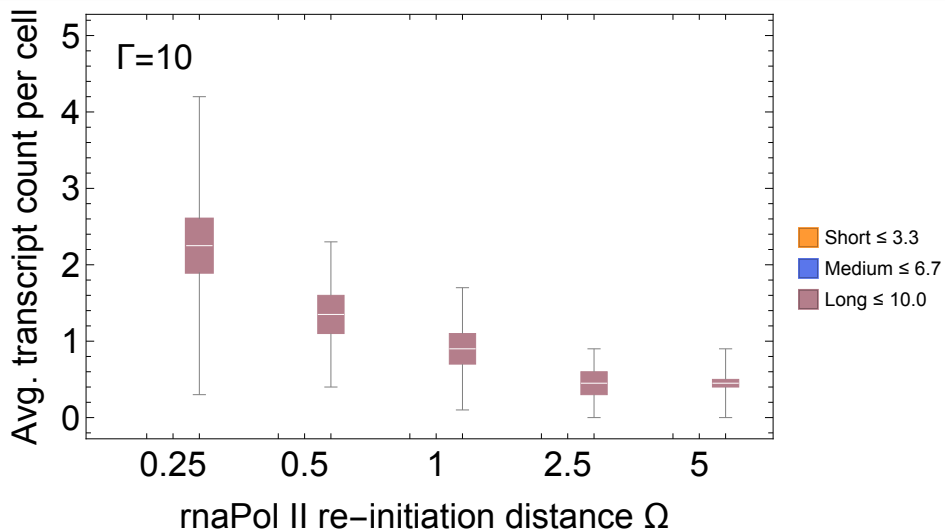
C



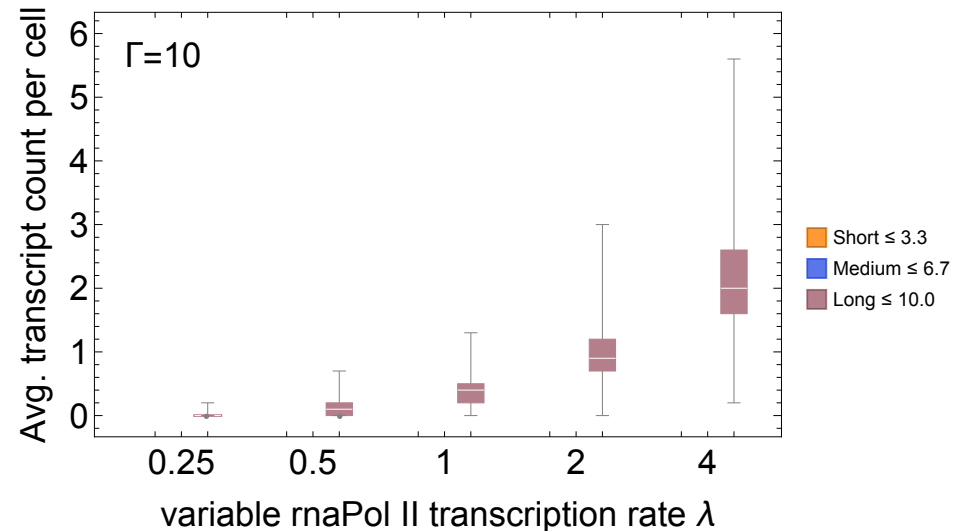
D



E

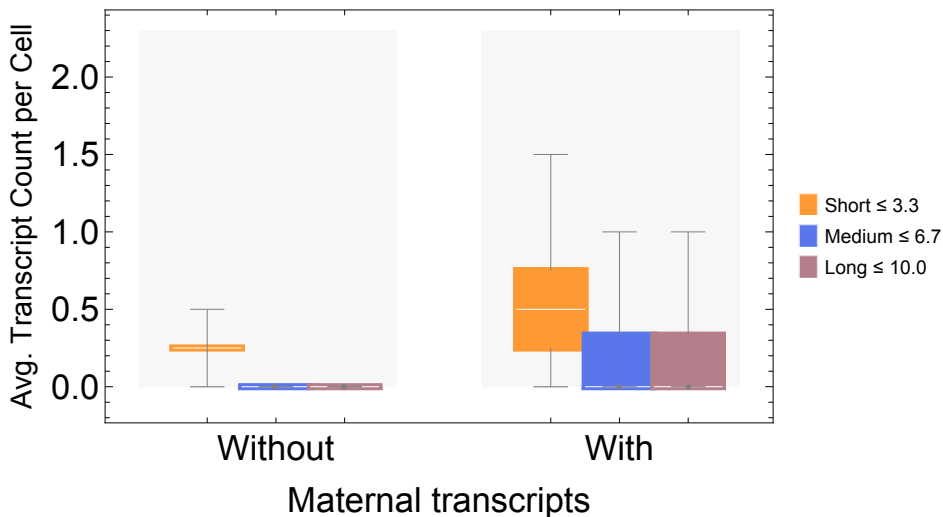
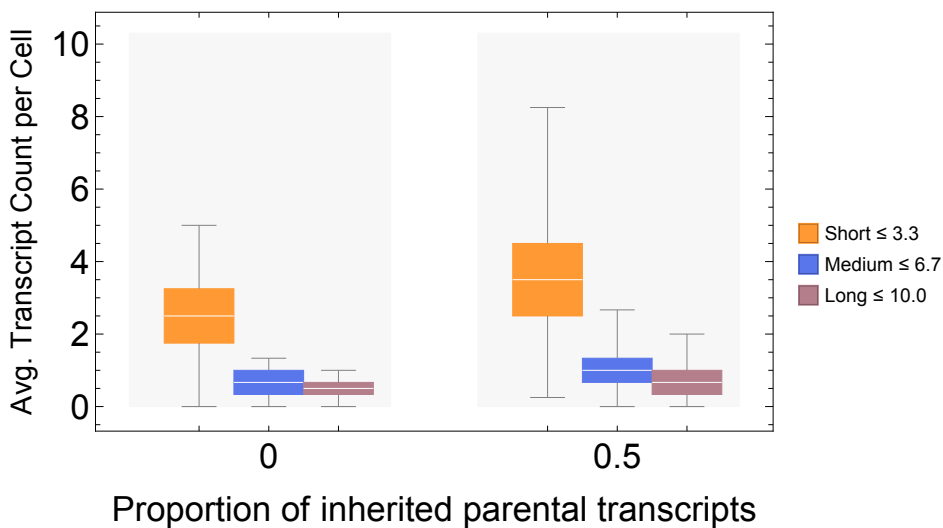


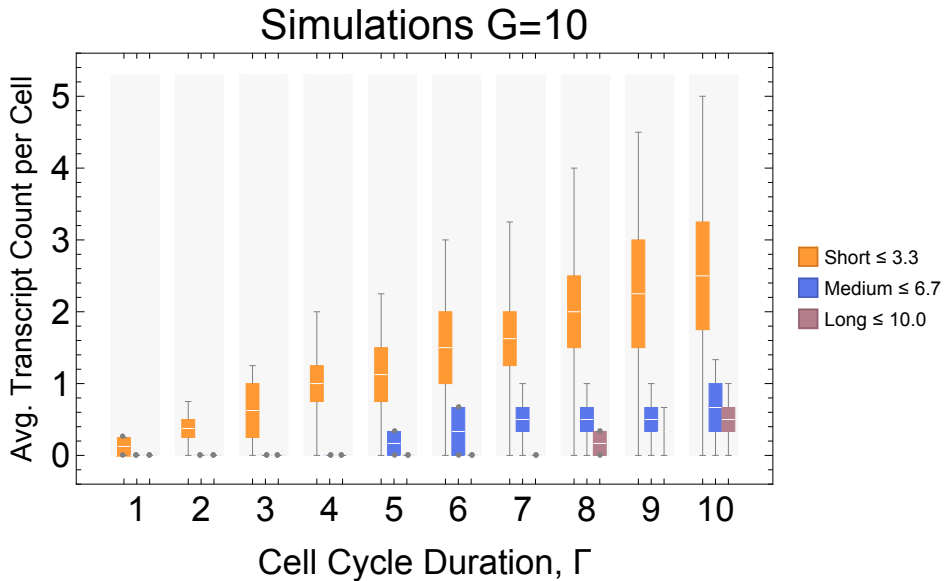
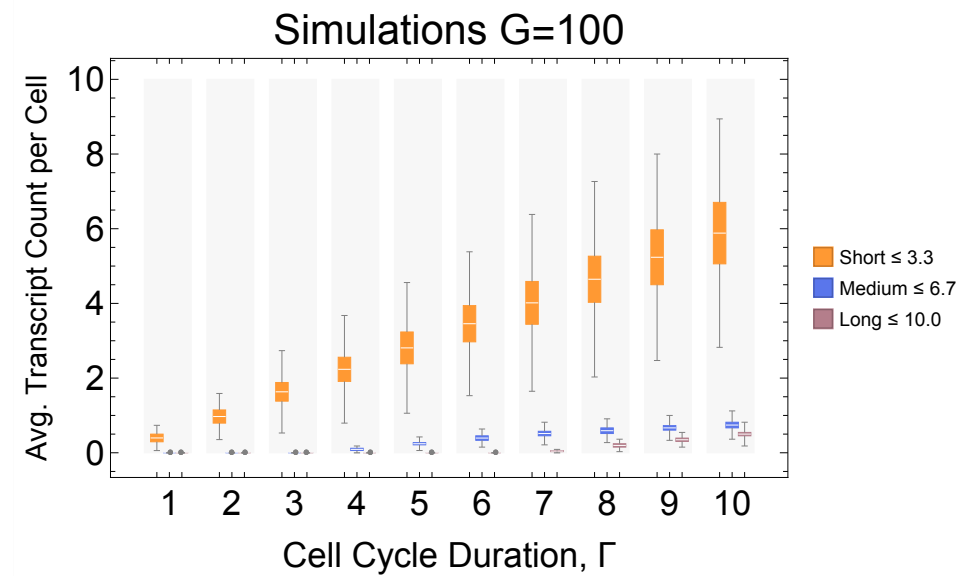
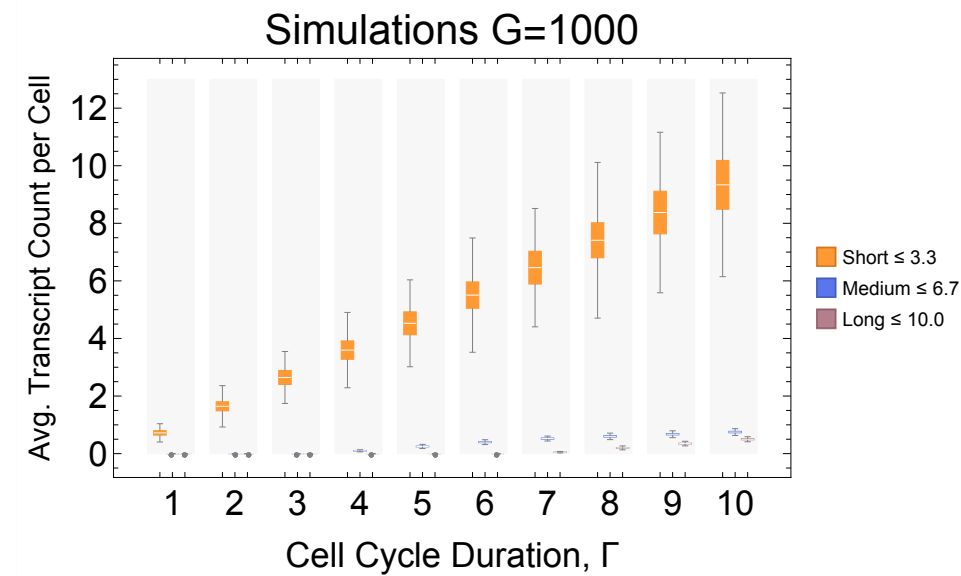
F



**A**

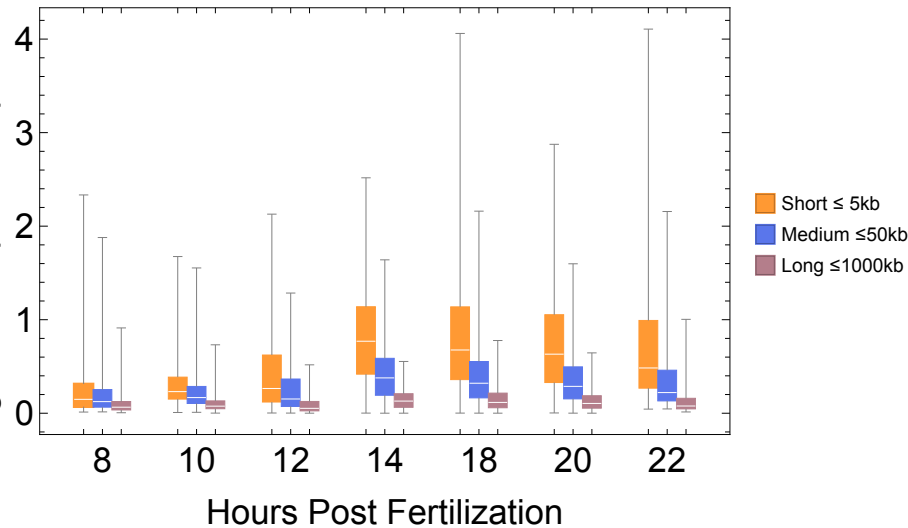
## Simulation

**B**

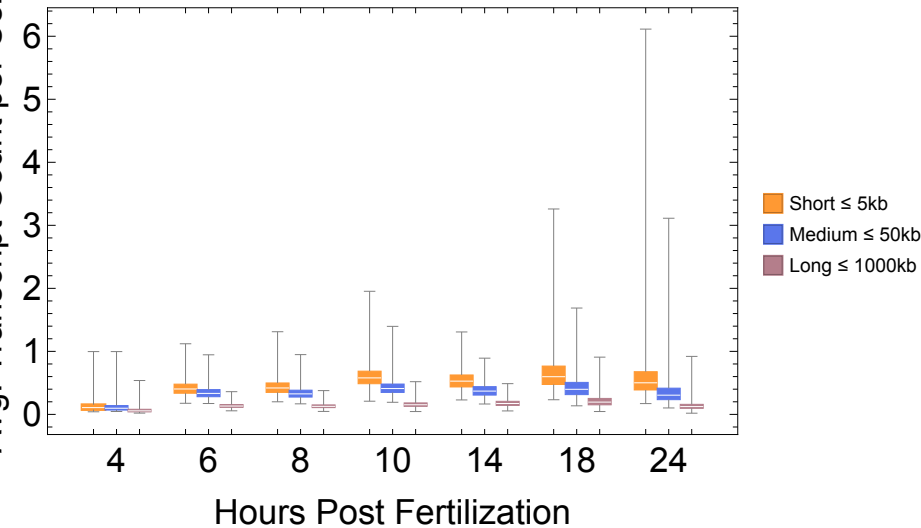
**A****B****C**

**A**

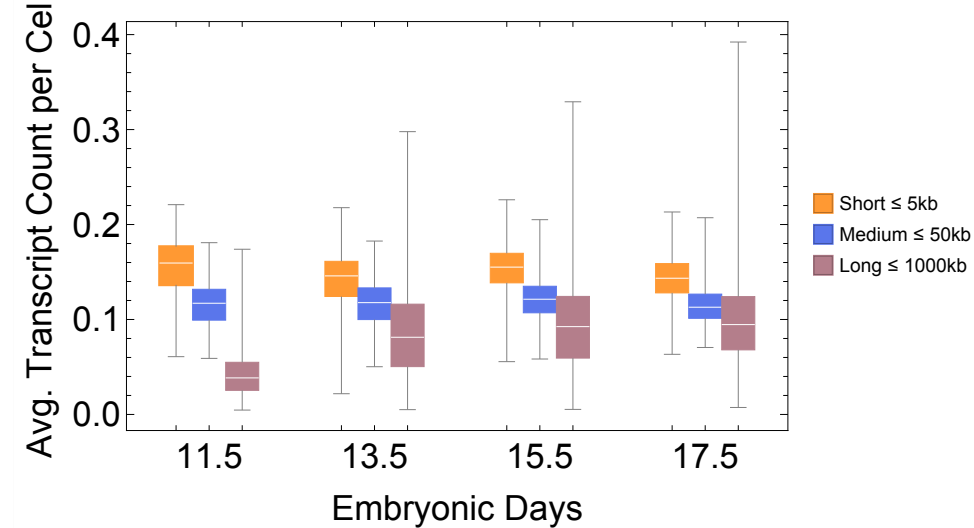
Avg. Transcript Count per Cell

*X. tropicalis***B**

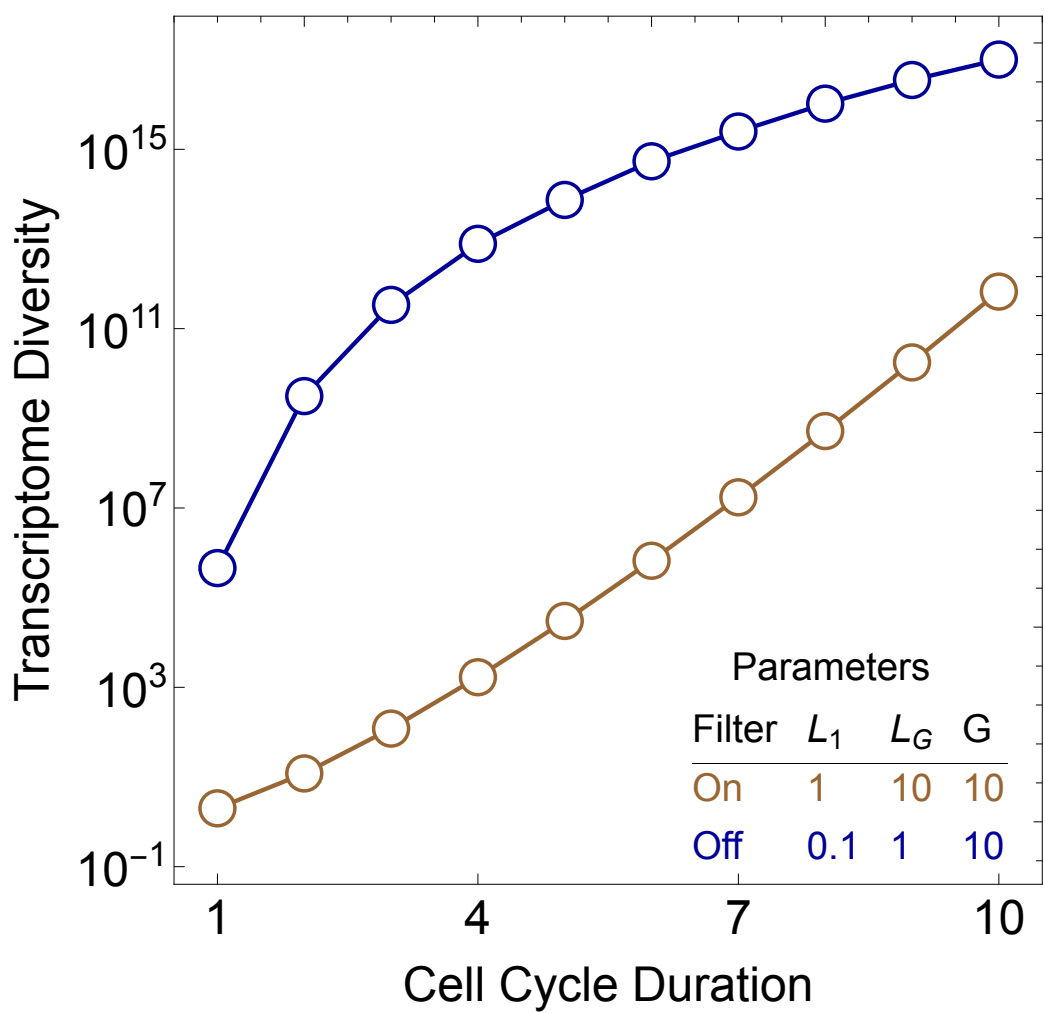
Avg. Transcript Count per Cell

*D. rerio***C**

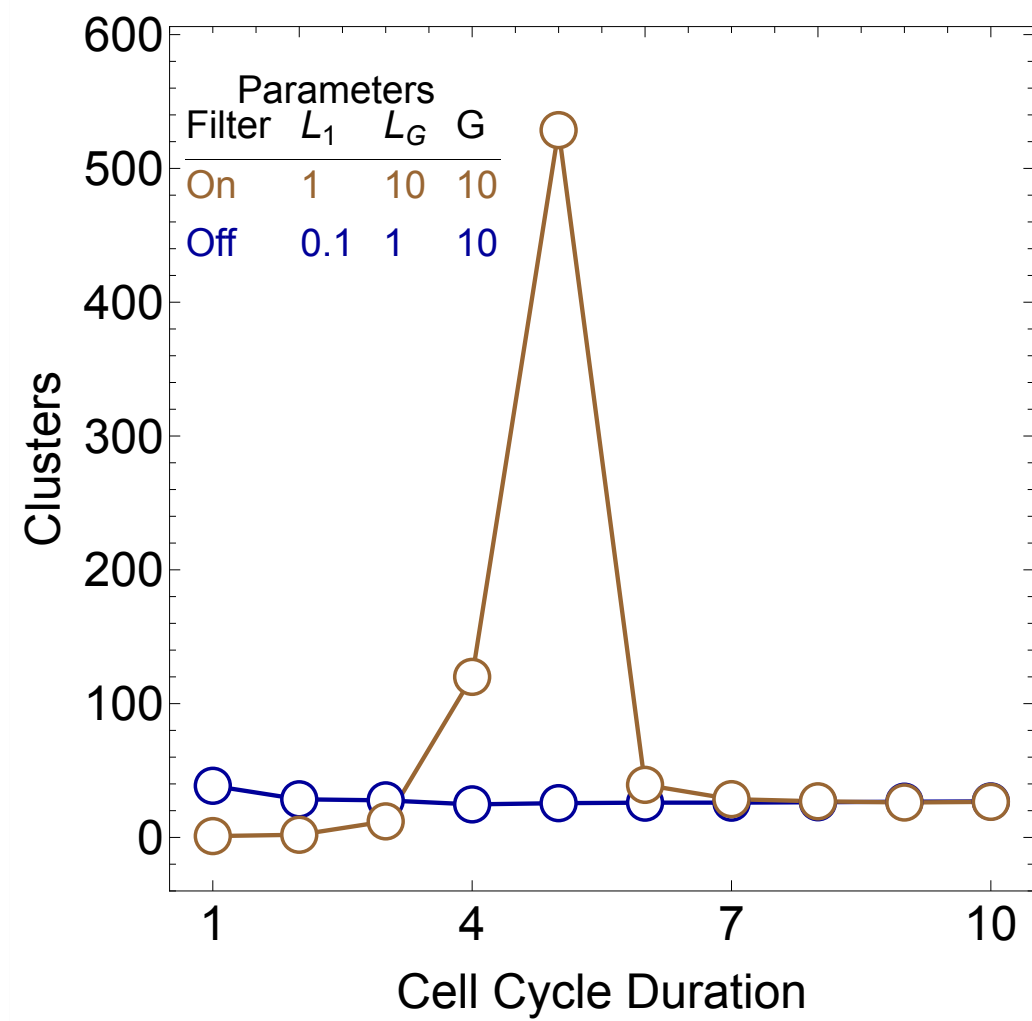
Avg. Transcript Count per Cell

*M. musculus*

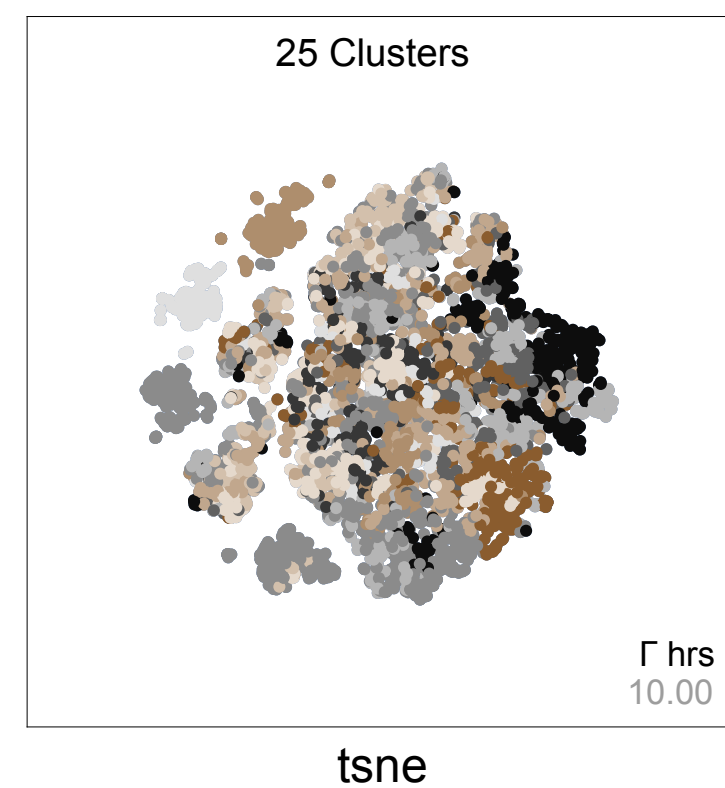
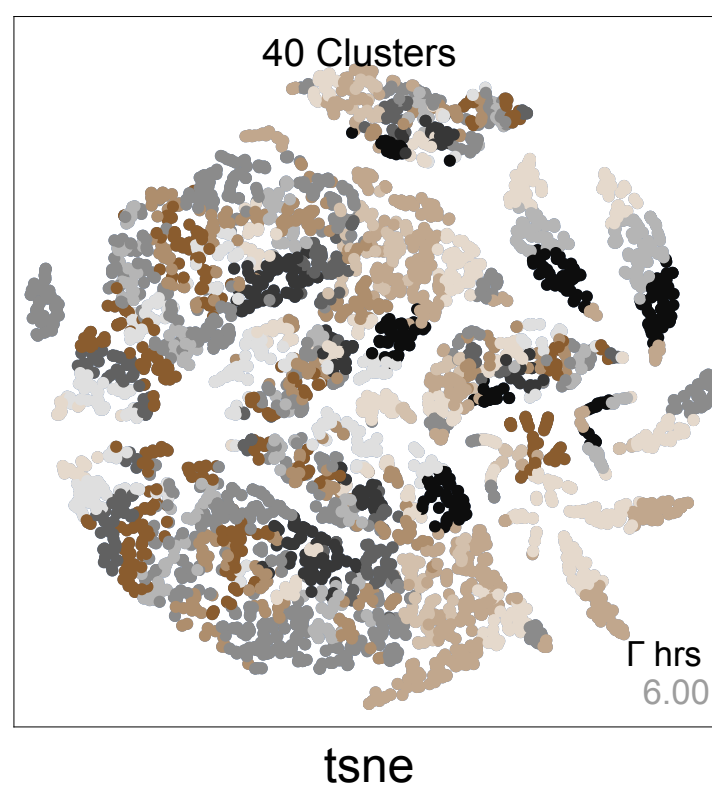
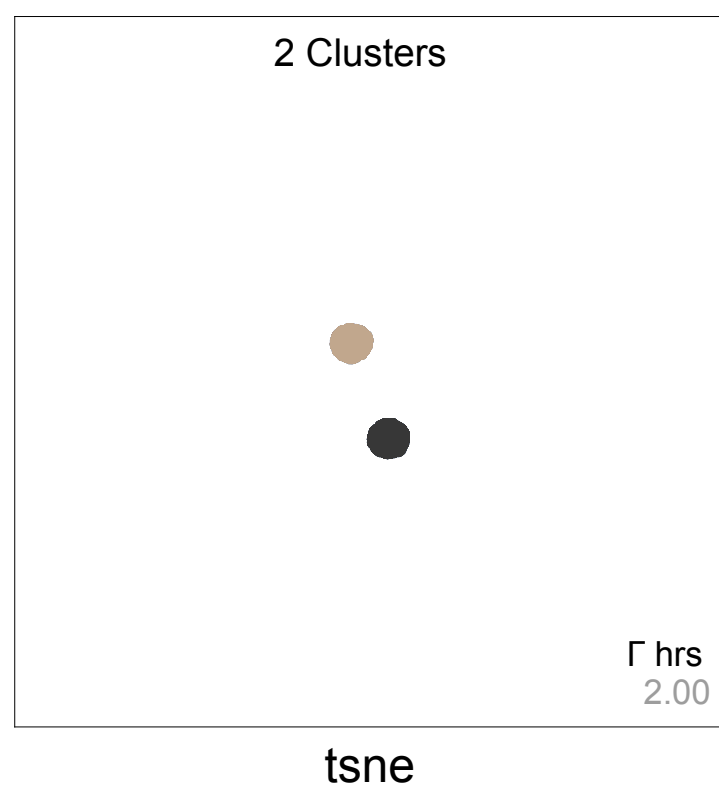
A



B

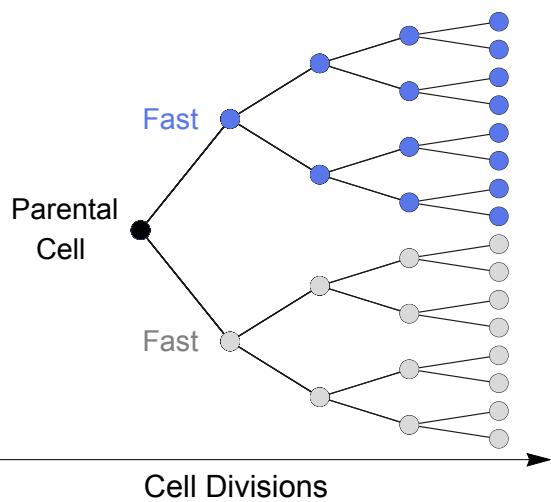


C



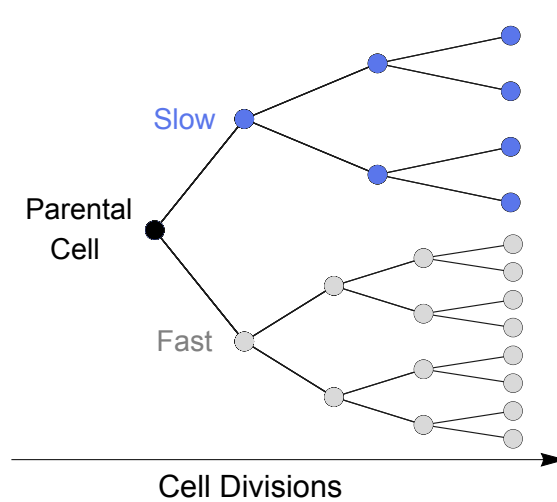
A

Scenario 1: Fast-Fast



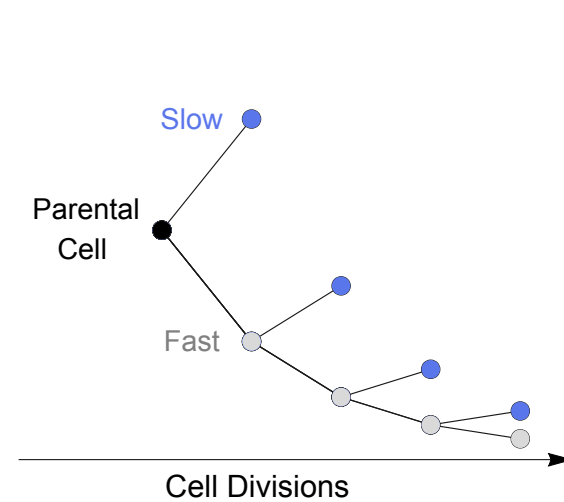
B

Scenario 2: Slow-Fast

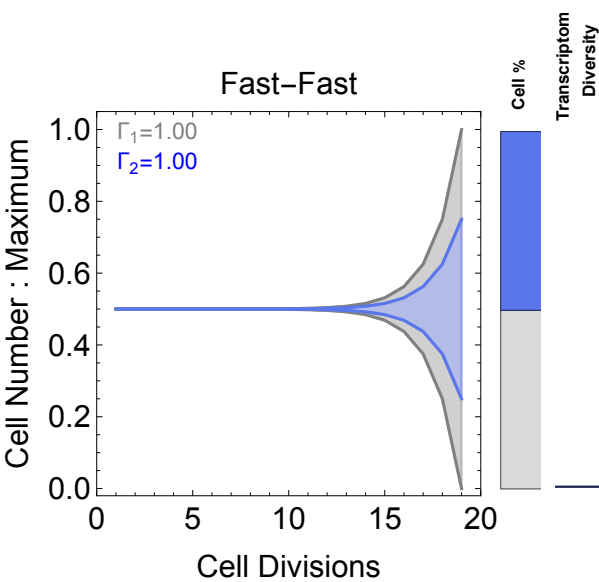


C

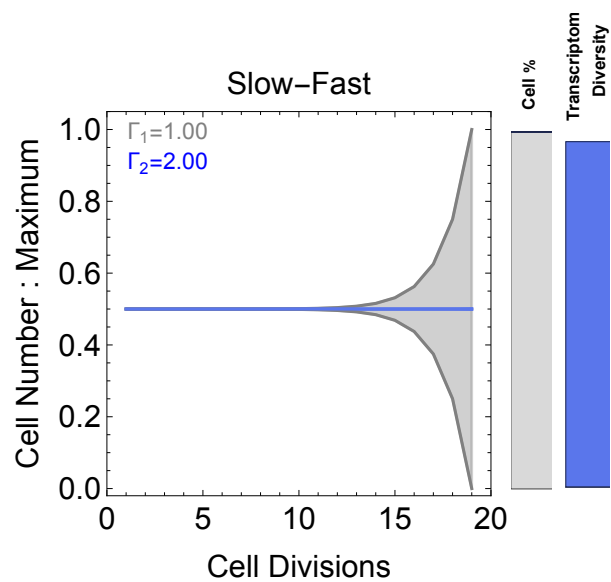
Scenario 3: Slow-Fast



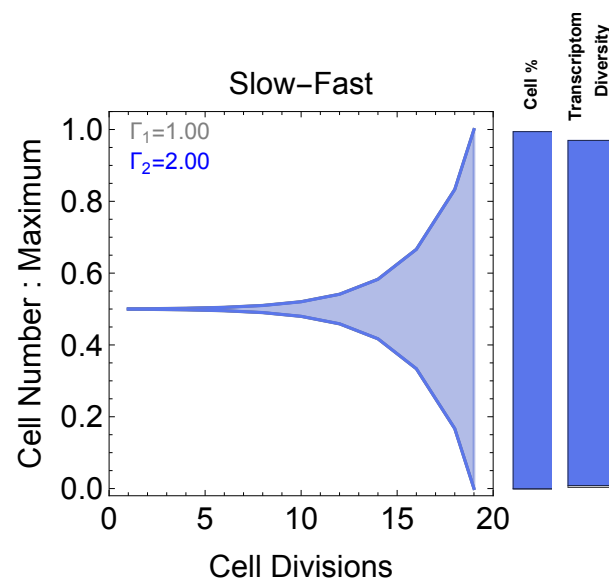
D



E

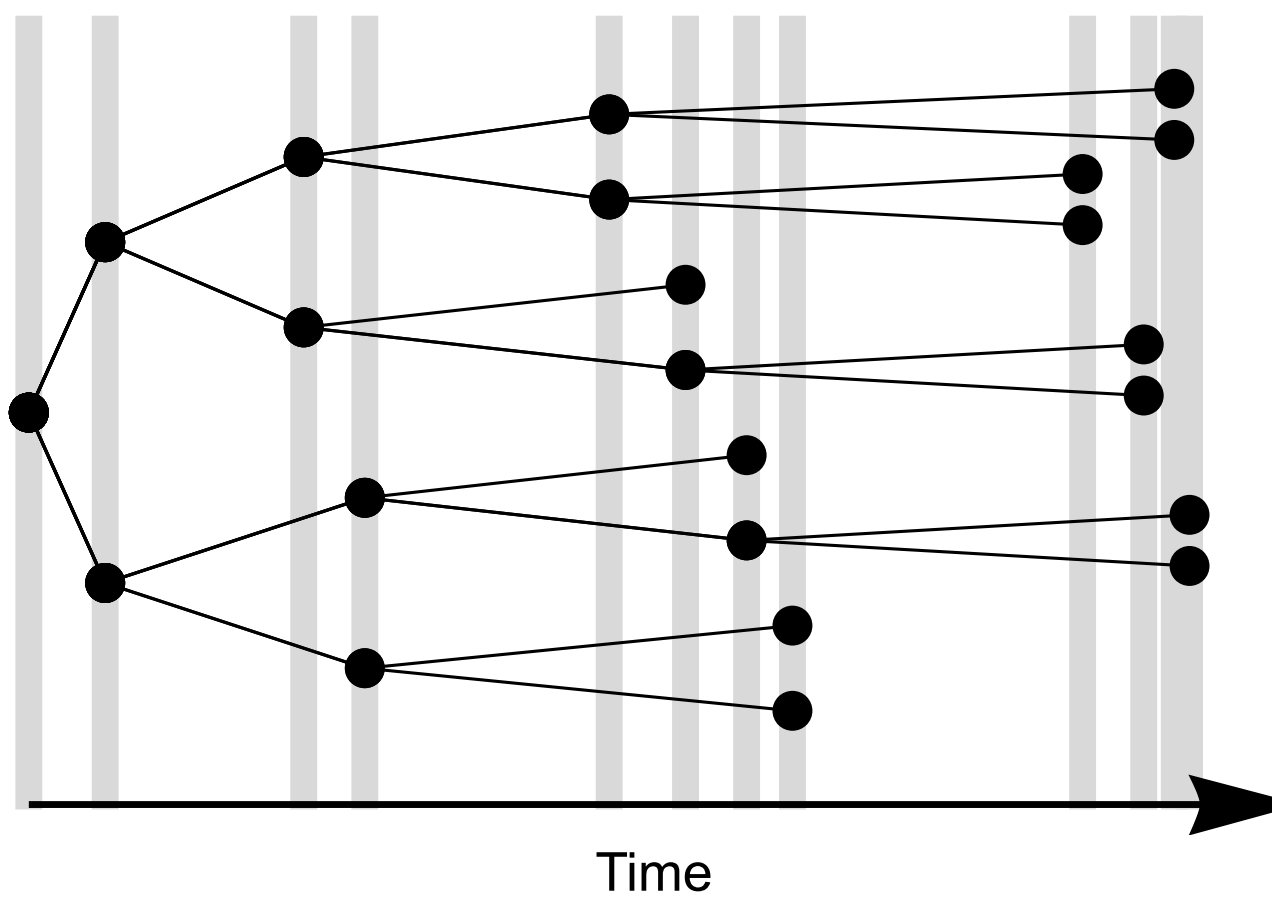


F



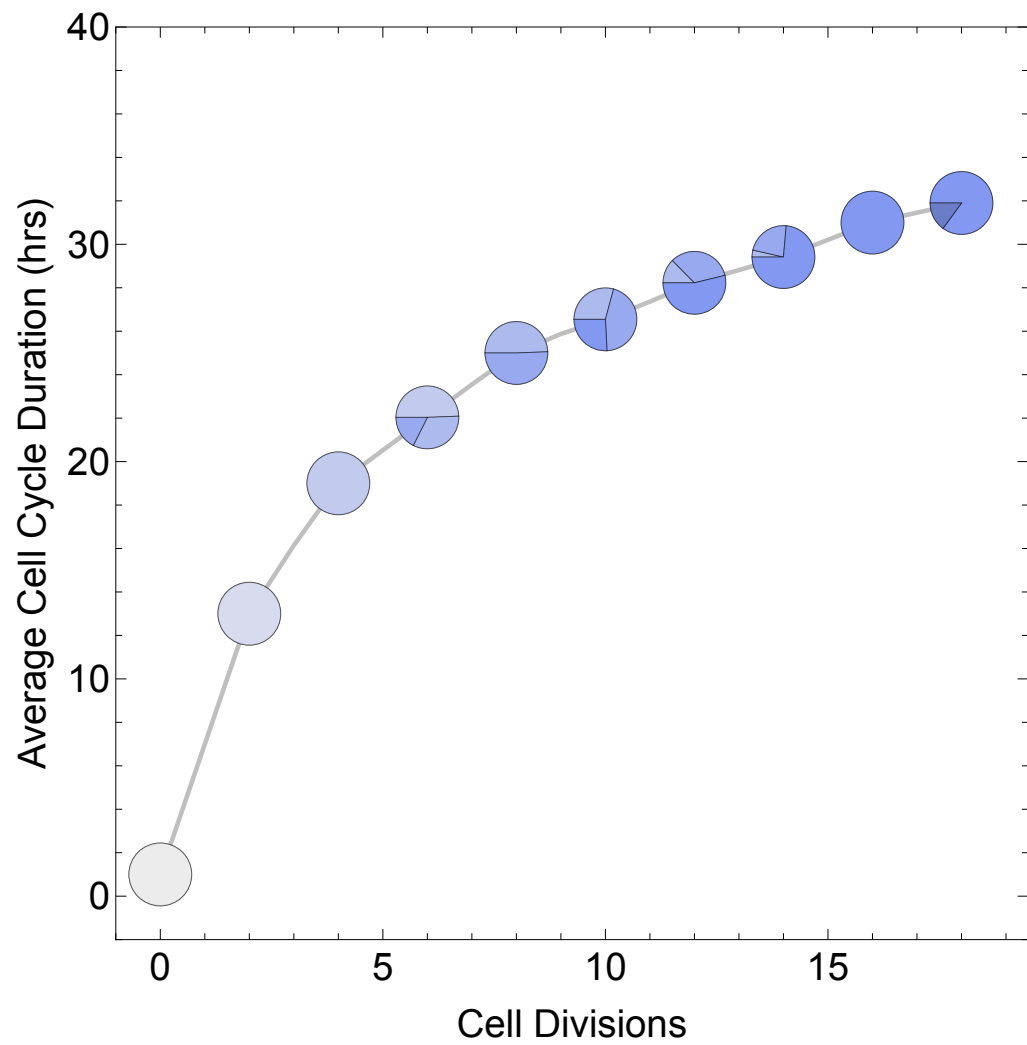
A

## Cell Divisions



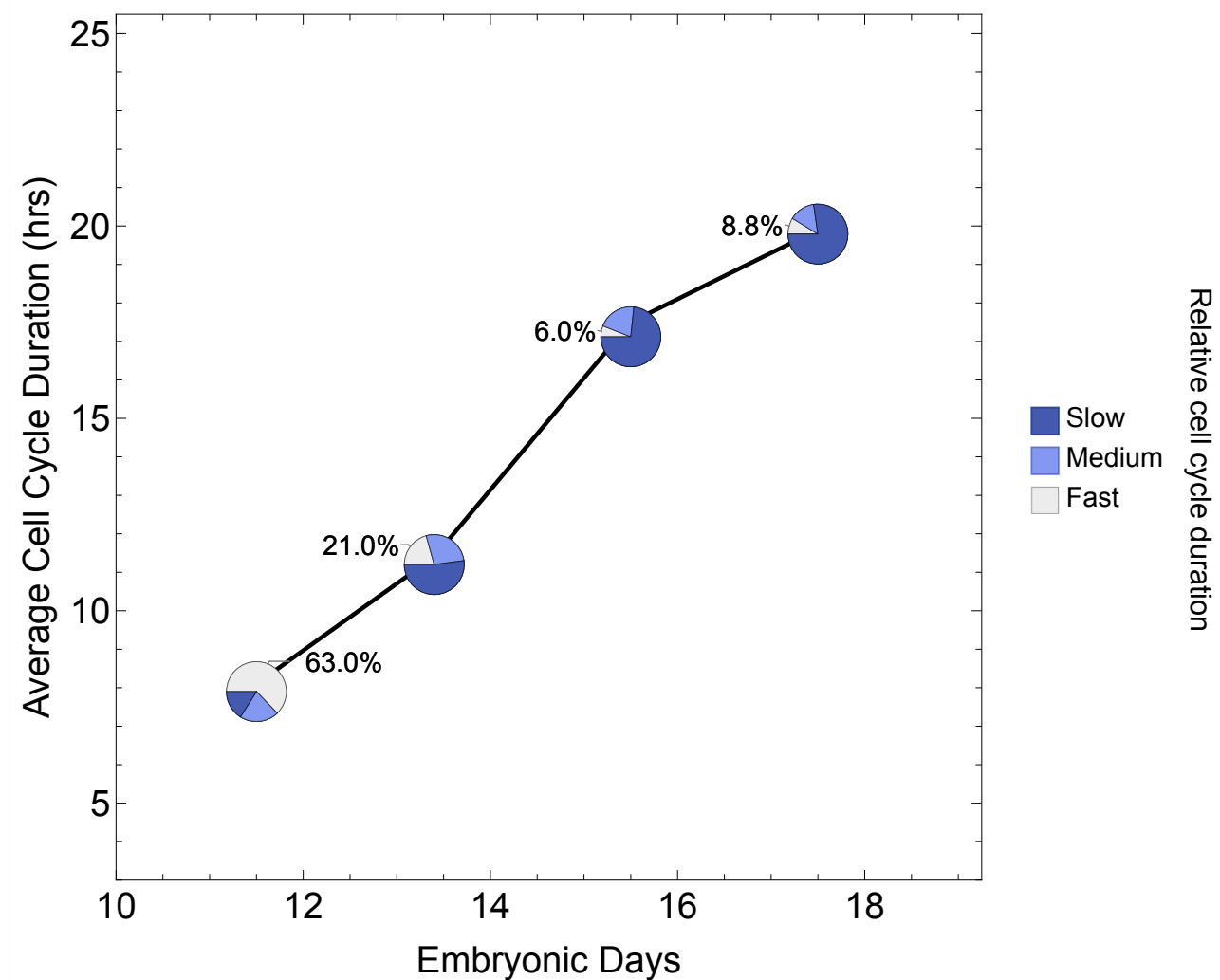
B

## Simulations

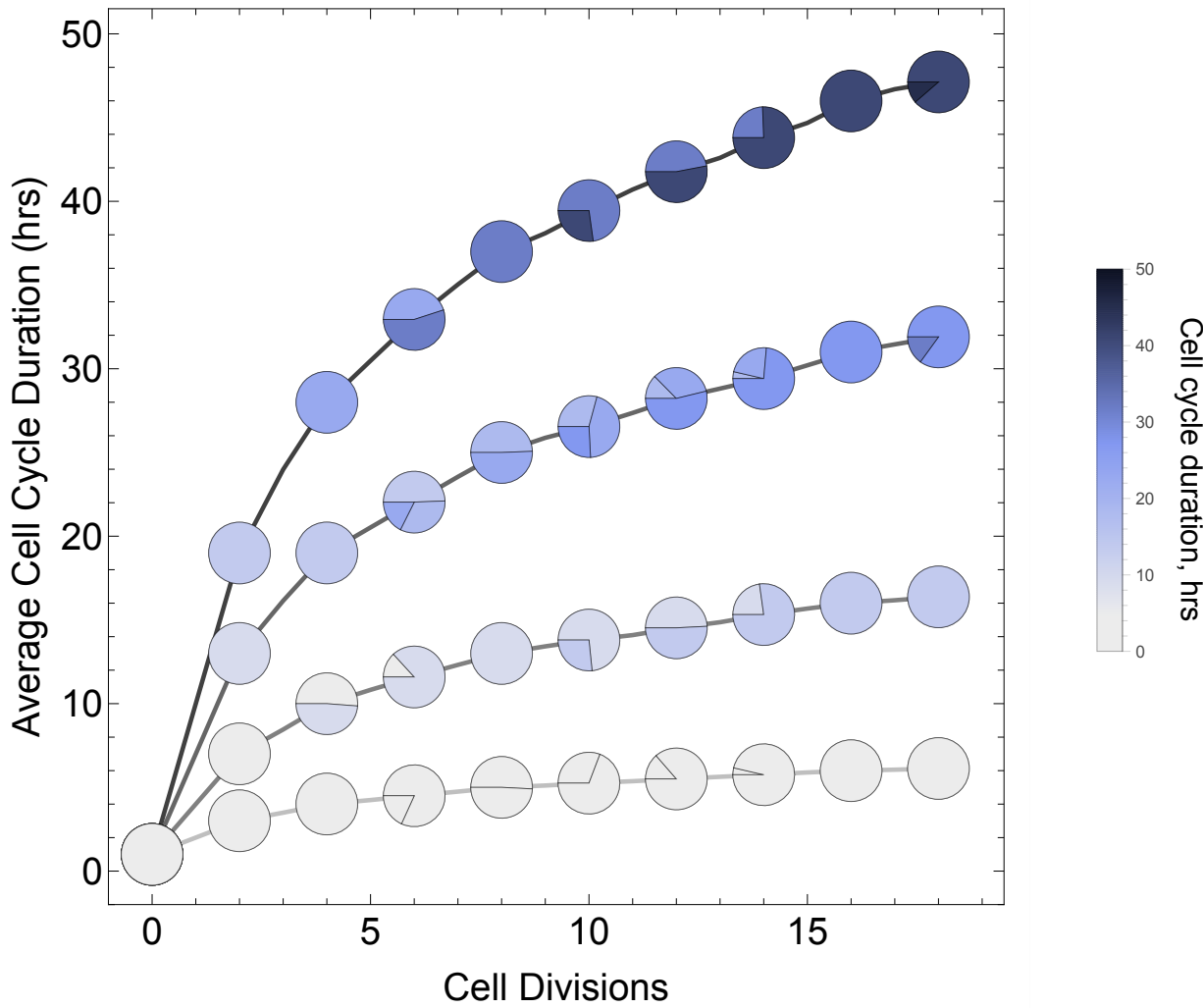


C

## M. musculus cortex

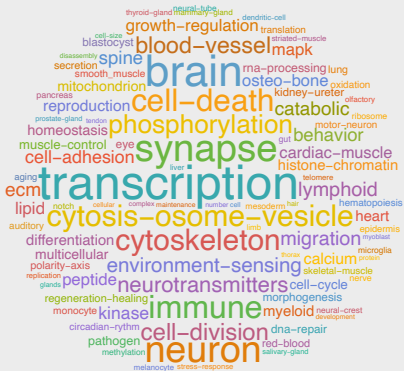


# Simulations



Increasing

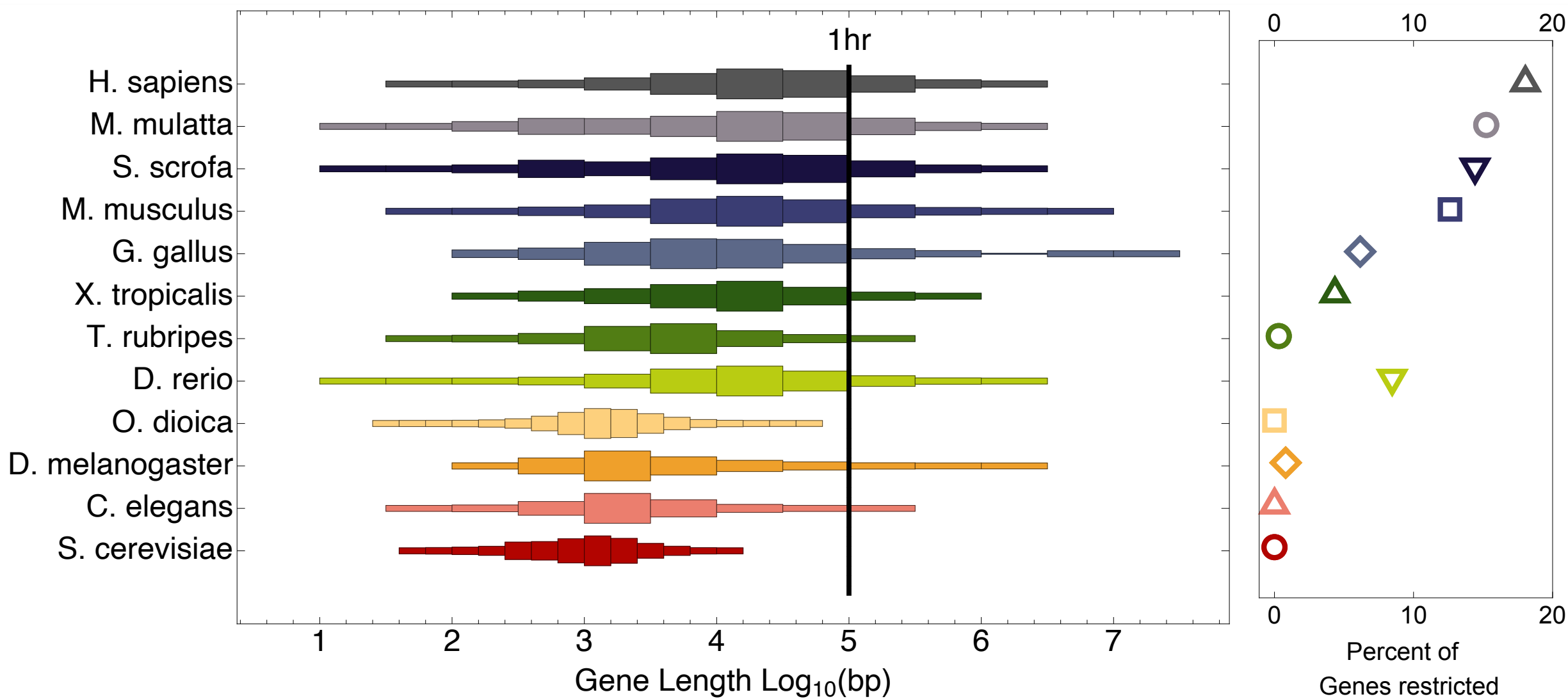
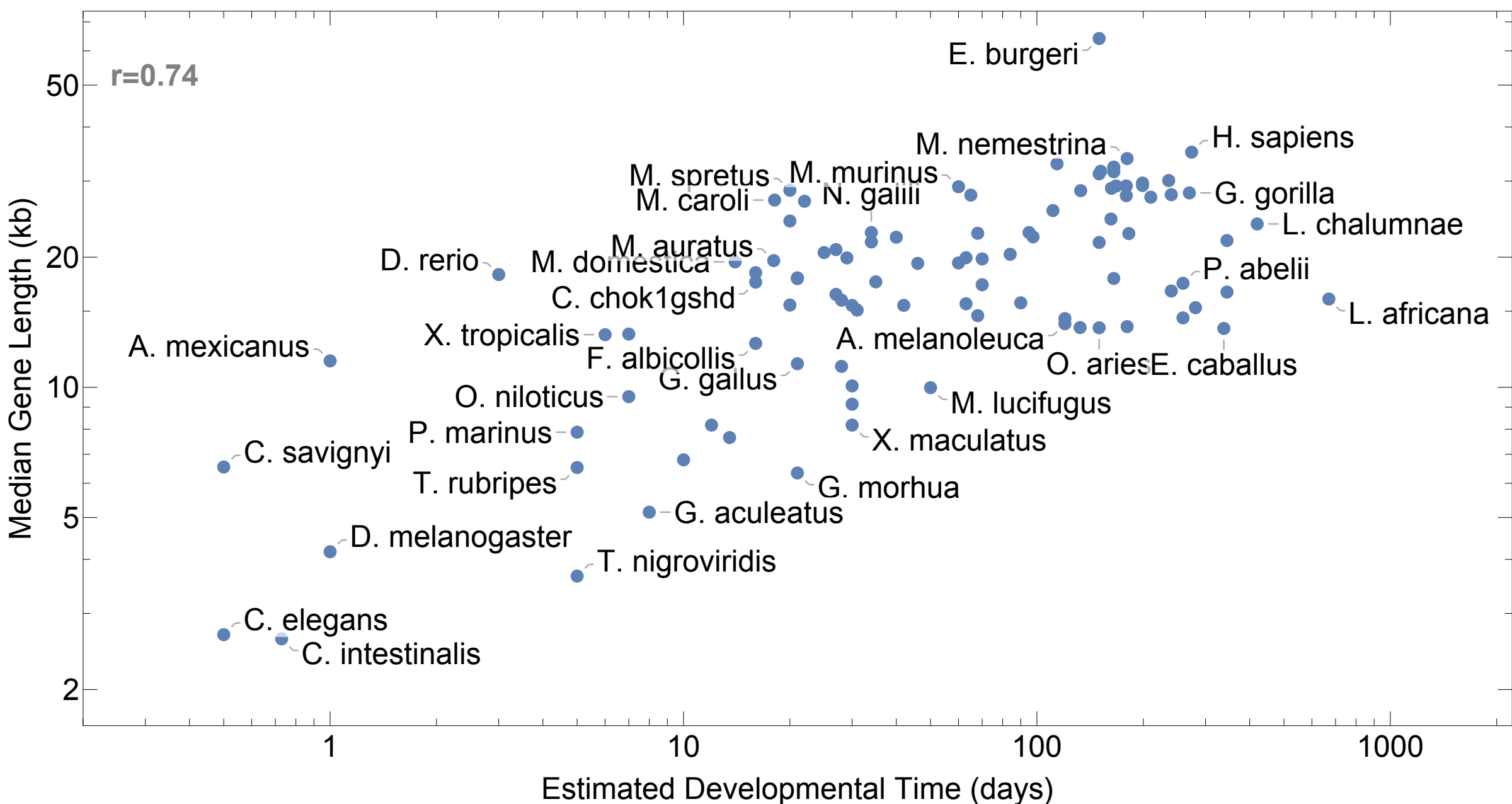
E11.5 < E13.5 < E15.5 < E17.5

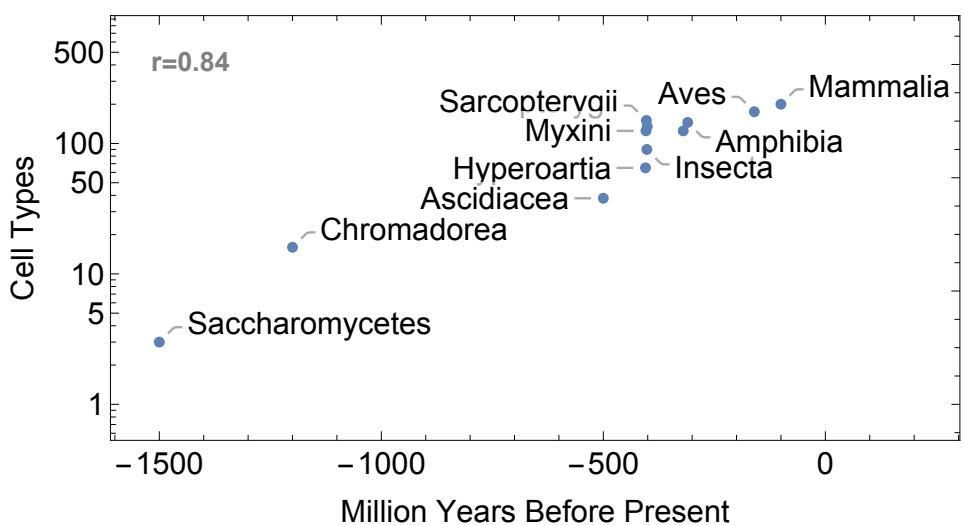
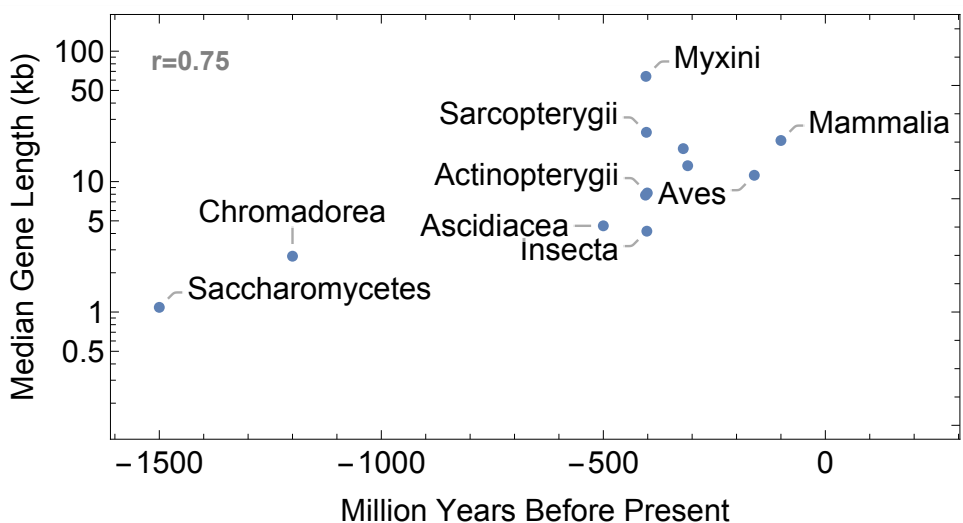
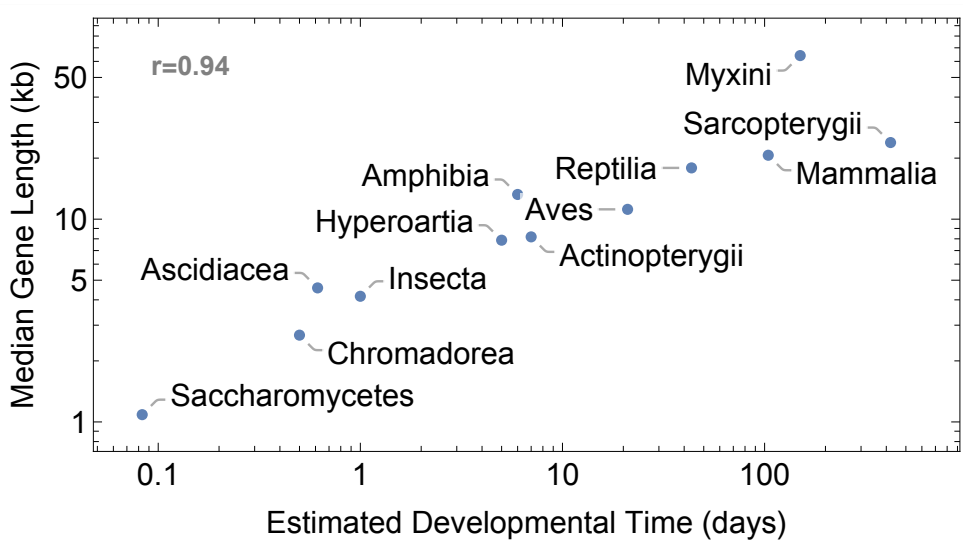


Decreasing

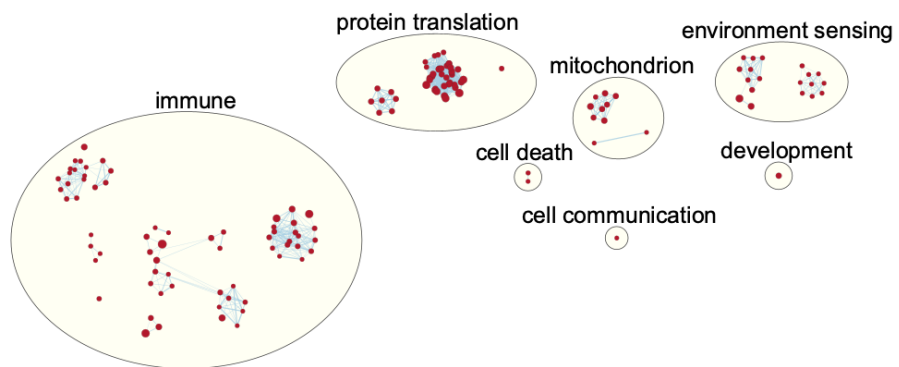
E11.5 > E13.5 > E15.5 > E17.5



**A****B**

**A****B****C**



**A****B**